

**Effect of autoantibodies targeting amphiphysin or glutamate decarboxylase
65 on synaptic transmission of GABAergic neurons**

**Einfluss von Autoantikörpern gegen Amphiphysin oder
Glutamatdecarboxylase 65 auf synaptische Transmission GABAerger Neurone**



Doctoral thesis for a doctoral degree
at the Graduate School of Life Sciences,
Julius-Maximilians-Universität Würzburg,

Section Neuroscience

submitted by

Christian Werner

from

Schweinfurt

Würzburg, 2014

Submitted on:

.....

Office stamp

Members of the *Promotionskomitee*:

Chairperson:

Primary Supervisor: Professor Dr. Claudia Sommer

Supervisor (Second): Professor Dr. Marie-Christine Dabauvalle

Supervisor (Third): Professor Dr. Erhard Wischmeyer

Supervisor (Fourth):

.....

(If applicable)

Date of Public Defence:

Date of Receipt of Certificates:

.....

Meiner Familie

Abstract

The number of newly detected autoantibodies (AB) targeting synaptic proteins in neurological disorders of the central nervous system (CNS) is steadily increasing. Direct interactions of AB with their target antigens have been shown in first studies but the exact pathomechanisms for most of the already discovered AB are still unclear. The present study investigates pathophysiological mechanisms of AB-fractions that are associated with the enigmatic CNS disease Stiff person syndrome (SPS) and target the synaptically located proteins amphiphysin or glutamate decarboxylase 65 (GAD65).

In the first part of the project, effects of AB to the presynaptic endocytic protein amphiphysin were investigated. Ultrastructural investigations of spinal cord presynaptic boutons in an established *in-vivo* passive-transfer model after intrathecal application of human anti-amphiphysin AB showed a defect of endocytosis. This defect was apparent at high synaptic activity and was characterized by reduction of the synaptic vesicle pool, clathrin coated vesicles (CCVs), and endosome like structures (ELS) in comparison to controls. Molecular investigation of presynaptic boutons in cultured murine hippocampal neurons with *d*STORM microscopy after pretreatment with AB to amphiphysin revealed that marker proteins involved in vesicle exocytosis (synaptobrevin 2 and synaptobrevin 7) had an altered expression in GABAergic presynapses. Endophilin, a direct binding partner of amphiphysin also displayed a disturbed expression pattern. Together, these results point towards an anti-amphiphysin AB-induced defective organization in GABAergic synapses and a presumably compensatory rearrangement of proteins responsible for CME.

In the second part, functional consequences of SPS patient derived IgG fractions containing AB to GAD65, the rate limiting enzyme for GABA synthesis, were investigated by patch clamp electrophysiology and immunohistology. GABAergic neurotransmission at low and high activity as well as short term plasticity appeared normal but miniature synaptic potentials showed an enhanced frequency with constant amplitudes. SPS patient IgG after preabsorption of GAD65-AB using recombinant GAD65 still showed specific synaptic binding to neurons and brain slices supporting the hypothesis that additional, not yet characterized AB are present in patient IgG responsible for the exclusive effect on frequency of miniature potentials.

In conclusion, the present thesis uncovered basal pathophysiological mechanisms underlying paraneoplastic SPS induced by AB to amphiphysin leading to disturbed presynaptic architecture. In idiopathic SPS, the hypothesis of a direct pathophysiological role of AB to GAD65

was not supported and additional IgG AB are suspected to induce distinct synaptic malfunction.

Zusammenfassung

Die Anzahl neu charakterisierter Autoantikörper (AAK) gegen synaptische Proteine bei Erkrankungen des zentralen Nervensystems (ZNS) ist stetig wachsend. Direkte Interaktionen der AAK mit ihren Zielantigenen konnten in ersten Studien belegt werden, jedoch besteht weiterhin Unklarheit über die exakten zugrunde liegenden Pathomechanismen.

In der vorliegenden Arbeit wurden pathophysiologische Mechanismen von AAK gegen die synaptisch lokalisierten Proteine Amphiphysin und Glutamatdecarboxylase 65 (GAD65) untersucht, die mit der ZNS Erkrankung Stiff Person Syndrom (SPS) assoziiert sind.

Im ersten Projektteil wurden die Effekte von AAK gegen das Endozytoseprotein Amphiphysin analysiert: in einem etablierten in-vivo Tiermodell konnten nach intrathekalem passiven Transfer von AAK gegen Amphiphysin ultrastrukturelle Untersuchungen von präsynaptischen Terminalen im Rückenmark eine Störung der Endozytose aufzeigen. Dieser Defekt, der bei hoher synaptischer Aktivität eintrat, war durch eine Verminderung synaptischen Vesikel-pools, Clathrin-ummantelter Vesikel und endosomähnlicher Strukturen charakterisiert. Molekulare Untersuchungen präsynaptischer Terminale kultivierter hippocampaler Zellkulturen mit *d*STORM Mikroskopie zeigten, dass an der Exozytose beteiligte synaptische Vesikelproteine (Synaptobrevin 2 und Synaptobrevin 7) ein verändertes Expressionsmuster innerhalb GABAerger Synapsen aufweisen. Die Expression von Endophilin, einem direkten Bindungspartner von Amphiphysin, war ebenso verändert. Zusammengefasst weisen diese Ergebnisse auf einen Organisationsdefekt GABAerger Synapsen hin, die durch anti-Amphiphysin AAK induziert sind und eine kompensatorische Umverteilung von Endozytoseproteinen vermuten lassen.

Im zweiten Teil der Arbeit wurden die funktionellen Effekte von SPS AAK gegen GAD65, dem geschwindigkeitsbestimmenden Enzym der GABA-Synthese, mittels Patch-Clamp Messungen und Immunhistologie untersucht. Die GABAerge synaptische Übertragung bei niedriger als auch hoher synaptischer Aktivität sowie die synaptische Kurzzeitplastizität wurden durch die IgG Fraktionen mit GAD65-AAK nicht beeinträchtigt. Die Frequenz von GABAergen Miniaturpotentialen war jedoch bei ansonsten gleichbleibender Amplitude erhöht. SPS-Patienten-IgG zeigte allerdings auch nach Präabsorbition von GAD65-AAK mit Hilfe von rekombinanten GAD65 eine spezifische Anfärbung neuronaler Synapsen, was die Hypothese von weiteren, funktionell wirksamen, aber noch nicht identifizierten AAK im Patienten-IgG unterstützt.

Zusammenfassend konnten in der vorliegenden Arbeit grundlegende pathophysiologische Mechanismen aufgezeigt werden, wie pathogene Antikörper gegen Amphiphysin die Struktur präsynaptischer Boutons beeinträchtigen können. Im Falle des idiopathischen SPS konnte

keine unterstützenden Befunde für die Hypothese einer direkten pathophysiologischen Rolle von GAD65 AAK erhoben werden. Nach den vorliegenden Ergebnissen wird das Vorhandensein weiterer, derzeit noch nicht beschriebener IgG AAK postuliert, die die synaptische Fehlfunktion erklären können.

INDEX

Summary	I
Zusammenfassung	III
Index	V
1. Introduction	1
1.1. Humoral autoimmunity in the CNS	1
1.2. Stiff person syndrome	2
1.3. Chemical synapses and the vesicle cycle	4
1.4. Amphiphysin	5
1.5. Scientific research question: anti-amphiphysin AB	8
1.6. Glutamate decarboxylase 65 (GAD65)	8
1.7. Scientific research question: anti-GAD65 AB.....	9
2. Material and methods	10
2.1. Animal experiments.....	10
2.2. Patient IgG and AB purification	10
2.3. Primary hippocampal cell culture	11
2.4. <i>In-vivo</i> rat model of SPS.....	12
2.5. Electron microscopy of rat spinal terminals.....	13
2.6. <i>d</i> STORM microscopy experiments	14
2.7. Confocal microscopy for analysis of GABAergic bouton size and IgG binding experiments.....	16
2.8. Whole cell patch-clamp recordings.....	17

2.9. Quantitative real time polymerase chain reaction (qRT-PCR)	18
2.10. Statistics	19
3. Results A: Impact of SPS anti-amphiphysin AB on synaptic structure	20
3.1. Sustained stimulation increases synaptic vesicle pool size and the amount of clathrin-coated vesicles in naïve GABAergic spinal cord interneurons	20
3.2. Pathogenic human anti-amphiphysin AB interfere with CME leading to stimulus-dependent presynaptic vesicle depletion	23
3.3. Different v-SNARE composition of GABAergic vesicle pools induced by anti-amphiphysin AB	28
3.4. Human AB to amphiphysin alter endophilin density and clustering in GABAergic presynaptic vesicle pools.....	31
4. Results B: Functional consequences induced by anti-GAD65 containing SPS-IgG	36
4.1. Normal basal GABAergic neurotransmission in presence of anti-GAD65 AB containing SPS-IgG.....	36
4.2. Normal short term plasticity and high frequency transmission after anti-GAD65 IgG incubation	37
4.3. Anti-GAD65 AB containing IgG increases frequency of mIPSCs	38
4.4. Microisland cultures as model system to investigate functional effects of pathogenic antineuronal AB	42
5. Discussion	44
5.1. Pathophysiological mechanisms of anti-amphiphysin AB	44
5.2. The role of anti-GAD65 AB in SPS	46
Reference list.....	49

Appendix A: Index of figures.....	56
Appendix B: Abbreviations	58
Affidavit & eidesstattliche Erklärung	61
Danksagung/Acknowledgements (in German).....	62
Publications.....	64
Curriculum Vitae	65

1. Introduction

1.1. Humoral autoimmunity in the CNS

The term of autoimmunity was first used by the Nobel laureate in medicine Paul Ehrlich. He described the state in which the immune system attacks own tissue instead of foreign invaders as „horror autotoxicus” (Silverstein, 2001). Humoral autoimmunity - in contrast to cell-mediated autoimmunity - is the form of immunity which is mediated by macromolecules in the extracellular fluids, e.g. serum or cerebrospinal fluid (CSF), most importantly by secreted autoantibodies (AB) (Whitney and McNamara, 1999). Identification of AB in serum or CSF and characterization of the respective target antigen are first prerequisites for characterization of a humoral autoimmune mediated disorder. Further, successful passive transfer of the respective AB in experimental animals and active immunization with target antigen reproducing patient symptoms as well as relief of disease symptoms by immunosuppressive therapies are mandatory to categorize suspected disorders as an autoimmune disease according to Witebsky’s postulates (Rose and Bona, 1993).

In the past decades, clinical neurology and neuroscience research has first focused on AB targeting peripheral nervous tissue in e.g. myasthenia gravis with AB to the acetylcholine receptor (Toyka et al., 1975) Guillian-Barré syndrome with AB to gangliosides (Buchwald et al., 1998a, Buchwald et al., 1998b) and Lambert-Eaton syndrome with AB to presynaptic Ca^{2+} channels (Fukunaga et al., 1983). In recent years, characteristic CNS disorders have been described to be associated with AB targeting neuronal proteins. Scientific reports highlight an increasing number of newly detected AB: autoantigens comprise ionotropic glutamate receptor subunits (Dalmau et al., 2008, Lai et al., 2009), $GABA_B$ -receptors (Lancaster et al., 2010), $GABA_A$ receptors (Petit-Pedrol et al., 2014), the leucine rich, glioma inactivated protein LGI1, the paranodal protein CASPR2 (Irani et al., 2010, Lai et al., 2010), and others. Interestingly, AB can not only be neuron-specific but also target antigens in astrocytes as reported for neuromyelitis optica (Bradl et al., 2009). Most of these recently described antigens are synaptic, extracellular located proteins and therefore easily accessible for potentially pathogenic AB. Some of these target antigens are known to be primarily intracellular located, e.g. amphiphysin and glutamate decarboxylase 65 (GAD65) in presynaptic terminals (Solimena et al., 1988, De Camilli et al., 1993). The cellular mechanism for AB uptake or an alternative mechanisms, how AB can directly interact with their target is still a matter of debate. There are first reports revealing functional effects of AB targeting these presynaptic antigens in animal models (Manto et al., 2007, Geis et al., 2009, Geis et al., 2010, Hansen et

al., 2013). The underlying pathophysiological impact of AB targeting surface or intracellular antigens resulting in distinct synaptic dysfunction have only been described in few recent reports in some of these disorders (Dalmau et al., 2008, Geis et al., 2009, Lai et al., 2009, Geis et al., 2010, Ohkawa et al., 2014).

1.2. Stiff person syndrome

Stiff person syndrome (SPS) is a rare CNS autoimmune disease with a reported prevalence of one case per million although prevalence may be underestimated because it is often misdiagnosed as a psychiatric disorder (Dalakas, 2008). Patient symptoms comprise muscle stiffness and superimposed muscle spasms of the lumbar, trunk and proximal limb muscles (Moersch and Woltman, 1956, Alexopoulos and Dalakas, 2010). Beside motor symptoms, patients also show also supraspinal symptoms of agoraphobia, panic attacks, and comorbid depression (Toro et al., 1994, Henningsen and Meinck, 2003). In general, symptoms can often be triggered by stress, unexpected sounds, and other external stimuli.

Etiology of SPS can be either idiopathic or paraneoplastic secondary to primarily breast and small cell lung cancer (Pittock et al., 2005). Paraneoplastic SPS is characterized by AB targeting the endocytic protein amphiphysin or the scaffolding protein gephyrin (De Camilli et al., 1993, Butler et al., 2000, Dalakas, 2009). In the far more frequent idiopathic variant of SPS, AB against glutamate decarboxylase 65 (GAD65) are prevailing (Solimena et al., 1988). Recently, in anti-GAD65 AB positive SPS patients also AB to additional epitopes have been described. In up to 70 % of patients, AB to the GABA_A receptor associated protein (GABARAP) were detected (Solimena et al., 1988, Raju et al., 2006). Figure 1 summarizes localization and function of already known SPS antigens. Amphiphysin is a protein involved in clathrin mediated endocytosis (CME) (Wigge and McMahon, 1998), GAD65 is the rate limiting enzyme required for gamma-aminobutyric acid (GABA) synthesis and involved of loading GABA into presynaptic vesicles (Asada et al., 1996, Tian et al., 1999), GABARAP is a postsynaptically localized protein involved in GABA_A receptor clustering (Chen et al., 2000), and the scaffolding protein gephyrin is essential for postsynaptic localization of GABA_A and glycine receptors (Essrich et al., 1998).

As mentioned above, most SPS patients are affected by the idiopathic form with associated AB to GAD65. Interestingly, patients that suffer from autoimmune diabetes mellitus type 1 (DM1) also typically have AB to GAD65 (Dalakas et al., 2000). However, in these patients the titer of DB1 associated anti-GAD65 AB is low in comparison to SPS related anti-GAD65 IgG and the AB seem to be directed only to conformational epitopes, which is not the case in

SPS (Butler et al., 1993, Daw et al., 1996, Dalakas et al., 2000). In a study of monozygotic twins suffering from SPS, anti-GAD65 binding to linear epitopes of GAD65 could be reduced by treatment with Rituximab while conformational epitopes and inhibition of enzymatic activity still remained (Rizzi et al., 2010). This observation underlines the assumption that the immune reaction in diabetic patients and SPS patients is different. Moreover, SPS associated anti-GAD65 AB target GAD65 preferentially at the N-terminal region of GAD65 and were shown to be synthesized intrathecally which may further support the hypothesis of a pathogenic role of these AB in SPS acting on CNS neurons (Kim et al., 1994, Jarius et al., 2010).

Treatment of SPS consists of symptomatic measures with drugs enhancing GABAergic transmission (benzodiazepines, baclofen), AB-removal by plasma exchange (Brashear and Phillips, 1991), and immunosuppression (Wessig et al., 2003, Baker et al., 2005). There exists one controlled study testing polyvalent intravenous immunoglobulins (Dalakas et al., 2001) in a series of idiopathic SPS patients showing improvement of disease symptoms. More recently, case reports and case series report beneficial outcome of SPS patients when treated with rituximab, a B-cell depleting monoclonal AB (Baker et al., 2005, Lobo et al., 2010, Fekete and Jankovic, 2012).

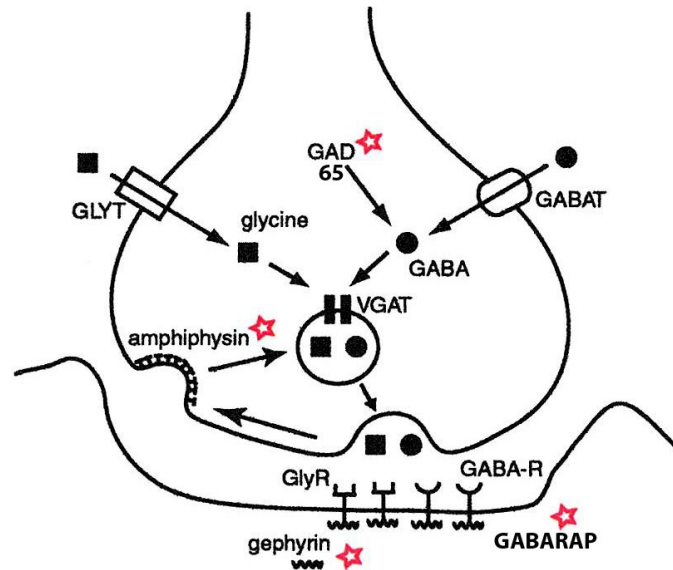


Fig 1 Summary of SPS antigens linked to GABAergic neurotransmission

Amphiphysin is an endocytosis protein playing a key role in clathrin mediated endocytosis. GAD65 is a presynaptic localized enzyme for rate limiting GABA synthesis. Postsynaptic localized gephyrin organizes localization of GABA_A receptors and glycine receptors. GABARAP is associated with postsynaptic GABA_A receptors regulating their opening kinetics [adapted from and cited in (Butler et al., 2000)]

1.3. Chemical synapses and the vesicle cycle

Communication between nerve cells in the brain relies predominantly on synaptic transmission using chemical synapses. Chemical synapses transmit synaptic signals by releasing chemical compounds called neurotransmitters which allows filtering, integration and summation of synaptic signals (Burns and Augustine, 1995). Chemical synapses form contacts between a presynaptic compartment (axonal bouton from a transmitting cell) and a postsynaptic compartment (dendrite) of a target cell receiving synaptic information via receptor mediated changes of postsynaptic membrane potential (Sudhof and Malenka, 2008). The presynaptic bouton stores and releases neurotransmitters using small sized synaptic vesicles (Figure 2) (Haucke et al., 2011). Synaptic vesicles can be allocated to different synaptic vesicle pools (Rizzoli and Betz, 2005), a ready release pool near the presynaptic membrane, a reserve pool, and a resting pool of vesicles. Different vesicle pool models regarding their functional role have been proposed but still need further validation (Denker and Rizzoli, 2010). Vesicle pools can be distinguished on the basis of their vesicular soluble N-ethylmaleimide-sensitive-factor attachment receptors (v-SNARE) composition. Synaptobrevin isoform 2 preferentially targets the readily releasable pool whereas isoform 7 primarily resides on resting pool vesicles (Hua et al., 2011). V-SNAREs form essential components of vesicular neurotransmitter exocytosis facilitating the fusion of vesicular membranes with presynaptic membrane via interaction with membrane bound t-SNAREs (Sudhof and Rizo, 2011). After exocytosis vesicles are recycled in a compensatory mechanism called endocytosis (Haucke et al., 2011) and it has been suggested previously that different modes of endocytosis might produce different molecular composition of vesicular proteins (Voglmaier and Edwards, 2007). Clathrin-mediated endocytosis (CME) has long been termed the dominant form of vesicular endocytosis (Granseth et al., 2006) although recent research also points to similar importance of other endocytosis mechanisms, namely kiss and run (He and Wu, 2007) and ultrafast endocytosis (Watanabe et al., 2013). CME is a rather slow endocytosis mechanism taking place several seconds after exocytosis (Heuser and Reese, 1973). CME is initiated by nucleation of a clathrin coated pit which is accomplished by adaptor proteins and membrane bending proteins like amphiphysin (Wu et al., 2009). Successive fission of synaptic vesicles is performed together with the guanosinetriphosphatase (GTPase) dynamin (Takei et al., 1999, Ferguson et al., 2007). The clathrin coat covering synaptic vesicles in CME is supposed to support molecular sorting of vesicular proteins (Schmid, 1997) and is shed after successful CME by uncoating proteins (Verstreken et al., 2003, Milosevic et al., 2011). Kiss and run endocytosis is characterized by a narrow, transient fusion pore openings for transmitter release retaining the morphology of synaptic vesicles, thus allowing fast coupling of endo- and exo-

Introduction

cytosis 20 times faster than CME (Fesce et al., 1994, Richards et al., 2005). Reports of ultra-fast endocytosis showed compensatory endocytosis within 50 to 100ms revealing an even faster endocytosis mechanism taking place at sites adjacent to active zones (Watanabe et al., 2013).

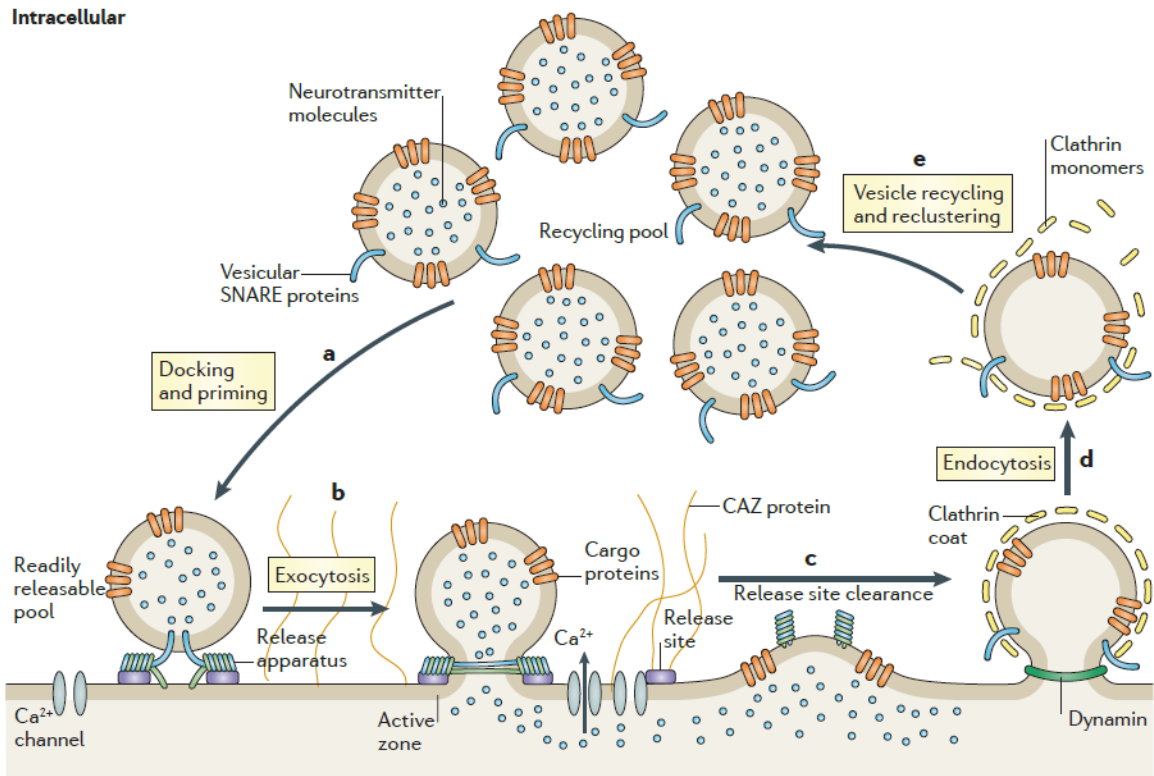


Fig 2 Overview of the presynaptic compartment of chemical synapses depicting exocytosis and endocytosis mechanisms

adapted from (Haucke et al., 2011) Scheme of presynaptic endocytosis and exocytosis with suggested coupling of both machineries; light blue: v-SNAREs, green: dynamin, yellow: clathrin coat surrounding synaptic vesicles.

1.4. Amphiphysin

Amphiphysin is a synaptic 128kD Protein involved in CME. There exist 2 isoforms of amphiphysin and both isoforms are highly concentrated in nerve terminals. Amphiphysin 1 shows dominant neuronal expression along with partial association with synaptic vesicles while isoform 2 is ubiquitously expressed (Di Paolo et al., 2002).

Amphiphysin structure (Figure 3) consists of a N-terminal alpha-helix domain, a membrane bending N-Bin-amphiphysin-RVs (BAR) domain, a proline rich domain (PRD), a clathrin - and AP-2-binding domain and a C-terminal src-homology 3 domain (SH3) (Wu et al., 2009).

During CME amphiphysin function involves curvature sensing (Peter et al., 2004) and bending of the presynaptic membrane (Arkhipov et al., 2009) during the membrane invagination

Introduction

step and recruitment of several endocytosis proteins. Its PRD domain binds to endophilin, a SH3 domain containing protein (Micheva et al., 1997, Chen et al., 2003) that is partially associated with presynaptic calcium channels (Chen et al., 2003) driving BAR domain mediated membrane invagination and uncoating of vesicles by recruiting the phosphatase synaptojanin (Verstreken et al., 2003).

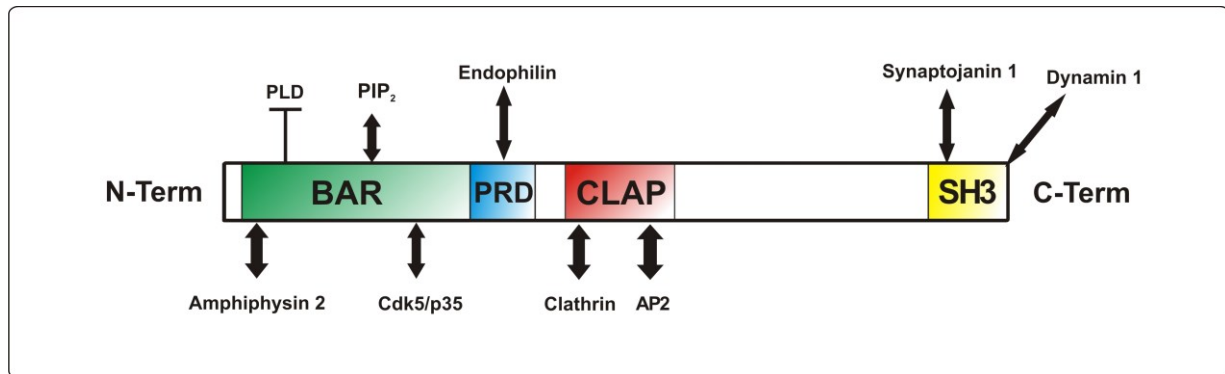


Fig 3 Amphiphysin structure and interaction partners.

Amphiphysin shows BAR domain mediated interaction with PIP₂, Amphiphysin 2, Cdk5/p35 and inhibits phospholipidase (PLD) upon binding. The PRD domain binds endophilin and the CLAP domain is the interaction hub for clathrin and the adaptor protein AP-2. At the C-terminal there are interactions of the SH3 domain with the phosphatase synaptojanin 1 and the vesicle pinching GTPase dynamin 1; adapted from (Wu et al., 2009)¹

Genetic absence of endophilin leads to accumulation of clathrin coated vesicular profiles. Further, endophilin was suggested to be essential for the fast mode of endocytosis (Llobet et al., 2011, Milosevic et al., 2011). The SH3 domain of amphiphysin is an interaction hub for dynamin 1 (David et al., 1996) and synaptojanin 1 (Micheva et al., 1997). The GTPase dynamin 1 is the neuronal isoform of dynamins and a key player of endocytosis. Dynamin is acting in concert with amphiphysin (Takei et al., 1999) and mediates synaptic vesicle fission from the presynaptic membrane by establishing collar rings around the neck of clathrin coated membrane invaginations (Roux et al., 2006) and pinching of synaptic vesicles into the presynaptic cytosolic space (Takei et al., 1995, Shupliakov et al., 1997, Praefcke and McMahon, 2004). Genetic knockout (KO) of dynamin 1 results in faster depression of inhibitory postsynaptic current (IPSC) peak amplitudes at high synaptic activity and increased vesicle diameter along with formation of clathrin coated pits. (Ferguson et al., 2007). The phos-

¹ All information in legend of Figure 3 is from (and cited in) Wu et al., 2009.

phatase synaptojanin is recruited in the late step of endocytosis (Perera et al., 2006) and its genetic deletion leads to enhanced depression of neurotransmission along with reduced vesicle pool size and increased number of clathrin coated vesicles (CCV) suggesting a role in vesicle uncoating process (Cremona et al., 1999).

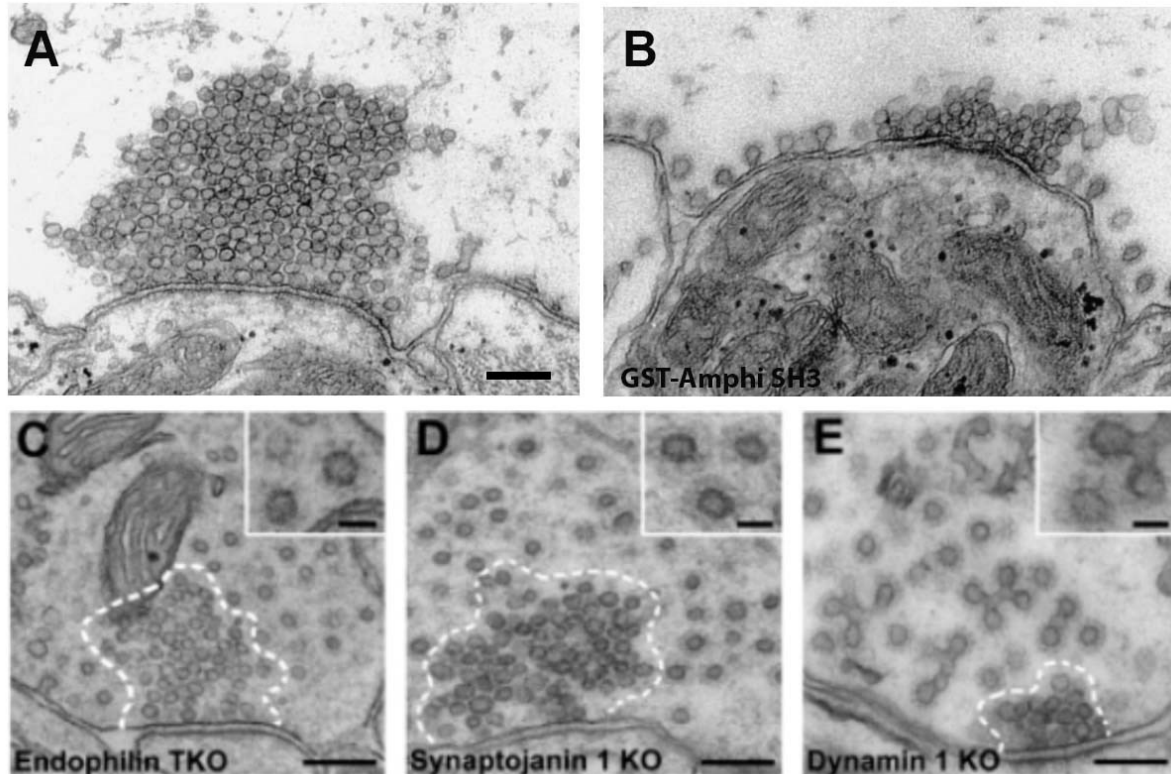


Fig 4 Structural deficits at disturbed endocytosis

Ultrastructural changes resulting from disturbed endocytosis. [A and B adapted from (Shupliakov et al., 1997), C-E adapted from (Milosevic et al., 2011)]. A) Reticulospinal synapse of lamprey at resting conditions. Note the accumulation of vesicles at the release site B) Stimulated (0.2 Hz, 30 min) lamprey reticulospinal synapse after injection of peptides targeting amphiphysin SH3 domain showing clathrin coated pits at the synaptic membrane. C) Presynaptic bouton of endophilin triple KO mouse showing several CCVs. D) Synaptojanin 1 KO synapse with multiple CCVs. E) Dynamin 1 KO synapse harbouring clathrin coated, partially elongated clathrin coated profiles. Scale bars = 200 nm.

Amphiphysin further interacts with clathrin and AP-2, PLD and cdk5 (Wu et al., 2009). Genetic ablation of amphiphysin 1 leads to concomitant reduction of amphiphysin 2, to reduced vesicle pools and enhanced depression of neurotransmission at high synaptic activity (Di Paolo et al., 2002). Injection of inhibitory peptides binding to amphiphysin SH3 domain resulted in clathrin coated intermediates stalled at the synaptic membrane. In paraneoplastic SPS, associated AB targeting amphiphysin SH3 domain (David et al., 1994) were shown reduce GABAergic neurotransmission leading to motor hyperexcitability and enhanced anxiety in experimental rats (Geis et al., 2010, Geis et al., 2012). Figure 4 summarizes different ultrastructural changes that result from inhibition of amphiphysin itself or depletion of its binding partners.

1.5. Scientific research question: anti-amphiphysin AB

In a previous report from our research group we could provide evidence that intrathecally applied SPS patient AB specifically targeting amphiphysin induce functional relevant defects in endocytosis in experimental rats. These deficits became evident in spinal GABAergic circuits resulting in reduced GABAergic presynaptic inhibition in the spinal cord as measured by smaller dorsal root potential amplitudes and reduced attenuation of the Hofmann reflex. Furthermore, using stimulated emission depletion (STED) microscopy an accumulation of adaptor proteins essential for CME was found in presynaptic terminals, corroborating the hypothesis of an AB-induced endocytosis defect in CNS neurons (Geis et al., 2010).

Based on these findings, we hypothesized AB-induced structural changes of vesicle pools in spinal presynaptic boutons as described in experiments using peptides to amphiphysin SH3 domain to block CME (Shupliakov et al., 1997). Vesicle pools may have different molecular composition of vesicular proteins due to engagement of compensatory endocytosis mechanisms (Voglmaier and Edwards, 2007). As amphiphysin has several interaction partners, AB to amphiphysin might disturb the docking of binding partners leading to differences in their synaptic distribution. Another assumption is that endophilin could fulfil compensatory endocytosis while amphiphysin is blocked by AB (Llobet et al., 2011). In a similar way, the uncoating factor synaptojanin could also be involved in pathologic processes as structural deficits of disturbed CME frequently show vesicles still equipped with their stabilizing clathrin coat (Milosevic et al., 2011). To test these hypotheses, ultrastructural investigations of spinal GABAergic presynapses were performed in the intrathecal passive-transfer rat model after repetitive application of purified patient anti-amphiphysin AB. Further, potentially AB-induced changes in synaptic architecture were investigated using super-resolution microscopic techniques in primary hippocampal neurons.

1.6. Glutamate decarboxylase 65 (GAD65)

Two different GAD isoforms catalyze synthesis of GABA (Battaglioli et al., 2003), the major inhibitory transmitter in the mammalian CNS. The larger isoform glutamate decarboxylase 67 (GAD67) is a cytosolic enzyme showing ubiquitous expression in the cell body and is predominantly saturated with its cofactor pyridoxal 5' phosphate (PLP) (Erlander and Tobin, 1991). GAD67 synthesizes the majority of GABA explaining why KO animals are not viable (Asada et al., 1997). The smaller isoform GAD65 is localized to inhibitory presynaptic boutons, is reversibly attached to synaptic vesicle membranes (Jin et al., 2003), and is involved in supplementary synthesis of GABA needed for synaptic transmission while KO animals show no significant reductions in GABA availability (Asada et al., 1996). GAD65 is localized

to presynaptic boutons as apoenzyme and becomes activated for additional GABA synthesis at high synaptic activation (Martin et al., 1991). Mice with genetic ablation of GAD65 are prone to seizures (Christgau et al., 1991, Christgau et al., 1992, Kash et al., 1997) and show deficits in fear consolidation and generalization (Seidenbecher et al., 2003, Bergado-Acosta et al., 2014). Deficiency of GAD65 leads to reduced GABA release at sustained synaptic transmission (Tian et al., 1999). Several diseases are characterized by AB targeting GAD65: cerebellar ataxia (Vianello et al., 2003), type 1 diabetes (Solimena, 1998) limbic encephalitis (Mata et al., 2010), and non-paraneoplastic SPS (Solimena et al., 1988, Solimena et al., 1990, Rakocevic et al., 2004). Animal models investigating IgG antibodies purified from patients with anti-GAD65 AB positive SPS reported motor dysfunction and increased fear related behavior *in-vivo* in experimental rats after intrathecal delivery or surface application of AB preparations. *In-vitro*, patient IgG was shown to reduce GABA synthesis (Manto et al., 2007, Geis et al., 2011, Hansen et al., 2013). Immunization of mice with recombinant GAD65 evoked production of AB that bind near GAD65 but interestingly also showed surface staining (Chang et al., 2013). Detailed investigations of SPS-associated anti-GAD65 AB on GABAergic transmission at the single cell level have not been investigated so far.

1.7. Scientific research question: anti-GAD65 AB

In *in-vivo* animal passive-transfer experiments using purified IgG of SPS patients with high titer of anti-GAD65 AB, IgG application led to motor symptoms, increased anxiety, cognitive dysfunction, and increased excitatory transmission (Geis et al., 2011, Hampe et al., 2013, Hansen et al., 2013, Vega-Flores et al., 2014). These findings along with patient symptoms and clinical relief to plasma exchange and immunotherapy suggests disturbed inhibitory tone in CNS networks. These observations led to the hypothesis of AB-induced reduction of presynaptic GABA synthesis. Reduced availability of presynaptic GABA would theoretically result in decreased evoked inhibitory postsynaptic currents (eIPSCs), especially at high frequency transmission as observed in GAD65 KO animals (Tian et al., 1999). AB binding might also cause changes in gene expression of GAD isoforms to compensate for the putative reduced GABA synthesis. These hypotheses have been addressed in the present work by investigating the influence of anti-GAD65 directed patient IgG-AB on GABAergic transmission in vital brain slices and in primary neurons using patch-clamp neurophysiology, confocal imaging of presynaptic boutons, and GAD65/67 gene expression analysis after IgG preincubation.

2. Material and methods

2.1. Animal experiments

All animal experiments were approved by the Bavarian and Thuringian state authorities and executed according to ARRIVE guidelines and good laboratory practice (Kilkenny et al., 2012). Animals were kept in standard cages with water and food ad libitum at a 12h light/dark cycle. C57BL/6 mice sacrificed for patch-clamp experiments and primary cell culture preparations were obtained from internal breedings of the animal facilities at the Department of Neurology of the University Hospital Würzburg or the Hans-Berger Department of Neurology, Jena University Hospital. Female Lewis rats were purchased from Harlan-Winkelmann (Borchen, Germany).

2.2. Patient IgG and AB purification

All biochemistry and molecular biology experiments including preparation of patient IgG fractions were mainly performed by Susanne Hellmig and PD Dr. Andreas Weishaupt (Department of Neurology, University hospital, Würzburg).

Anti-amphiphysin AB

The clinical details of the SPS patient who had a paraneoplastic SPS with very high titers of anti-amphiphysin AB have been reported (Wessig et al., 2003). Commercial enzyme immuno-dot assay was used to determine titers of anti-amphiphysin AB by measuring means of with rabbit antisera raised against recombinant amphiphysin 1 as a positive control (H.P. Seelig, Karlsruhe, Germany). Titres before the first plasma exchange were $1-2 \cdot 10^8$.

Anti-GAD65 AB

SPS IgG #1 and SPS IgG #2 containing high-titer anti-GAD65 AB and control IgG from a patient with chronic inflammatory polyneuropathy as well as a control IgG from a patient with a tumor in the orbita (initially diagnosed as therapy-resistant optic neuritis), both without detectable serum AB were purified from therapeutic plasma exchange material as described previously (Sommer et al., 2005). The IgG fractions were dialyzed, freeze dried and stored at -20°C . Lyophilized IgG was dissolved in normal saline before use.

Affinity purification of specific AB using recombinant proteins

The recombinant human glutathione S-transferase-amphiphysin and glutathione S-transferase-SH3 domain fusion protein, the gene encoding for amphiphysin protein and the construct containing its wild-type SH3 domain (Grabs et al., 1997) were expressed and purified as described before (Geis et al., 2010). Recombinant human GAD65 was kindly provided by Diarect (Freiburg, Germany). Purification of human immunoglobulin from patient plasma filtrates was performed as described (Buchwald et al., 1998b, Sommer et al., 2005). Anti-amphiphysin and anti-GAD65 AB were depleted by affinity chromatography according to established protocols (Geis et al., 2010). Successful depletion of anti-GAD65 AB was confirmed by western blotting of recombinant human GAD65 followed by anti-human IgG detection (Werner et al., 2014). Eluates containing specific AB and fractions depleted from specific AB were dialyzed separately against distilled water, freeze dried and stored at -20°C. Lyophilized IgG was reconstituted in normal saline just before use.

2.3. Primary hippocampal cell culture

Reagents were obtained from Life Technologies (Darmstadt, Germany) it not stated otherwise. E18 embryos of pregnant C57BL/6mice were used for cell culture preparations. After dissection of embryonal hippocampi, meninges and surrounding tissue were removed followed by enzymatic digestion with 0.25% w/v trypsin EDTA for 5 minutes at 37°C. Trypsin was inactivated by two generous flushes of Hank's Balanced Salt Solution (HBSS) supplemented with Penicillin Streptomycin (PS; 1% final concentration) and 10mM HEPES®. Cells were mechanically separated by trituration in Neurobasal® medium supplemented with glutamine (1%), B27® (2%) and PS (1%) using a narrowed glass pipette. Concentration of cells in suspension was assessed with a haematocytometer (Hartenstein, Würzburg, Germany).

For dSTORM experiments cells were plated at a density of 50.000 cells on poly-D-lysine (PDL) coated 18mm diameter coverslips. 12mm diameter coverslips were used for confocal microscopic investigations (Langenbrinck, Emmendingen, Germany). Primary neurons were used for experiments at day 14 in vitro (DIV 14).

Microisland cultures were prepared according to established protocols (Allen, 2006). Briefly, 12mm diameter coverslips were covered with 0.15% type IIA agarose (Sigma Aldrich, Taufkirchen, Germany) as growth limiting agent. At the following day small islands of PDL containing rat tail collagen (0.25 mg/ml collagen + 0.05 mg/ml PDL in distilled H₂O, Sigma Aldrich, Taufkirchen, Germany) were applied on agarose coated coverslips using a glass atomizer (Carl Roth, Karlsruhe, Germany). Cells were prepared as described for standard

Material and methods

primary hippocampal cell culture above and a total of 10.000 cells were applied on 12mm diameter coverslips. Cells were cultured in standard Neurobasal medium[®] containing 10% fetal bovine serum (FBS) for 24h. After 24h medium was replaced with standard Neurobasal medium[®] lacking additional FBS. Microislands were used for experiments at DIV 10.

For gene expression experiments $1 \cdot 10^6$ primary hippocampal cells were seeded in PDL coated cell culture flasks (#690160, Greiner Bio One, Frickenhausen, Germany) and used for gene expression experiments at DIV 10.

2.4. *In-vivo* rat model of SPS

Catherization and intrathecal AB application

Placement of intrathecal catheters and AB injections were performed by Prof. Dr. Christian Geis. PE10 plastic catheters (Schubert Medizinprodukte, Wackersdorf, Germany) with an inner diameter of 0.28 mm, an outer diameter of 0.61 mm and an internal length of 7,0 mm were placed in subarachnoid space of experimental Lewis rats in a similar way as described in the original report (Yaksh and Rudy, 1976). In deep anesthesia with Isoflurane[®] (Abott GmbH, Wiesbaden, Germany) the catheters were inserted through the occipital membrane and the internal tip of the catheter ended just above the lumbar enlargement of the spinal cord. In case of paralysis experimental animals were euthanized immediately after the surgery. Following a recovery period of at least 7 days the first IgG application was performed (concentration = 10mg/ml, injected volume = 10 μ l) followed by a rinse with 10 μ l 0.9% saline. The first five injections were applied daily, the following 5 injections every second day and the final two injections three days apart. This experimental procedure has been evaluated to induce typical disease signs and underlying neurophysiological changes with reduced GABAergic presynaptic inhibition in rats in previous studies (Geis et al., 2010).

Stimulation of Ia afferents

After completing the IgG application series, animals were deeply anaesthetized with intraperitoneally injected Narcoren[®] (Merial GmbH, Hallbergmoos, Germany, diluted 1:10 with 0.1% saline [Braun, Melsungen, Germany]). Ia afferents were stimulated by supramaximal excitation of the right tibial nerve (8-9V, 10 Hz) using a Grass S88 stimulator (Grass Technologies, West Warwick, Rhode Island, USA). Stimulation was performed continuously for 60 s ensuring a sustained period of high synaptic activity. The stimuli were applied unilaterally, the contralateral side represented conditions of basal activity. At the end of stimulation (during the last seconds of stimulation to exclude fixation of tissue in the compensatory period

Material and methods

after stimulation), spinal cord of experimental animals was fixed with 2.5% glutaraldehyde, 1% paraformaldehyde in PBS by transcardial perfusion using a slow peristaltic pump (Ismatec, Wertheim-Mondfeld, Deutschland) followed by a rinse with 0.1M PBS. After fixation, lumbar spinal cord (L4-L5) and tibial nerve were removed, washed with 0.1M PBS and kept in 30% sucrose solution at 4°C overnight.

2.5. Electron microscopy of rat spinal terminals

Tissue processing for electron microscopy (EM)

All reagents were obtained from Sigma Aldrich (Taufkirchen, Germany) if not stated otherwise. The extracted spinal cord was cut in hemisegments using a sharp razorblade (Wilkinson Sword, Solingen, Germany). From each resulting hemisegment 45 µm slices were cut in 0.1M PBS using a Leica VT1000S tissue chopper (Leica, Ratingen, Germany) in 0.1M PBS. Slices were fixed in osmium tetroxide (1% in 0.1M PBS), followed by several washing steps in 0.1M PBS. Uranylacetate (2% in 70% ethanol) was used for contrast enhancement, dehydration included a rising ethanol concentration series with a final rinse in propylenoxide (100%). Slices were embedded en bloc in epoxy resin on aclar foil (Serva, Heidelberg, Germany). Tissue blocks were cut to ultrathin slices (70 nm) on an ultratome (Ultracut E, Leica, Wetzlar). Sections were mounted on formvar coated mesh grids (Plano, Wetzlar, Germany).

Postembedding immuno EM

Sections were washed in Tris buffered saline containing 0.1% Triton-X 100, adjusted to pH 7.6 (TBST 7.6) and immunoreacted overnight with a primary antibody to GABA (1:1500, rabbit polyclonal, Millipore). Slices were etched in periodate (2% in distilled H₂O) and sodium-metaperiodate (10% in distilled H₂O, at 50°C) for 30 seconds each following a rinse in TBST 7.6 and TBST 8.2. Gold-conjugated secondary antibodies (1:80, Aurion-Biotrend) were applied in TBST 8.2 for 2h at RT. Gold particles were enhanced with silver particles using R-GENT SE-EM according to manufacturer protocols (Aurion, Wageningen, Netherlands) and slices were contrast enhanced with uranyl acetate (2% in 70% ethanol) and Reynolds' lead citrate (Reynolds, 1963).

EM recordings and image analysis

EM photographs were captured on a LEO 912 AB electron microscope or Leo 906 E electron microscope (Zeiss SMT, Oberkochen, Germany). Images were documented via a slow scan CCD camera (Zeiss SMT, Oberkochen, Germany) or a ProScan Slow Scan CCD (ProScan,

Material and methods

Lagerlefeld, Germany), respectively. Image acquisition and storage was performed with corresponding iTEM software (Soft Imaging System, Irvine, USA).

For analysis, a square grid of roughly $100\mu\text{m}^2$ was chosen randomly next to a ventral horn motoneuron. This square was screened for synaptic boutons. Silver particles or presynaptic structures (vesicles, clathrin coated vesicles (CCV), endosome-like structures (ELS) were counted manually using MacBiophotonics ImageJ (Wayne Rasband, www.macbiophotonics.ca). CCV were characterized by a clathrin triskelia surrounding conventional synaptic vesicles and ELS structures were identified as oval shaped, enlarged organelles in comparison to synaptic vesicles. Density of GABA (enhanced silver particles) and vesicle subforms were calculated by dividing the counts by the area of bouton minus the mitochondrial area. GABA rich and GABA poor terminals were defined by taking the median of all calculated GABA densities and splitting the terminals apart at this value. Calculations were performed in Excel and statistics were done in Sigmaplot 12.

2.6. dSTORM microscopy experiments

AB treatment and stimulation

Primary neurons were incubated with affinity purified specific AB targeting the SH3 domain of amphiphysin (specAmph) and IgG of a control patient that are described previously (Geis et al., 2010) for 6h at 37°C ($100\mu\text{g}/\text{ml}$). The experimenter was blinded to treatment conditions.

Stimulation of primary hippocampal neurons

Neurons were stimulated with a customized stimulation chamber RC-49FS (Warner Instruments, Hamden, UK). Electrical fields of $\sim 10\text{V}/\text{cm}$ at a frequency of 10Hz for 90s (pulse duration = 1ms) were applied across platinum electrodes with a spacing of approximately 10mm using a Grass stimulator S88. Stimulation of neurons was performed in artificial cerebrospinal fluid (ACSF) containing 119mM NaCl, 2.5mM KCl, 2mM CaCl_2 , 2mM MgCl_2 , 25mM HEPES and 30mM glucose. Control coverslips were placed in ACSF for 90s until fixation without stimulation.

Immunocytochemistry for dSTORM microscopy

Immediately after stimulation cells were fixed with ice-cold 4% paraformaldehyde (PFA) for 20min and permeabilized with 0.1% Triton-X (Sigma Aldrich, Taufkirchen, Germany) for 30min at room temperature (RT).

Primary antibodies	concentration	manufacturer	order ID	species
synaptobrevin 2	1 : 2000	Synaptic systems	104211	mouse monoclonal
synaptobrevin 7	1 : 2000	Synaptic systems	232011	mouse monoclonal
endophilin	1 : 1000	Synaptic systems	159002	rabbit polyclonal
synaptojanin	1 : 500	Synaptic systems	145003	rabbit polyclonal
VGAT	1 : 1000	Synaptic systems	131004	guinea pig polyclonal
synaptophysin	1 : 1000	Chemicon	AB9272	rabbit polyclonal
PGP 9.5.	1 : 500	Paesel & Lorei	5304793	rabbit polyclonal
Secondary antibodies	---	---	---	---
Alexa 647	1 : 500	Life technologies	A21237	goat anti-mouse
Alexa 647	1 : 500	Life technologies	A21246	goat anti-rabbit
Alexa 488	1 : 500	Life technologies	A21206	goat anti-guinea pig
Cy3	1 : 500	Dianova	106-165-003	goat anti-guinea pig
Cy3	1 : 500	Jackson immunoresearch	111-165-003	goat anti-rabbit
Rhodamin	1 : 500	Jackson immunoresearch	706-296-148	goat anti-guinea pig

Table 1 Antibody list for fluorescence microscopy

Primary antibodies (see Table 1) were incubated for 1h at RT in PBS containing 10% normal bovine (BSA) and 10% normal goat serum (NGS). Coverslips were then washed six times for 10 minutes and subsequently incubated with respective secondary antibodies (see Table 1) in blocking solution (10% BSA, 10% NGS) overnight at 4°C. Incubation was again followed by washing steps as described above. Samples were kept in PBS until recording started.

dSTORM microscopy

Coverslips were fixed in a custom built imaging chamber and placed on a vibration isolated, customized Olympus IX71 inverted microscope. Samples were imaged in 1ml 100mM mercaptoethylamine (MEA) in PBS with pH adjusted to 7.9 using a 60x Tif objective (numerical aperture = 1.49). Fluorophores were excited with an Ibeam Smart 640s (Toptica Photonics, Gräfelfing, Germany) at 640 nm and a Nano laser (Quioptiq photonics, Göttingen, Germany) at 532 nm using respective filter sets while keeping laser powers (75mW at 640 nm; 1mW at 532 nm) constant during the experiment. Tif illumination was only slightly used yielding a better z axis resolution. Photons were collected using two EMCCD (Andor Ixon Ultra, BFI

Material and methods

Optilas, Gröbblingen, Germany) cameras keeping detector gain and frame rate constant throughout the experiment.

Analysis of dSTORM recordings

Recorded tiff-format videos (15.000 frames) were processed in rapidstorm software (Wolter et al., 2012) to obtain density matrices with z-dimensions representing localization counts. The following processing parameters were applied in rapidstorm: minimum localization strength = 1000, pixel size = 127 nm, PSF FWHM = 320. A custom written python script (kindly provided by Thorge Holm) was used to rearrange matrices to text image format. Text images were fed into ImageJ (Wayne Rasband, www.macbiophotonics.ca) for further calculations. For calculation of sum of localization counts a region of interest (ROI) was created in ImageJ by applying a (constant) threshold on the epifluorescent signal of vesicular GABA transporter (VGAT). A binary mask was created and converted to ROIs for quantification of integrated density in ImageJ. Parallel computations of raw values in Microsoft Excel confirmed reliability of ImageJ output.

Analysis of clusters inside GABAergic boutons was performed by computing the distances between each maximum residing in every singular VGAT ROI. Coordinates of cluster centroids were calculated by ImageJ (using constant parameters for detection, threshold = 2) and distances were calculated by a custom written script in Sigmaplot (Systat, Erkrath, Germany). Thus, shorter distances represent enhanced clustering and longer distances dispersed signal.

2.7. Confocal microscopy for analysis of GABAergic bouton size and IgG binding experiments

AB incubation and staining procedure

Commercial antibodies for immunofluorescence staining are listed in Table 1. Primary hippocampal cells were treated with purified patient IgG at a concentration of 100µg/ml for 6h. The researcher was blinded to treatment conditions. Following incubation, neurons were fixed in ice-cold 4% PFA for 10min followed by permeabilization with 0.1 % Triton-X 100. Blocking solution to saturate unspecific binding sites contained 10% bovine serum albumin (BSA) and was applied for 30 min at RT. Primary antibodies targeting synaptophysin and VGAT (Table 1) were incubated overnight at 4°C in 2% BSA. Alexa 488 goat anti-rabbit and Rhodamin anti guinea-pig were used as secondary antibodies. Antibodies were applied for 2h at RT fol-

Material and methods

lowed by washing in PBS (4 x 15 mins), DAPI® (Life Technologies, Darmstadt, Germany) staining, and embedding in Mowiol (Sigma Aldrich, Taufkirchen, Germany). This protocol was also applied for immunostaining of PGP 9.5 (Table 1) and synaptophysin in microisland cultures. For IgG binding experiments, DIV14 primary neurons fixed with ice-cold 4% PFA and 30µm free floating murine coronal brain sections were incubated with patient IgG (10 µg/ml) over night at 4°C followed by Cy3 goat anti-human secondary antibody (table 1) for 2h at room temperature.

Confocal microscopy and image analysis

Confocal images were captured on a confocal laser scanning microscope (Zeiss LSM 710, Jena, Germany) using a 40x oil objective, keeping lasers power and PMT (photomultiplier tube) voltage constant. Tiff images were acquired sequentially as z-stacks and maximum projections of z-stacks were generated in FIJI image analysis software (Schindelin et al., 2012). Resulting images were converted to 16-bit and background signal subtraction was performed. Areas were calculated after setting constant thresholds for VGAT and synaptophysin signals. The area ratio was defined by the division of synaptophysin area by VGAT area. VGAT signals as defined by thresholds were used as a region of interest for synaptophysin intensity quantification. For visualization of neurons and brain slices used in binding studies, the same confocal microscope was used. Images of slices were captured using a 20x air objective and primary hippocampal cells with a 40x oil objective (Zeiss). Processing of images was performed as described for quantification of vesicle pools but omitting background subtraction and thresholding procedures.

2.8. Whole cell patch-clamp recordings

15-25 day old C57BL/6-mice were sacrificed and acute hippocampal slices (300µm) were prepared from brain hemisegments in ice cold slicing solution (40mM NaCl, 25mM NaHCO₃, 10mM glucose, 150mM sucrose, 4mM KCL, 1.25mM NaH₂PO₄, 0.5mM CaCl₂, 7mM MgCl₂; purged with 95% CO₂/5% O₂) using a Campden vibratome (Campden Instruments, Loughborough, UK). Slices were incubated in slicing solution containing 100µg/ml of the respective IgG-solution at 32°C for at least 30 min. During recordings slices were fixed with a custom made thin platinum ring with nylon strings and superfused with extracellular solution (125mM NaCL, 25mM NaHCO₃, 25mM glucose, 2.5mM KCl, 1.25mM NaH₂PO₄, 2mM MgCl₂ purged with 95% CO₂/5% O₂). GABAergic IPSC were recorded with a HEKA EPC10 patch clamp amplifier (HEKA, Lambrecht, Germany). Recording electrodes were pulled from thick-walled

Material and methods

borosilicate glass (GB200F-10, Science Products, Hofheim, Germany) with an Sutter instruments micropipette puller p97 (Science Products, Hofheim, Germany) and were filled with intracellular recording solution containing 140mM KCl, 10mM Hepes, 10mM EGTA, 2mM Na₂ATP, 2mM MgCl₂ yielding a final resistance of 3-5 MΩ. Positioning of electrodes was performed using piezo driven micromanipulators (Unit Mini 3 Axes, Luigs & Neumann, Ratingen, Germany). Dentate granule cells (GC) were voltage clamped at -70mV in whole cell configuration. Recordings were rejected if resting potential changed during experiments, series resistance was higher than 20 MΩ, or cells had resting potentials more positive than -50mV. Evoked IPSCs were isolated by applying 10μM CNQX and 50μM AP-5 to recording solution to block AMPA and NMDA currents, respectively (Tocris Bioscience, Ellisville, USA). Minimal stimulation of GABAergic axons was performed as described before (Edwards et al., 1990, Allen and Stevens, 1994, Geis et al., 2010). In brief, GABAergic afferents of molecular layer basket cells were stimulated (200μs, 0.3Hz) using an Isoflex stimulation isolation unit (A.M.P.I., Jerusalem, Israel). 1μM Tetrodotoxin (TTX; Sigma Aldrich, Germany) was added for recording of miniature IPSC.

For recording of IPSC in microisland cultures, intracellular and extracellular solutions including blockers were used as described and autaptic neurons were voltage clamped at -70mV. eIPSC were evoked by a 1ms depolarization step to 0mV. Recordings were filtered at 2.9 kHz and 10 kHz. Igor Pro was used for analysis of recordings (Wavemetrics, Lake Oswego, OR, USA).

2.9. Quantitative real time polymerase chain reaction (qRT-PCR)

At DIV 10, in each experiment 1*10⁶ primary hippocampal cells, grown in 25 cm² cell culture flasks (#690160, Greiner Bio One, Frickenhausen, Germany) were incubated with 100μg/ml anti-GAD65 antibody containing SPS-IgG #1 or control IgG #1 (CIDP patient) for 3h at 37°C. Following incubation with IgG, RNA was extracted with RNeasy[®] mini kit (Quiagen, Hilden, Germany). Here, culture medium was removed from preincubated cells and exchanged by RLT[®] lysis buffer supplemented with 20μl β-mercaptoethanol (Roth, Karlsruhe, Germany). After 2 min incubation time cells including lysis buffer were scraped into Eppendorf cups with a cell scraper (Hartenstein, Würzburg, Germany) and further processed according to manufacturer protocol. Purity and concentration was assessed by measuring absorption of RNA solution using a Nanodrop[®] device (Wilmington, USA).

Reagents for reverse transcription and qRT-PCR were obtained from Life Technologies (Darmstadt, Germany) if not stated otherwise. RNA was handled on ice if not other specified.

Material and methods

250ng RNA was used as input for reverse transcription of each sample. After addition of 5µl random hexamer to RNA, mixture was incubated for 3 min at 85°C using a heating block (TS-100, ThermoShaker, Hartenstein) and subsequently stored on ice for further steps. 2µl Oligo-DT und 60.2 µl premix (10µl 10x buffer; 22µl 25mM MgCL₂; 20µl dNTP; 2µl RNASE Inhibitor; 6.2µl Multiscribe) were added to the solution. RNA was reverse transcribed to cDNA using the following program: 10 min at 25°C, 60 min at 48°C and 5 min at 95°C.

qRT-PCR primers for Gad1 (Kit ID: Mm00725661_s1), Gad2 (Kit ID: Mm00484623_m1, GAPDH (Kit ID: Mm99999915_g1) und 18s rRNA (Nr.: 4319413E) were obtained as Taqman[®] gene expression assays at Life technologies (Darmstadt, Germany). Premix (2µl mastermix, 0.25µl primer (250nM), 1.75µl distilled H₂O) and sample were mixed in a 4:5 ratio and 9µl of final reaction solution was applied to each well.

Gad 1 and Gad 2 were recorded as triplets and cDNA of housekeeping genes as well as negative controls as duplets. qRT-PCR was performed using a StepOnePlus[®] qRT-PCR device from Life Technologies (Darmstadt, Germany) repeating the following cycles: 20s at 95°C, 40 repetitions of 1s at 95°C followed by 20s at 60°C. CT values were calculated as described (Livak and Schmittgen, 2001).

2.10. Statistics

Statistical comparisons and plots were made in Microsoft Excel and Systat Sigmaplot 12 (Erkrath, Germany). Samples were compared with non-parametric Mann-Whitney U test and with one-way ANOVA following Tukey post-hoc test for groupwise comparisons. Graphs report mean and standard error of mean if not stated otherwise.

3. Results A: Impact of SPS anti-amphiphysin AB on synaptic structure

3.1. Sustained stimulation increases synaptic vesicle pool size and the amount of clathrin-coated vesicles in naïve GABAergic spinal cord interneurons

The consequences of sustained high frequency Ia afferent stimulation on the presynaptic vesicle pool of naïve spinal cord interneurons were investigated in boutons next to ventral horn motoneurons at the lumbar spinal cord level using EM. Prior to perfusion with fixative, Ia afferents of the rat tibial nerve were unilaterally stimulated at 10 Hz for 60 s. This heterosynaptic activation of local GABAergic neurons (Figure 5 A) allows investigation of presynaptic inhibition in spinal circuits that was shown to be disturbed by specific anti-amphiphysin AB in a previous report (Geis et al., 2010).

We measured vesicle pool size, density of CCVs, and ELS in spinal presynaptic boutons of in the L4-5 levels of spinal cord hemisegments (stimulated vs. unstimulated condition). Presynaptic spinal terminals can use multiple neurotransmitters in parallel (Somogyi, 2002). To focus on primary GABAergic boutons, we defined this type of bouton population by applying a threshold on GABA immunoreactive postembedding signal and analyzed this subgroup of boutons in addition to the total number of all perisomatic boutons regardless of transmitter specificity located adjacent to ventral horn motoneurons (Figure 5 B).

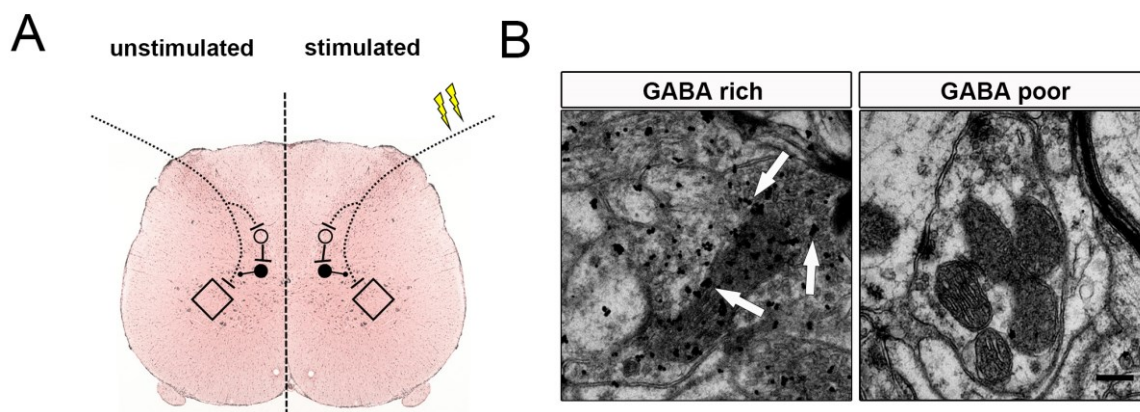


Fig 5 Experimental setup and categorization of synapse types

A) Scheme of experimental setup depicting unilateral stimulation of Ia afferents targeting ventral horn motoneurons (rhombus: motoneuron; white circle: excitatory neuron; block circle: local GABAergic inhibitory neuron). Flashes represent stimulation of peripheral Ia afferent) B) Example micrographs of spinal boutons with high GABA immunoreactivity (arrows, GABA rich) or low reactivity (GABA poor). Scale bar = 250 nm.

Results A: Impact of SPS anti-amphiphysin AB on synaptic structure

In control animals which received non-reactive control patient IgG intrathecally, sustained stimulation increased the size of the presynaptic vesicle pool (Figure 6; unstimulated = $32.5 \pm 0.3 \text{ n}/\mu\text{m}^2$, $n = 51$; stimulated = $47.3 \pm 4.2 \text{ n}/\mu\text{m}^2$, $n = 52$ analyzed boutons).

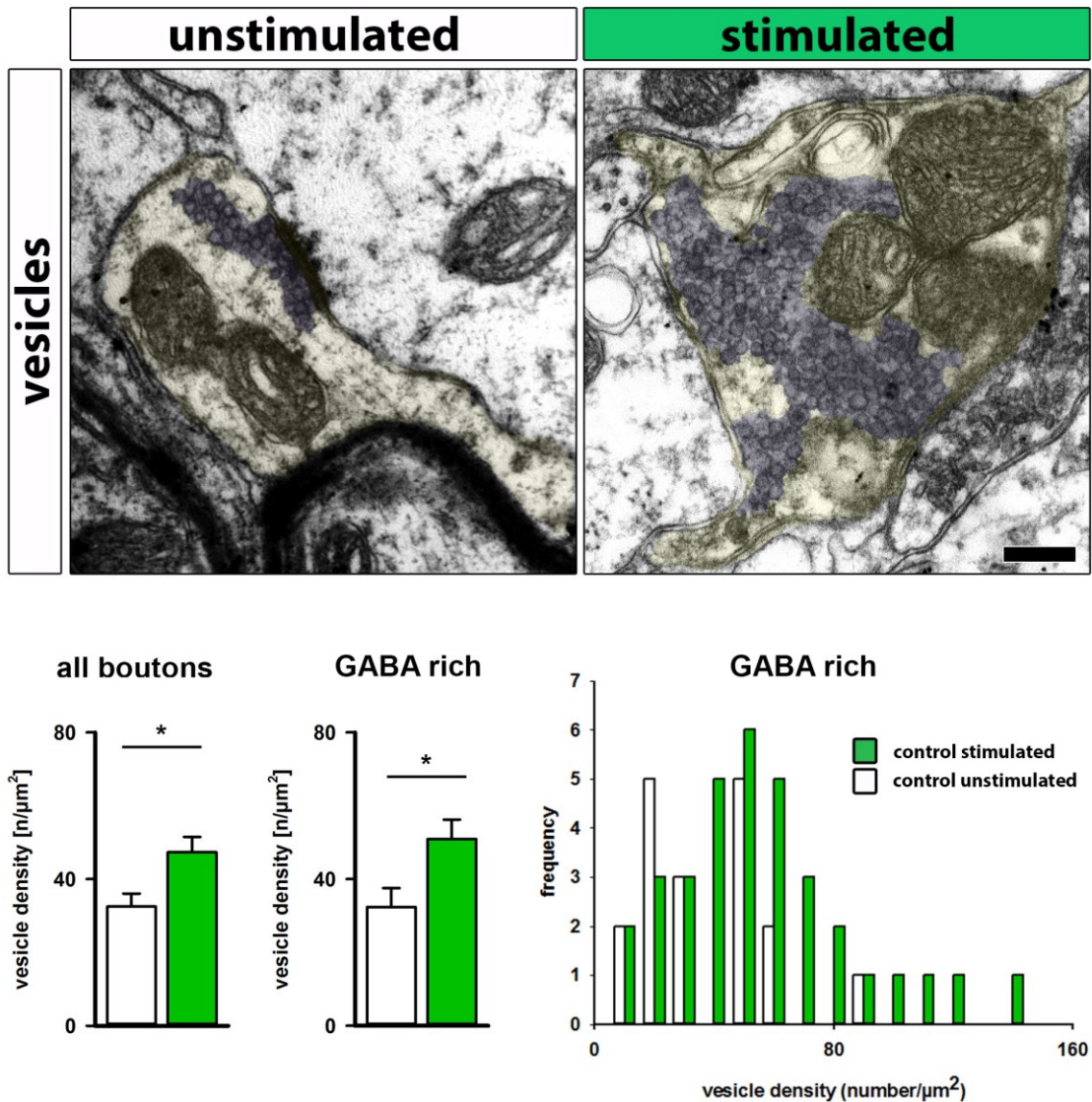


Fig 6 Increased synaptic vesicle density in stimulated spinal boutons (control condition).

EM micrographs show unstimulated and stimulated spinal boutons of controls (scale bar: 250 nm). Boutons are marked with decent yellow. Quantification of vesicle (purple) density of all boutons and in the subgroup of GABA rich presynapses revealed larger synaptic vesicle pool size in stimulated conditions compared to basal neuronal activity. Frequency distribution histogram shows a shift towards a higher number of boutons with high vesicle density (GABA rich boutons; $*p < 0.05$).

At low synaptic activity only few endocytic intermediates (CCV and ELS) were found whereas stimulation evoked accumulation of these intermediates within the synaptic vesicle pools.

Results A: Impact of SPS anti-amphiphysin AB on synaptic structure

(Figure 7, [CCV]: unstimulated = 3.2 ± 0.6 n/ μm^2 , n = 40; stimulated = 6.2 ± 1.3 n/ μm^2 , n = 52; Figure 8, [ELS]: unstimulated = 1.0 ± 0.3 n/ μm^2 , n = 44; stimulated = 2.0 ± 0.5 n/ μm^2 , n = 53).

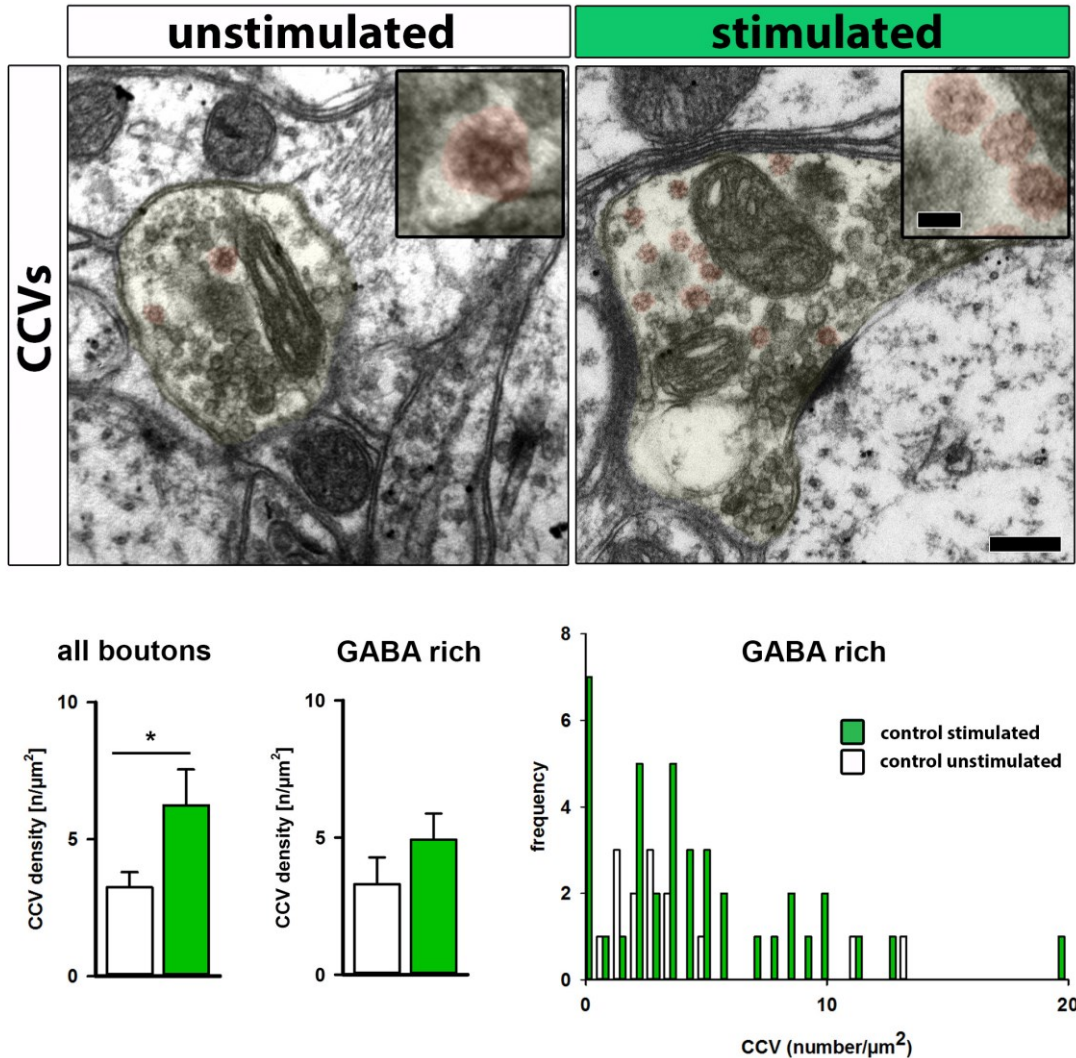


Fig 7 Increased CCV intermediates at high synaptic activity in spinal boutons (control condition).

EM microscopic images of unstimulated and stimulated spinal cord synapses showing CCVs. In stimulated boutons several CCVs were detected (in red) compared to only few in unstimulated pre-synaptic compartments. Insets present detailed structure of CCVs with visible triskelia surrounding the vesicle core structure. Synapses predominantly using GABA as neurotransmitter show a similar trend but no significant changes in CCV density. Frequency distribution histogram represents data distribution of CCV density analysis of GABA-rich terminals. Scale bar: 250 nm, scale bar of insets: 50 nm; * $p < 0.05$.

Collectively, the results obtained from control animals indicate that spinal cord presynapses keep step with long-duration, high-frequency stimulation by generating an activity-induced

Results A: Impact of SPS anti-amphiphysin AB on synaptic structure

bulk of presynaptic vesicles including enlarged endocytic intermediates that are known from studies of ultrafast endocytosis (Kittelmann et al., 2013, Watanabe et al., 2013).

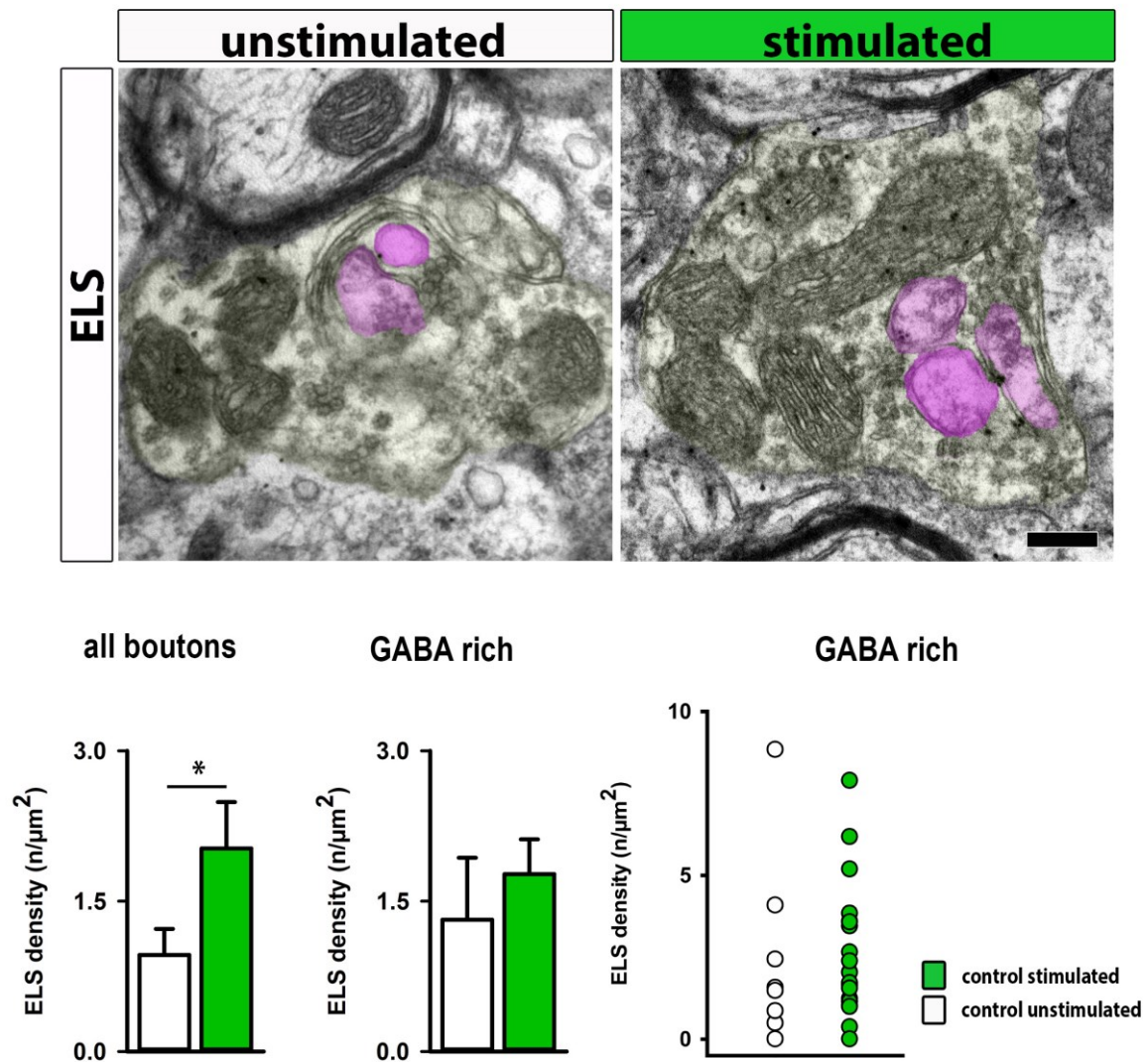


Fig 8 Increased number of ELS upon stimulation in spinal boutons (control condition). EM micrographs of spinal boutons enriched with enlarged organelles defined as ELS. These structures are identified by their increased size relative to synaptic vesicles. Note the increase of ELS at high synaptic activity compared to low synaptic activation. Bar graph depicts a significant difference between the activity patterns. Stimulation induced increase of ELS was not significant for GABA rich boutons. Dot plot shows data distribution of ELS density in individual boutons. Scale bar: 250 nm, * $p < 0.05$.

3.2. Pathogenic human anti-amphiphysin AB interfere with CME leading to stimulus-dependent presynaptic vesicle depletion

Next, the impact of anti-amphiphysin AB on the ultrastructure of spinal terminals was investigated in the same experimental setting using intrathecal application of affinity-purified human AB specific to amphiphysin (specAmph).

Results A: Impact of SPS anti-amphiphysin AB on synaptic structure

Spinal synaptic boutons of rats treated intrathecally with specAmph showed a markedly reduced synaptic vesicle pool size after stimulation (Figure 9, unstimulated = 54.0 ± 3.8 n/ μm^2 , n = 109; stimulated = 29.3 ± 3.3 n/ μm^2 , n = 66). This remarkable decrease at stimulated synapses was also observed when focussing on boutons with high GABA immunoreactivity (Figure 9, unstimulated = 57.8 ± 6.0 n/ μm^2 , n = 47; stimulated = 32.2 ± 5.8 n/ μm^2 , n = 25).

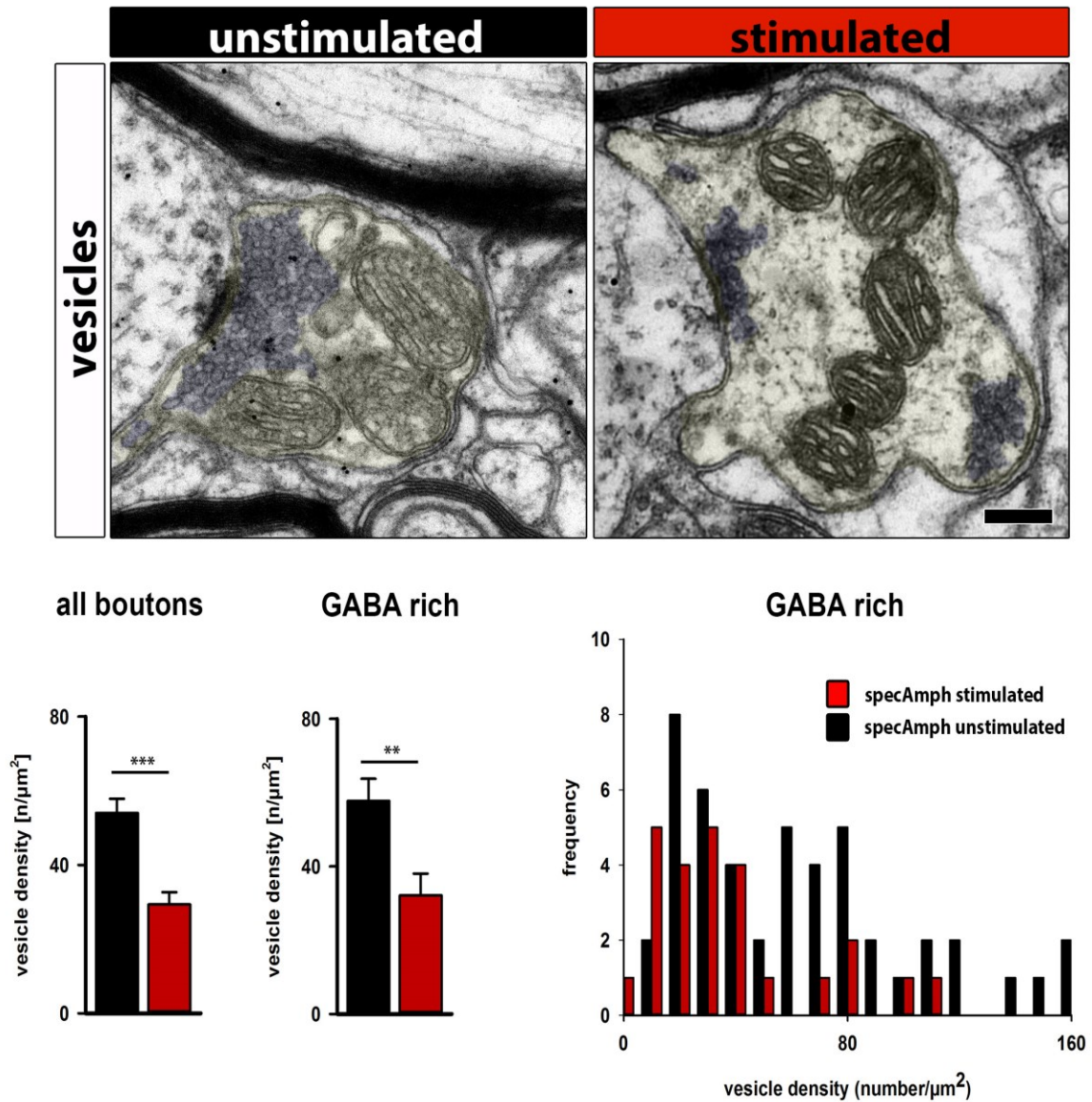


Fig 9 Reduced vesicle density in stimulated boutons after intrathecal passive-transfer with specAmph AB

EM micrographs of unstimulated and stimulated spinal boutons (scale bar: 250 nm). Boutons are marked with yellow and synaptic vesicles in light purple. Quantification of vesicle density in all boutons and in the subgroup of GABA rich presynapses shows a reduced vesicle density at high synaptic activity. Frequency distribution histogram represents data distribution of vesicle density inside GABA rich boutons with a shift towards terminals with reduced vesicle density; ** $p < 0.01$, *** $p < 0.001$.

Results A: Impact of SPS anti-amphiphysin AB on synaptic structure

Frequency distribution histogram in GABA rich boutons revealed a massive left shift with smaller vesicle pools after stimulation compared to low synaptic activity (Figure 9). Moreover, quantification of endocytic intermediates showed an even more remarkable depletion of CCVs in anti-amphiphysin AB treated animals (Figure 10).

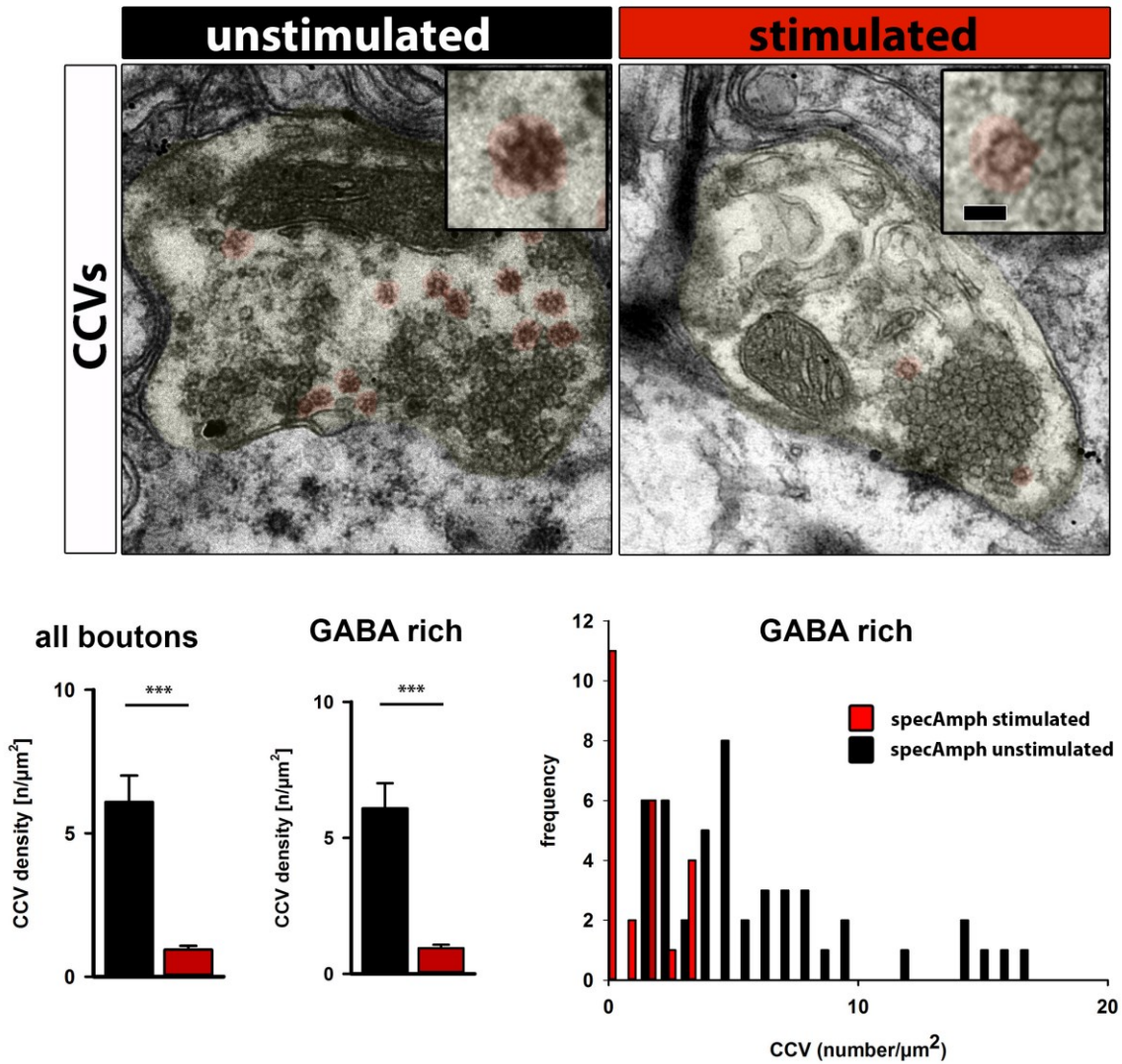


Fig 10 Depletion of CCV during high synaptic activity after intrathecal passive-transfer with specAmph AB

EM micrographs depicting CCVs (marked in red) in unstimulated and stimulated spinal cord presynapses (scale bar: 250 nm). Insets highlight detailed structure of CCVs with visible snowflake-like tri-skellia edging (scale bar: 50 nm). Analysis of CCV density of all stimulated boutons reveals comparatively high number of vesicles equipped with clathrin coat already in resting conditions which were almost completely abolished after stimulation. The same observation was made in synapses with high levels of GABA. Frequency distribution histogram represents CCV density analysis of GABA rich terminals showing a massive shift towards boutons with low number of CCV upon stimulation.

***p<0.001.

Results A: Impact of SPS anti-amphiphysin AB on synaptic structure

Here, frequency distribution histogram clearly depicts an almost complete depletion of boutons with higher density of CCV during stimulation (Figure 10).

Similarly, reduction of ELS in presynaptic boutons after sustained stimulation was evident, although not reaching significance due to the overall low number of ELS (Figure 11; unstimulated = $1.8 \pm 0.2 \text{ n}/\mu\text{m}^2$, $n = 110$; stimulated = $1.0 \pm 0.2 \text{ n}/\mu\text{m}^2$, $n = 64$; $p = 0.061$).

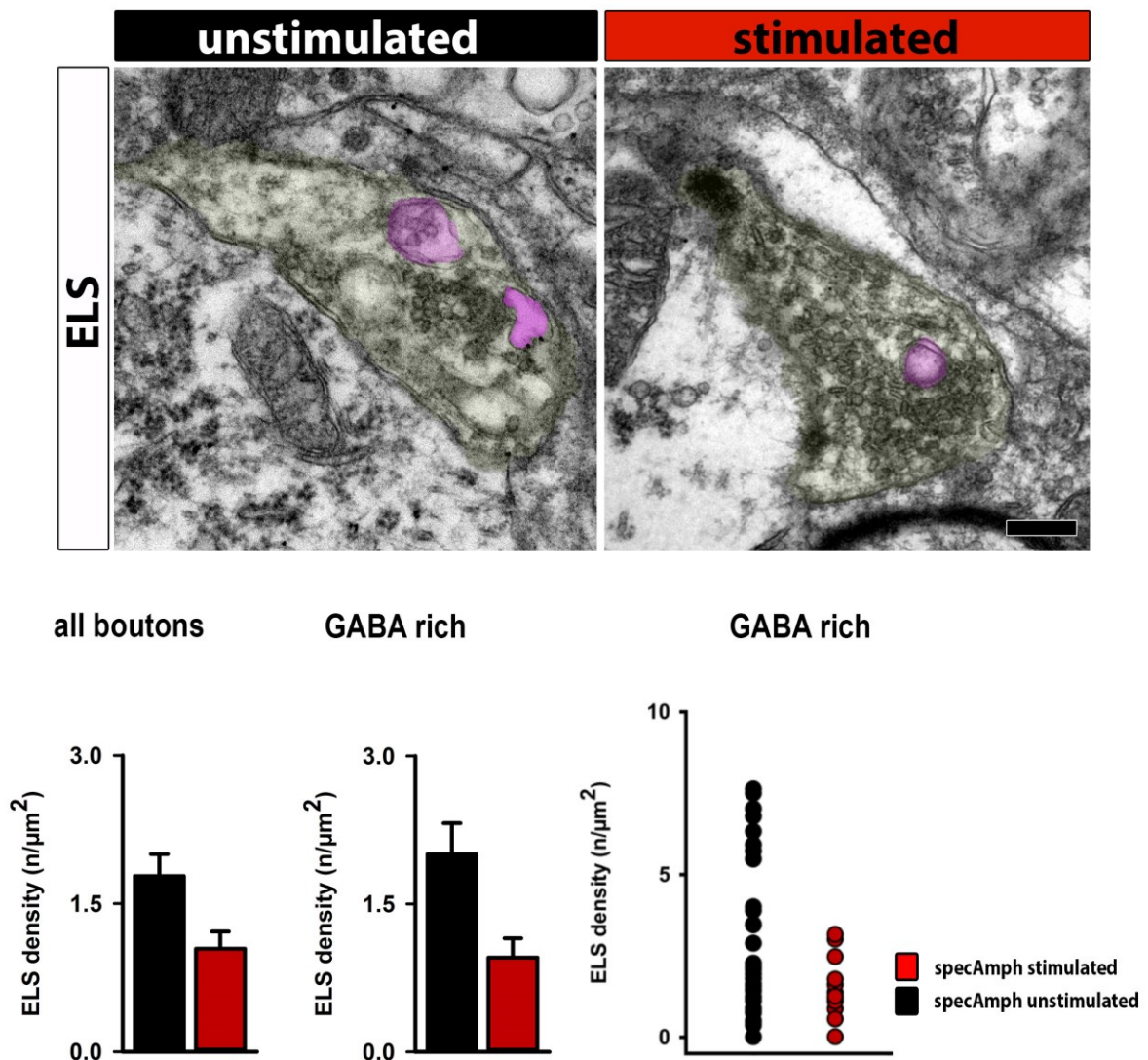


Fig 11 Reduction of ELS in spinal cord boutons after intrathecal passive-transfer with specAmph AB

EM microscopic images of ELS in unstimulated and stimulated spinal cord synapses (scale bar: 250 nm). Analysis of ELS density of all stimulated boutons shows a not significant reduction of ELS at high synaptic activity in presence of anti-amphiphysin AB. Dot plot highlights distribution of boutons according density of ELS with a shift towards terminals with low number of ELS.

Group analysis comparing all experimental conditions further elucidates the opposing effect of anti-amphiphysin AB on endocytic function in spinal presynapses after sustained Ia affer-

Results A: Impact of SPS anti-amphiphysin AB on synaptic structure

ent stimulation. In resting conditions with basal synaptic activity, presynaptic boutons of rats with intrathecal application of anti-amphiphysin AB showed a significant increased density of vesicles, CCV, and ELS in comparison to controls (Table 2). This contrasting vesicle recruitment after anti-amphiphysin IgG administration already in resting conditions was also evident in the subgroup of predominantly GABAergic boutons (Table 2, right column). In controls, sustained stimulation led to a significant increase of vesicle pool formation and number of CCV. In sharp contrast, sustained high frequency stimulation had a reversed effect with massive depletion of vesicles and endocytic intermediates in spinal boutons after chronic intrathecal application of pathogenic AB to amphiphysin.

A vesicle density

	vesicles - all boutons [$n/\mu\text{m}^2$]		vesicles - GABA rich [$n/\mu\text{m}^2$]	
control unstim	32.5 ± 3.6		32.3 ± 5.2	
control stim	47.3 ± 4.2		50.9 ± 5.3	
specAmph unstim	54.0 ± 3.8		57.8 ± 6.0	
specAmph stim	29.3 ± 3.3		32.2 ± 5.8	

B CCV density

	CCVs - all boutons [$n/\mu\text{m}^2$]		CCVs - GABA rich [$n/\mu\text{m}^2$]	
control unstim	3.2 ± 0.6		3.3 ± 1.0	
control stim	6.2 ± 1.3		4.9 ± 1.0	
specAmph unstim	6.1 ± 0.9		6.2 ± 1.2	
specAmph stim	0.9 ± 0.1		0.8 ± 0.2	

C ELS density

	ELS - all boutons [$n/\mu\text{m}^2$]		ELS - GABA rich [$n/\mu\text{m}^2$]	
control unstim	1.0 ± 0.3		1.3 ± 0.6	
control stim	2.0 ± 0.5		1.8 ± 0.3	
specAmph unstim	1.8 ± 0.2		2.0 ± 0.3	
specAmph stim	1.0 ± 0.2		1.0 ± 0.2	

Table 2 Group comparison of vesicle, CCV, and ELS density analysis. * $p < 0.05$, ** $p < 0.01$, *** $p < 0.001$

Collectively, *in-vivo* long-term intrathecal application of AB to amphiphysin induces massive changes in spinal presynaptic vesicle endocytosis with increased compensatory vesicle recruitment including endocytic intermediates already at basal activity levels which is then nearly completely decompensated during sustained stimulation.

3.3. Different v-SNARE composition of GABAergic vesicle pools induced by anti-amphiphysin AB

The massive structural endocytosis deficits in the animal experiments induced by anti-amphiphysin AB revealed profound changes in presynaptic vesicle pools. To gain insight into molecular equipment of vesicle pools, for differentiation which part of vesicle pool is predominantly affected, and to investigate if compensatory endocytic mechanisms take place, we performed *d*STORM *super-resolution* microscopy with specific commercial immunofluorescence antibodies. Here, we chose primary hippocampal cell culture as experimental model system which reduces circuit complexity and offers low background for quantification of fluorescent signals. Cultures of primary neurons were preincubated with purified IgG fractions and stimulated by applying electric fields with similar stimulation parameters as in the *in-vivo* experiments. Molecular composition of synaptic vesicle pools was analyzed by measuring the quantity of the two neuronal v-SNARE isoforms synaptobrevin 2 (syb2) and synaptobrevin 7 (syb7) that were reported to be expressed on different forms of vesicle pools. Syb2 is known to be predominantly localized to ready releasable vesicles and syb7 shows preferential localisation to resting pool vesicles (Hua et al., 2011). As *in-vivo* experiments here and previous studies highlight a major effect of anti-amphiphysin AB on GABAergic transmission, we constrained our analysis to GABAergic synapses by recording the quantity of syb localisation counts in regions of interests (ROIs) defined by the epifluorescent signal of presynaptic VGAT, a reliable marker of GABAergic presynaptic terminals (Figure 12).

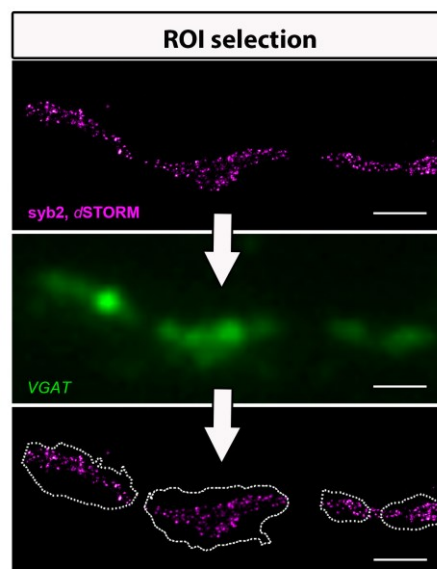


Fig 12 Scheme for analysis of *d*STORM signals

Scheme for quantification of signals using ROIs of epifluorescent VGAT (green) signal, dashed lines highlight calculated ROIs, scale bars: 250 nm.

Results A: Impact of SPS anti-amphiphysin AB on synaptic structure

Syb2 signal density in GABAergic presynapses showed no changes at control conditions comparing low and high synaptic activity. Interestingly, sustained stimulation of GABAergic synapses pretreated with pathogenic anti-amphiphysin AB increased syb2 localization count density inside GABAergic ROIs (Figure 13; controls unstimulated = 2.4 ± 0.3 n/nm², n = 51 analyzed ROIs; controls stimulated = 2.3 ± 0.1 n/nm², n = 100, specAmph unstimulated = 2.6 ± 0.3 n/nm², n = 85; specAmph stimulated = 4.8 ± 1.1 n/nm², n = 70).

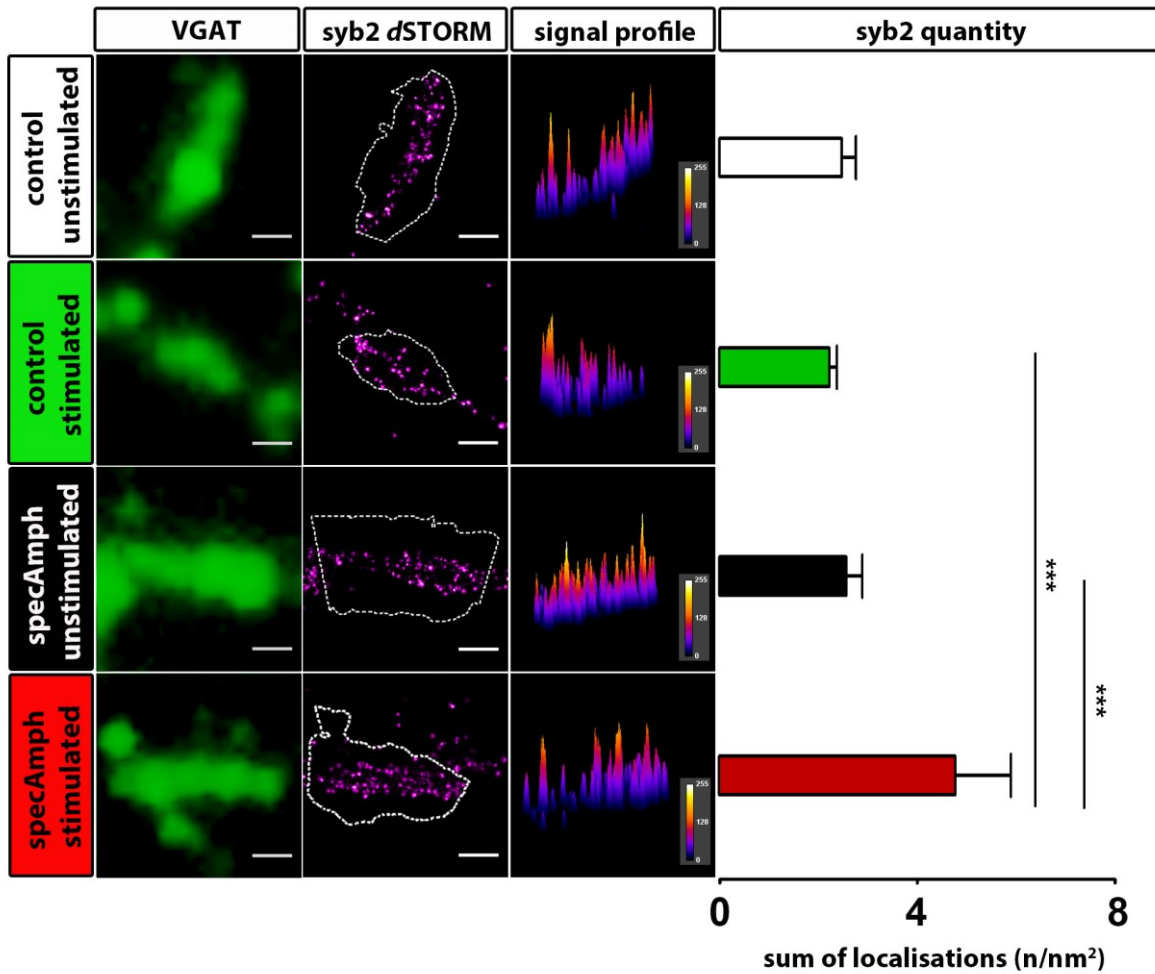


Fig 13 specAmph AB induce increase of syb2 expression inside GABAergic presynapses
 Density of v-SNARE synaptobrevin 2 (syb2, magenta, *d*STORM) over GABAergic boutons marked with vesicular GABA transporter (VGAT, green, epifluorescence) and corresponding signal intensity profiles of representative examples. Quantitative analysis of syb-2 reveals similar localization counts in unstimulated and stimulated control boutons. Stimulated specAmph pretreated boutons show an increased quantity of syb2 compared to unstimulated specAmph pretreated terminals or stimulated control terminals. Scale bars: 500 nm, range of heatmaps: 0-255 bits. ***p < 0.001

This increase of syb2 signal was also highly significant in comparison to stimulated control presynapses. In the next set of experiments we investigated impact of specAmph AB on density of v-SNARE syb7 targeting predominantly resting pool vesicles. Analysis of syb7

Results A: Impact of SPS anti-amphiphysin AB on synaptic structure

densities showed overall low signal inside GABAergic synapses which is in line with reports measuring a higher amount of syb2 copies with respect to other synaptic vesicle proteins (Takamori et al., 2006). Quantification of syb7 signal revealed a gradual increase of syb7 density in GABAergic presynapses of control boutons following stimulation (Figure 14, controls unstimulated = 0.22 ± 0.03 n/nm², n = 79; controls stimulated = 0.38 ± 0.07 n/nm², n = 72). In contrast, after pretreatment with affinity-purified anti-amphiphysin IgG, syb7 quantity was markedly reduced upon stimulation (Figure 14, specAmph unstimulated = 0.16 ± 0.06 n/nm², n = 98; specAmph stimulated = 0.05 ± 0.01 n/nm², n = 78).

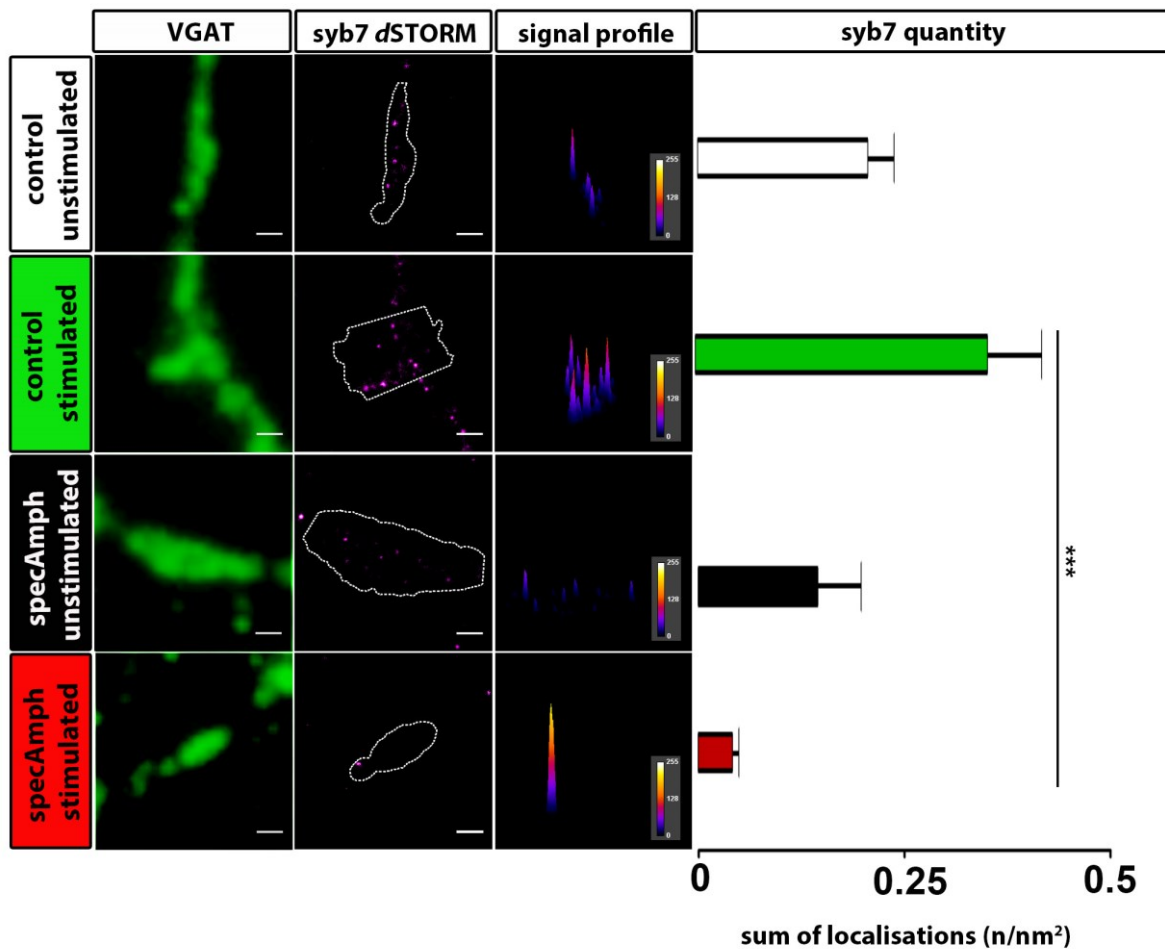


Fig 14 specAmph AB mediate decrease of syb7 upon stimulation

Analysis of signal quantity of vesicular SNARE synaptobrevin 7 (syb7, magenta, dSTORM) using VGAT signal (green) as a mask for GABAergic boutons (scale bar: 500 nm). Analysis reveals a nominal increase of syb7 localization count in controls by stimulation. Contrary, in specAmph pretreated neurons, syb7 quantity is gradually decreased at high synaptic activity. In comparison to stimulated control conditions, analysis reveals a highly significant reduction of syb7 signal in stimulated GABAergic boutons after specAmph application; scale bars: 500 nm, range of heatmaps: 0-255 bits. ***p < 0.001

Results A: Impact of SPS anti-amphiphysin AB on synaptic structure

Together, endocytic dysfunction induced by AB targeting amphiphysin influences synaptic vesicle pool dynamics by changing v-SNARE expression pattern of synaptic vesicles in GABAergic vesicle pools towards a relative increase of presumably ready releasable vesicle equipped with syb2 at the cost of the resting pool.

3.4. Human AB to amphiphysin alter endophilin density and clustering in GABAergic presynaptic vesicle pools

In-vivo experiments clearly demonstrated that repetitive intrathecal administration of anti-amphiphysin IgG results in enhanced density of CCV at basal synaptic activity. This finding suggests that compensatory mechanisms may contribute to the endocytic machinery during the pathological influence of anti-amphiphysin AB. We therefore investigated the direct amphiphysin interaction partners endophilin and synaptojanin. These proteins are not involved in membrane fission and the respective KO mouse models show similar synaptic pathology at resting conditions as observed in our passive-transfer model in presence of AB targeting amphiphysin (Milosevic et al., 2011).

We analyzed the quantity of endophilin signal over GABAergic vesicle pools in primary neurons at different activation patterns. Control GABAergic synapses had a reduction of endophilin signal after sustained stimulation (Figure 15; control unstimulated = 1.02 ± 0.14 n/nm², n = 107; control stimulated = 0.60 ± 0.08 n/nm², n = 106). Against this, after preincubation with pathogenic anti-amphiphysin AB, stimulation evoked nominal but not significant increase of endophilin signal inside GABAergic terminals (Figure 15; specAmph unstimulated = 0.76 ± 0.07 n/nm², n = 154; specAmph stimulated = 1.02 ± 0.25 n/nm², n = 114).

In addition to the absolute number of synaptic proteins, proper localization is essential for endocytic function. We therefore analyzed clustering of endophilin proteins by measuring distance between endophilin signal maxima (Figure 16). After stimulation, the mean distance between maxima was increased when neurons were preincubated with specAmph IgG indicating dispersion of endophilin signal during high synaptic activity. In control condition, stimulation did not change clustering of endophilin (Figure 17; control unstimulated: 2386 ± 343 nm, n = 71, control stimulated: 1770 ± 158 nm, n = 92, specAmph unstimulated: 2261 ± 225 nm, n = 69, specAmph stimulated: 2962 ± 325 nm, n = 78). Accordingly, frequency distribution histograms revealed a higher number of GABAergic synapses with longer distances between endophilin maxima at stimulation after application of specific anti-amphiphysin IgG.

Results A: Impact of SPS anti-amphiphysin AB on synaptic structure

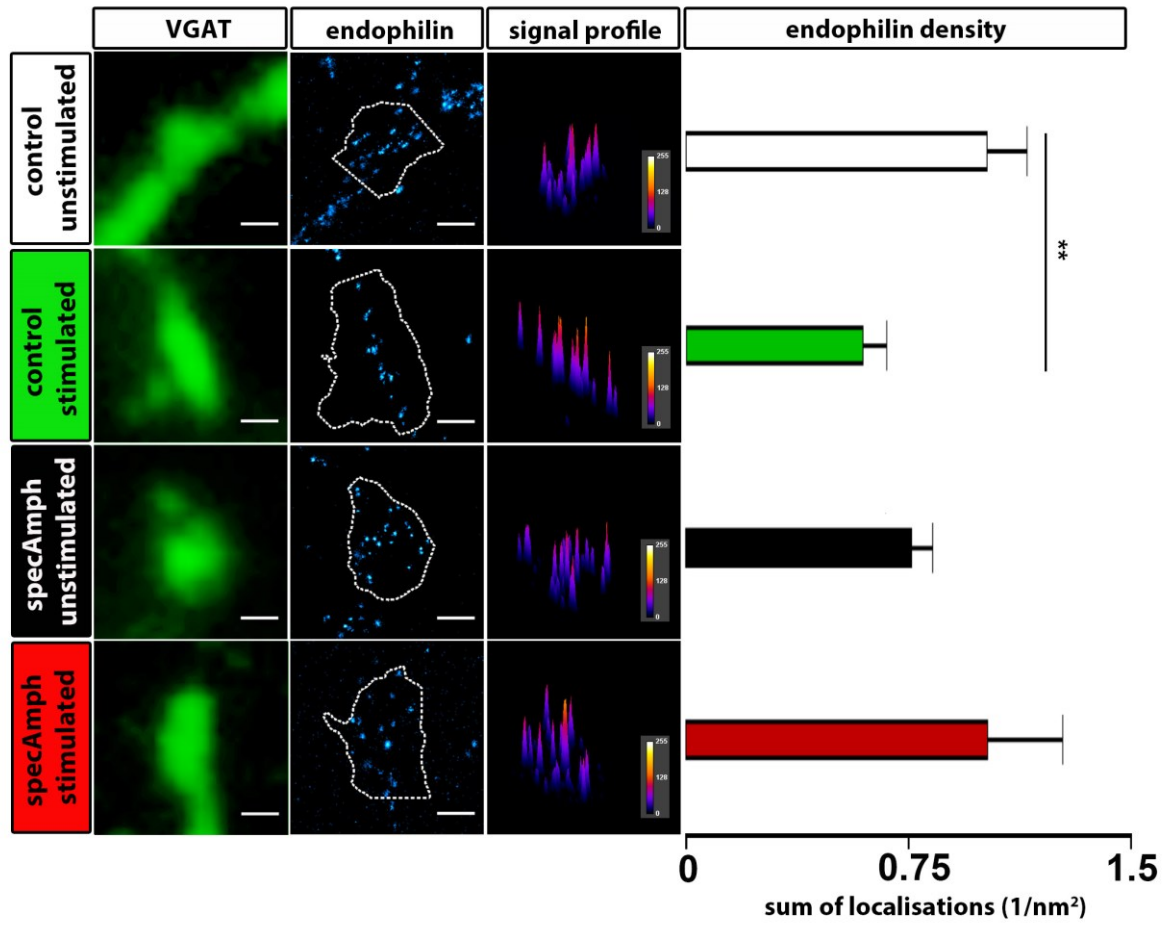


Fig 15 Stimulation induced different endophilin expression pattern in GABAergic boutons dependent on IgG preincubation

Analysis of endophilin (cyan) expression in GABAergic boutons (green). Controls show reduced localization count of endophilin signal over GABAergic vesicle pools upon stimulation. Pretreatment with specAmph leads to a reverse regulation with a slight increase of endophilin quantity after stimulation; scale bars: 500 nm, range of heatmaps: 0-255 bits. ** $p < 0.01$.

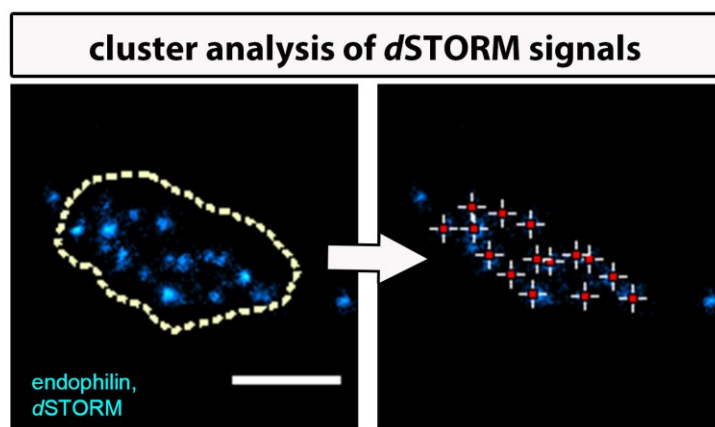


Fig 16 Scheme of cluster analysis of dSTORM signals

Crosshairs depict detected signal maxima, dashed lines show analyzed ROI, scale bar: 250 nm.

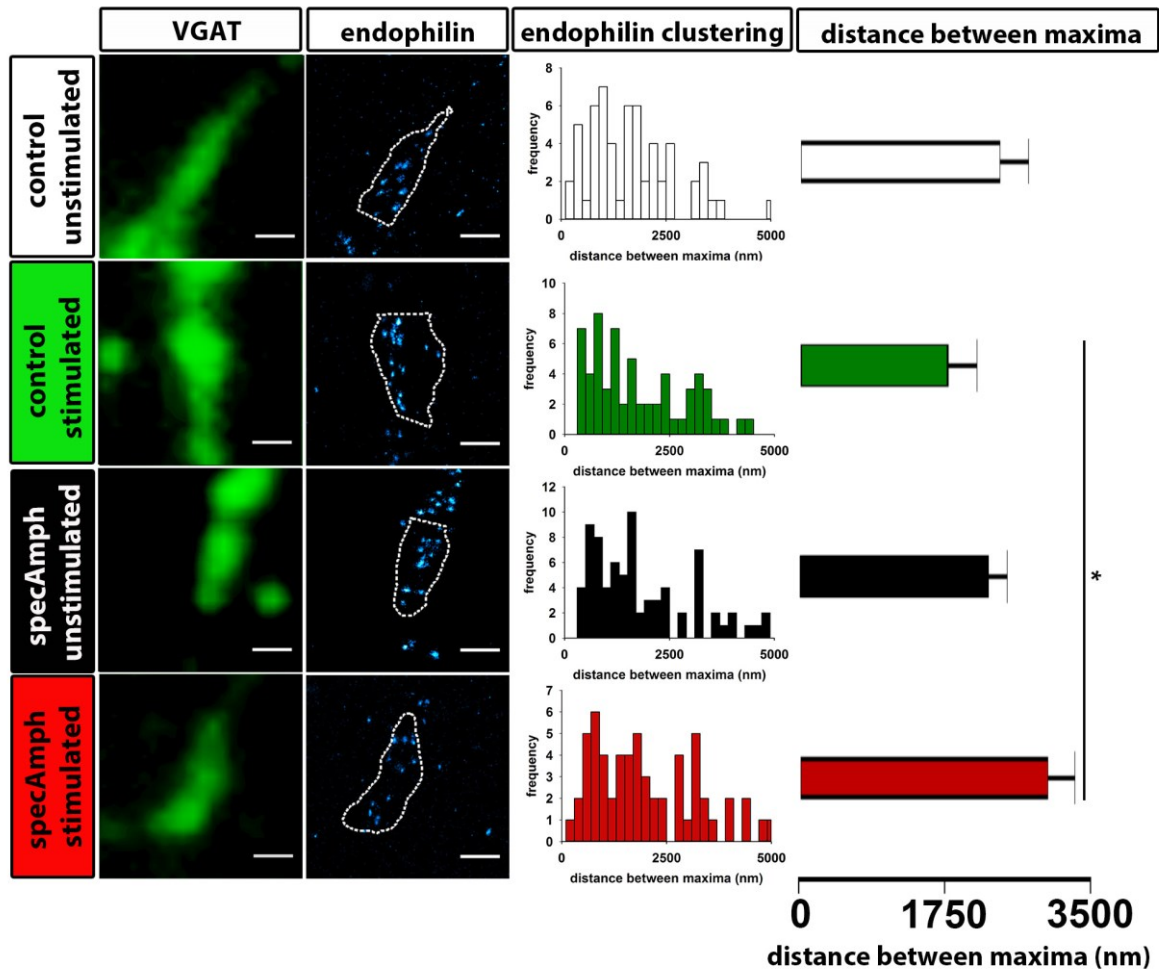


Fig 17 Stimulation evoked dispersion of endophilin signal maxima in presence of specAmph AB

Images show endophilin signal (cyan, *d*STORM) in GABAergic synapses (green, epifluorescence). Frequency distribution histograms show a population of GABAergic synapses with increased distance between endophilin maxima after stimulation and specAmph preincubation. Analysis of point distance between endophilin signal maxima of unstimulated versus stimulated GABAergic boutons reveals nearly equal distances between endophilin clusters comparing unstimulated and stimulated control boutons. Stimulated specAmph boutons show dispersion of endophilin signal compared to stimulated controls; scale bars: 500 nm, range of heatmaps: 0-255 bits; * $p < 0.05$

Different from endophilin, quantity as well as synaptic localization of the phosphatase synap-
tojanin was unchanged between experimental groups (Figure 18, quantity of synap-
tojanin localization counts : controls unstimulated = 0.27 ± 0.04 n/nm², n = 93; controls stimulated =
 0.30 ± 0.04 n/nm², n = 135, specAmph unstimulated = 0.33 ± 0.06 n/nm², n = 141; specAmph
stimulated = 0.38 ± 0.05 n/nm², n = 90; Figure 19, distance between synap-
tojanin maxima: controls unstimulated = 711 ± 74 nm, n = 58; controls stimulated = 827 ± 85 nm, n = 69, spe-
cAmph unstimulated = 704 ± 67 nm, n = 59; specAmph stimulated = 923 ± 92 nm, n = 54).

Results A: Impact of SPS anti-amphiphysin AB on synaptic structure

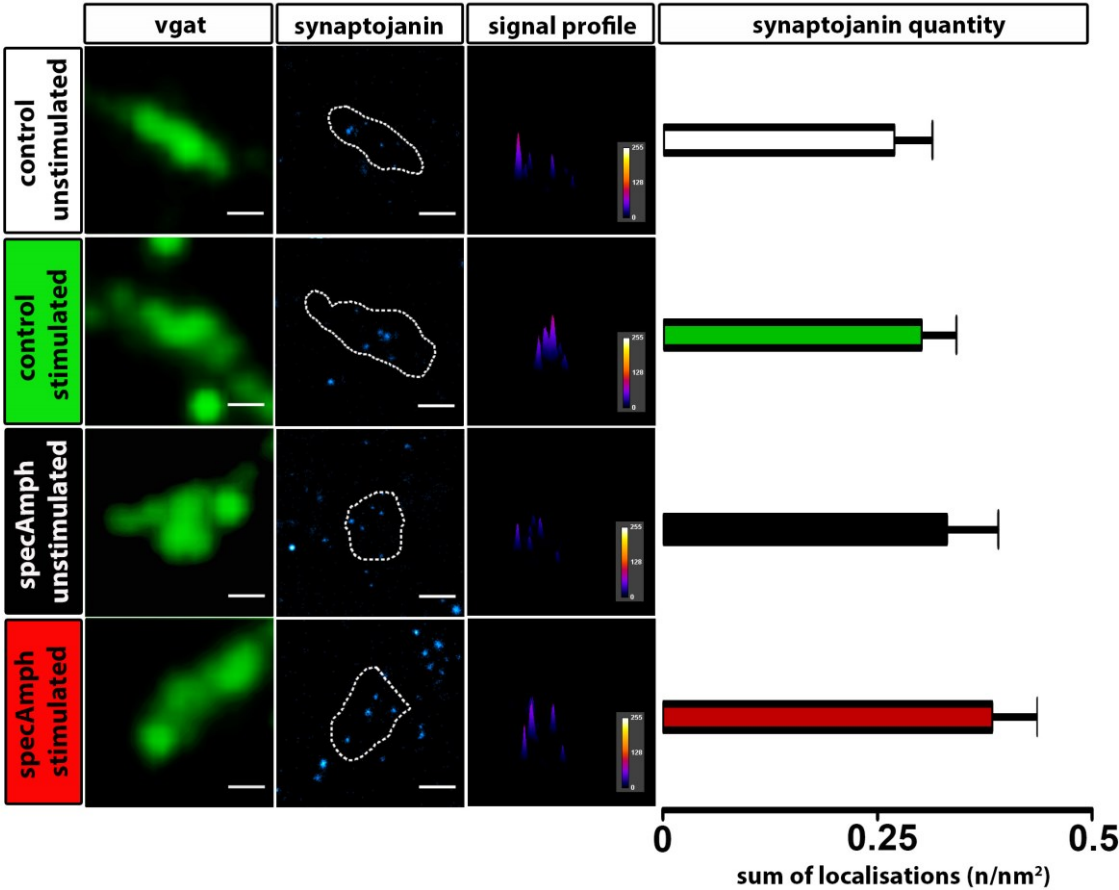


Fig 18 Synaptojanin expression in GABAergic boutons is unaffected by AB targeting amphiphysin
 Quantitative analysis of synaptojanin signal (cyan, dSTORM) in GABAergic synapses (green, epifluorescence) results in similar amount of synaptojanin in GABAergic synapses in all experimental groups; scale bars: 500 nm, range of heatmaps:0-255 bits.

Results A: Impact of SPS anti-amphiphysin AB on synaptic structure

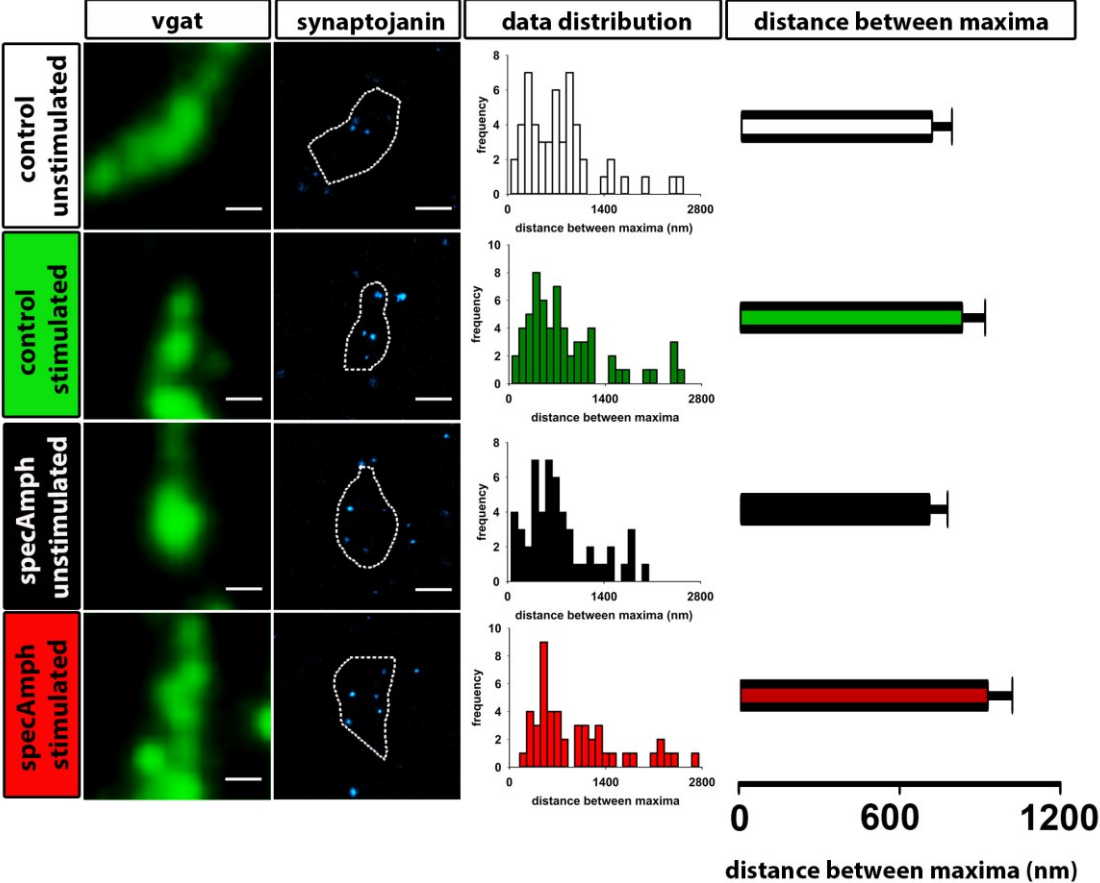


Fig 19 Stable synaptojanin clustering in presence of AB to amphiphysin
 Quantitative analysis and frequency distribution histograms of synaptojanin (cyan, dSTORM) in GA-BAergic synapses (green, epifluorescence) reveal nearly equal distances between synaptojanin clusters comparing all experimental groups without additional peaks of subgroups; scale bars: 500 nm, range of heatmaps: 0-255 bits.

4. Results B: Functional consequences induced by anti-GAD65 containing SPS-IgG²

4.1. Normal basal GABAergic neurotransmission in presence of anti-GAD65 AB containing SPS-IgG

IgG AB from SPS patients containing high titer of anti-GAD65 AB have been shown to cause motor deficits, increased anxiety, cognitive dysfunction, and increased excitatory synaptic potentiation (see introduction for detailed information). These findings and SPS patient symptoms with motor overexcitation and increased anxiety suggesting defective inhibitory tone led to the hypothesis that a defective GABAergic transmission due to AB-induced GAD65 dysfunction might be the underlying pathomechanism.

To evaluate hypothesized AB mediated functional defects of GABAergic transmission whole cell voltage clamp recordings were performed at hippocampal granule cells in brain slices preincubated with anti-GAD65 AB containing IgG or control IgG. Granule cells were excited by stimulation of molecular layer basket cell afferents forming GABAergic synaptic contacts onto granule cells and inhibitory postsynaptic currents (IPSC) were recorded (Figure 20 A).

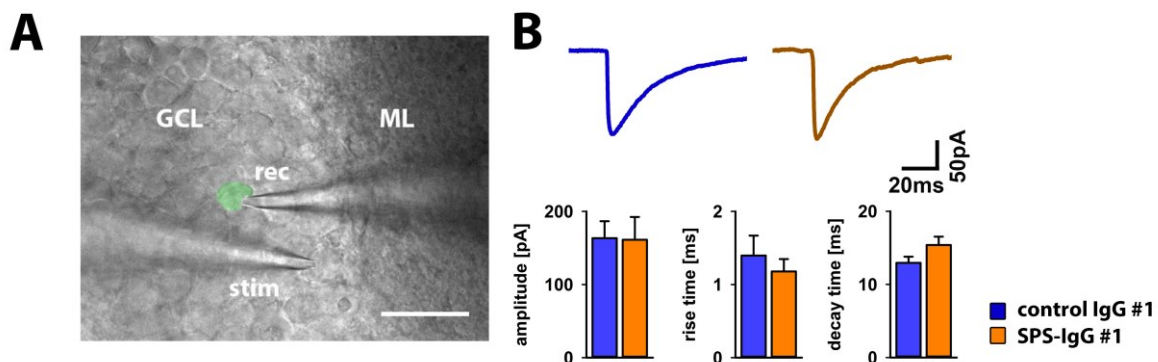


Fig 20 Similar GABAergic eIPSC amplitude and kinetic characteristics in presence of anti-GAD65 AB containing IgG

A) Experimental setup for recording IPSCs in acute hippocampal slices. GABAergic basket cell axons were stimulated in the inner third of the granule cell layer. IPSC evoked by minimal stimulation of GABAergic basket cell axons residing in the inner third of the granule cell layer were recorded in granule cells that were monosynaptically connected. GCL = granule cell layer, ML = molecular layer, rec = recording electrode, stim = stimulation electrode; scale bar: 20 μ m B) Analysis of single-evoked IPSC from dentate gyrus granule cells after preincubation with control IgG or SPS-IgG demonstrates no change in eIPSC amplitudes and kinetics. Upper traces show averaged responses of representative individual neurons.

Results B: Functional consequences induced by anti-GAD65 containing SPS-IgG

Whole cell patch clamp recordings from hippocampal granular cells after minimal stimulation of GABAergic afferences were unchanged after incubation with SPS-IgG and control IgG in amplitude (Figure 20 B; control IgG #1 = 163.5 ± 23.1 pA; SPS-IgG #1 = 161.2 ± 31.2 pA; $p = 0.824$) and eIPSC kinetics (Figure 20 B; [rise time]: control IgG #1 = 1.2 ± 0.2 ms; SPS-IgG #1 = 1.4 ± 0.3 ms; $p = 0.524$; [decay time]: controls = 15.4 ± 1.1 ms, SPS-IgG #1 = 12.9 ± 0.9 ms; $p = 0.134$); n [control IgG #1] = 15, n [SPS-IgG #1] = 10).

4.2. Normal short term plasticity and high frequency transmission after anti-GAD65 IgG incubation

IPSCs can also vary depending on preceding activity which can be evaluated in paired pulse experiments. Depending on synapse type, inter-stimulus intervals, and experimental conditions synapses can undergo synaptic facilitation or depression.

This mechanism called short-term plasticity is depending on intracellular calcium levels, vesicles available for exocytosis and vesicular release probability. We measured short-term plasticity and vesicular GABA loading at short inter-pulse intervals, using the paired pulse paradigm applying different interstimulus intervals. For all tested intervals there was paired pulse depression without any difference between the experimental groups (Figure 21 A; values of the test pulse are given in relation to the preceding pulse; 50 ms: control IgG #1 = 0.97 ± 0.07 , n = 6; SPS-IgG #1 = 0.89 ± 0.14 , n = 8, $p = 0.645$; 100 ms: control IgG #1 = 0.92 ± 0.06 , n = 11,; SPS-IgG #1 = 0.96 ± 0.01 , n = 9, $p = 0.761$; 250 ms: control IgG #1 = 0.89 ± 0.09 , n = 11, SPS-IgG #1 = 0.84 ± 0.05 , n = 13, $p = 0.720$; 500 ms: control IgG #1 = 0.90 ± 0.04 , n = 6, SPS-IgG #1 = 0.94 ± 0.04 , n = 8, $p = 0.652$).

AB-mediated effects may have been masked at low synaptic activity. Therefore GABAergic basket cell axons were stimulated using high frequency (10 Hz) train stimulation. In both groups, high-frequency stimulation induced depression was as expected without any differences between preincubation of control or SPS-IgG (Figure 21 B).

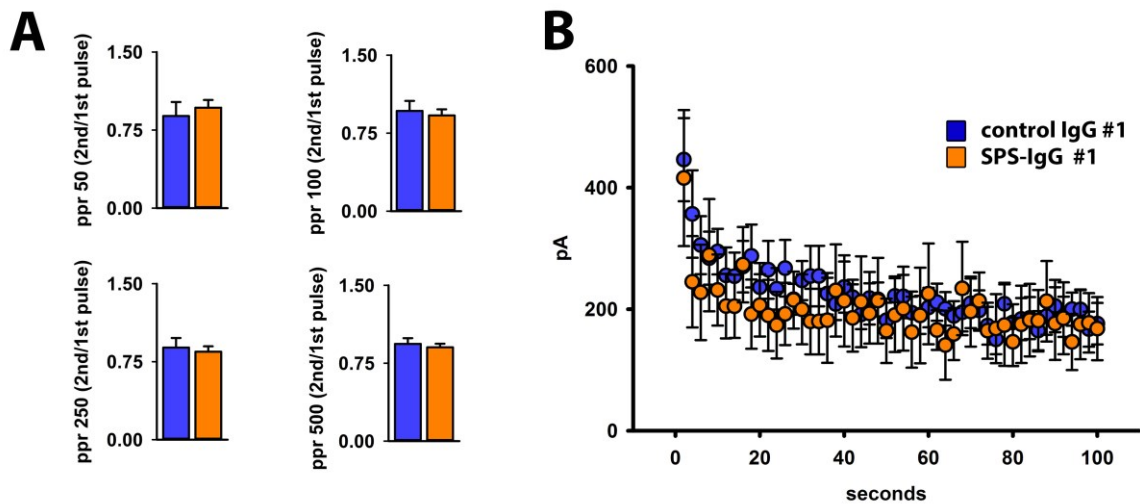


Fig 21 SPS-IgG with anti-GAD65 AB does not affect short term plasticity or high frequency transmission of a basket cell – granule cell GABAergic synapse

A) Paired stimulation at tested interpulse intervals revealed depression of the second pulse without differences between tested groups. B) IPSC peak amplitude during high frequency stimulation of GABAergic basket cell axons was not compromised by anti-GAD65 IgG preincubation (bin size = 5; n [control IgG] = 9, n [SPS-IgG] = 6).

4.3. Anti-GAD65 AB containing IgG increases frequency of mIPSCs

To investigate single fusion of GABAergic vesicles miniature IPSCs were recorded in absence of action potentials. Miniature potentials are spontaneous quantal currents that presumably represent single vesicular fusions releasing only one vesicle quantum from the pre-synaptic active zone for binding to postsynaptic target receptors. Frequency of mIPSCs is limited by release probability whereas mIPSC amplitude is determined by transmitter content of release-ready vesicles, postsynaptic receptor characteristics, and receptor location in the synapse. To characterize AB-mediated changes in single vesicular fusion we measured mIPSC amplitudes and frequencies in presence of the sodium channel blocker tetrodotoxin (TTX).

In two separate experiments, preincubation with SPS-IgG from different patients lead to a significant increase of mIPSC frequency in acute hippocampal slices compared to the respective controls (Figure 22; control IgG #1 = $0.62 \text{ Hz} \pm 0.14 \text{ Hz}$, n[control IgG #1] = 8, SPS-IgG #1 = $1.29 \pm 0.26 \text{ Hz}$, n[SPS-IgG #1] = 7, $p=0.038$; control IgG #2 = $0.68 \pm 0.07 \text{ Hz}$, n[control IgG #2] = 6, SPS-IgG #2 = $0.91 \pm 0.10 \text{ Hz}$, n[SPS-IgG #2] = 7; $p=0.035$).

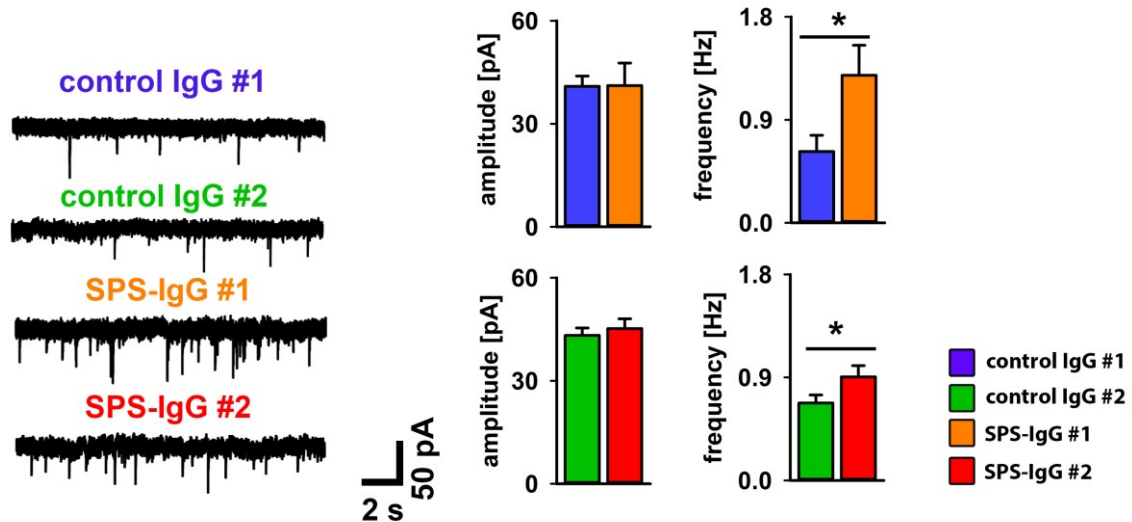


Fig 22 GAD65-IgG increases release probability of spontaneous GABAergic transmission

Traces show representative mIPSC recordings of control IgG #1 and #2 and of SPS-IgG (patient #1 and patient #2) pretreated neurons. mIPSC amplitude was not different while incubation with SPS-IgG led to an increase in the frequency of miniature potentials; * $p < 0.05$

Against this, mIPSC amplitudes were not affected by SPS-IgG (Figure 22; control IgG #1 = 43.2 ± 2.2 pA, $n[\text{control IgG \#1}] = 8$, SPS-IgG #1 = 40.9 ± 3.0 pA, $n[\text{SPS-IgG \#1}] = 7$, $p = 0.977$; control IgG #2 = 43.2 ± 2.2 pA, $n[\text{control IgG \#2}] = 6$, SPS-IgG #2 = 45.2 ± 2.8 pA, $n[\text{SPS-IgG \#2}] = 7$; $p = 0.534$) suggesting that individual vesicles were loaded with similar content in both experimental groups contradicting the hypothesis of reduced GABA availability.

Increased mIPSC frequency might result from a compensatory increased amount and therefore more frequent vesicular fusions of vesicles in GABAergic boutons. To test this hypothesis, the size of GABAergic vesicle pools was quantified in-vitro using confocal microscopy of axonal boutons of primary hippocampal neurons preincubated with SPS-IgG and non-reactive control IgG. The number of synaptic vesicles was identified by signal quantification of the vesicle marker synaptophysin (syphy) in VGAT positive GABAergic presynaptic terminals. To verify that VGAT area is a normalization factor with only minor variability, we compared VGAT area between both experimental groups. Calculated mean VGAT positive area per bouton showed no relevant fluctuations (Figure 23, control IgG #1 = $6.55 \pm 0.84 \mu\text{m}^2$, SPS patient-IgG #1 = $7.80 \pm 1.72 \mu\text{m}^2$; $p = 0.959$) confirming VGAT as reliable normalization factor. The size of GABAergic synaptic vesicle pools identified by the area of syphy immunoreactivity normalized by VGAT area showed similar percentage in SPS-IgG treated neurons in comparison to controls (Figure 23, control IgG #1 = $71.2 \pm 8.4 \%$, SPS-IgG #1 = 72.3 ± 6.3

Results B: Functional consequences induced by anti-GAD65 containing SPS-IgG

%; $p = 0.798$). Moreover, calculations of integrated density (Figure 23, control IgG #1 = 496.234 ± 108.459 bits/ μm^2 , SPS-IgG #1 = 573.3 ± 146.6 bits/ μm^2 ; $p = 0.878$) and mean-grey values over VGAT positive synapses (Figure 23, control IgG #1 = 75.5 ± 12.4 , SPS-IgG #1 = 72.0 ± 8.2 , $p = 0.967$) also revealed no differences in syphy signal. These results confirm that the size of GABAergic vesicle pools is not affected by SPS-IgG and cannot be responsible for the observed increased frequency of vesicular release.

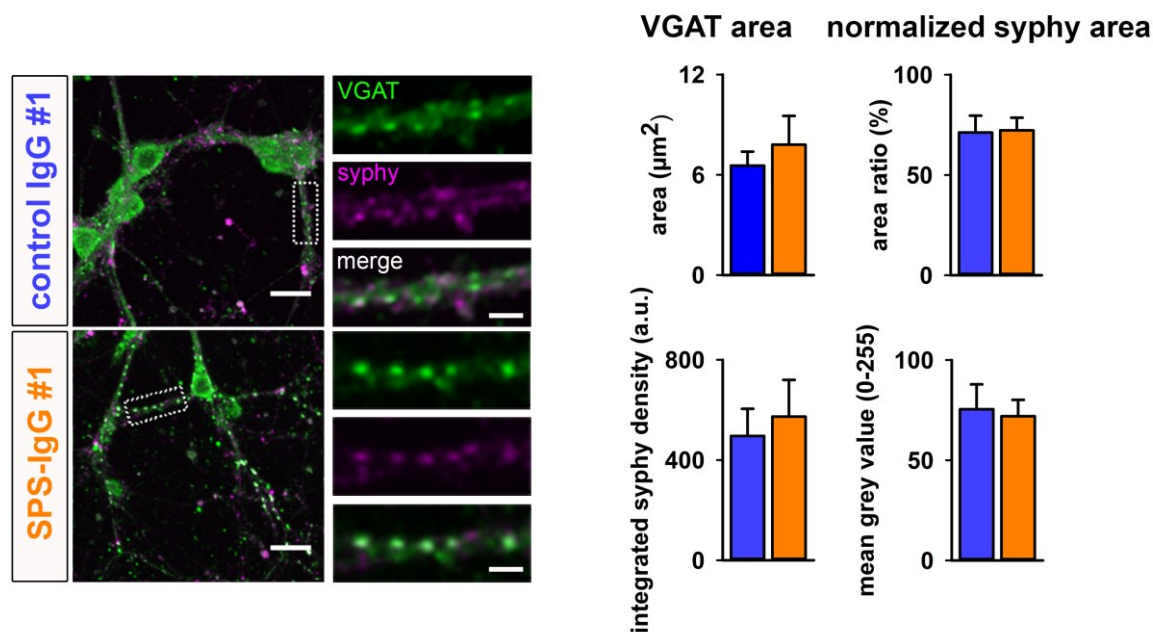


Fig 23 Increased mIPSC frequency cannot be attributed to larger GABAergic vesicle pools

Representative confocal images of control IgG and SPS-IgG treated neurons. The overview microphotograph shows merged images of neurons after VGAT (green) and syphy (magenta) double-staining. ROIs were defined on proximal axonal synapses (dotted rectangle) and taken for further analysis (scale bar: $20 \mu\text{m}$). High magnification images (right) of dotted areas in the overview images show individual and merged color channels demonstrating similar syphy signal over VGAT signals in both treatment groups (scale bar: $5 \mu\text{m}$). The VGAT area (mean area per bouton) was unchanged in both experimental groups. Syphy areas normalized to VGAT areas were nearly identical implicating a similar vesicle pool size in control IgG and SPS-IgG preincubated neurons. Integrated syphy intensity and mean grey values, both determined in VGAT positive presynaptic boutons, corroborate the finding of similar vesicle pool size comparing both experimental groups.

Studies from GAD65 KO animals showed no compensatory gene expression changes of its isoform GAD67 (Asada et al., 1996). Acute inhibition by AB targeting existing GAD65 might induce different regulations. To test the hypothesis of compensatory, AB-induced changes in gene expression, mRNA levels of GAD isoforms (*gad65*, *gad67*), were determined using qRT-PCR of *gad65* and *gad67* after preincubation of primary hippocampal cell cultures with pathogenic SPS-IgG vs. control IgG.

Experiments revealed no significant gene expression changes for *gad65* (Figure 24, results are given as delta CT value; control IgG #1 = 9.56 ± 0.40 , SPS-IgG #1 = 8.81 ± 0.32 ; $p = 0.212$; $n = 11$ for both groups) or *gad67* (Figure 24, control IgG #1 = 7.75 ± 0.32 SPS-IgG #1

Results B: Functional consequences induced by anti-GAD65 containing SPS-IgG

= 6.98 ± 0.20 ; $p = 0.101$; $n = 11$ for both groups) suggesting no compensatory gene expression regulation mediated by anti-GAD65 AB containing SPS-IgG.

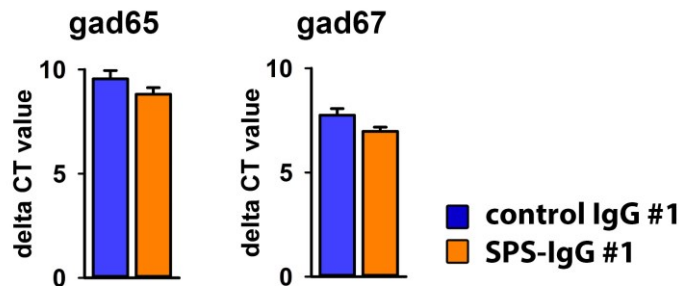


Figure 24 Anti-GAD65 AB containing IgG induces no gene expression changes of gad isoforms

Plots compare qRT-PCR comparative thresholds (delta CT) of gad65 and gad67 mRNA normalized to two housekeeping genes (18s, GAPDH) purified from cells pretreated with control or SPS-IgG.

From these different experiments and consisting results it became clear that AB to GAD65 cannot account for the observation of increased release probability. Since polyclonal purified IgG-fractions were used in the patch-clamp experiments, additional IgG-AB to other target proteins than to GAD65 may be present. To investigate whether SPS patient IgG contains further possible pathogenic AB we performed immunohistological experiments with fractions depleted of GAD65 AB after affinity purification of SPS-IgG #2 with recombinant GAD65 (SPSIgG #2^{preabsorbed}). Western blotting on recombinant human GAD65 corroborated the successful and complete depletion of AB to GAD65 from SPS-IgG #2 (Figure 25 B). Binding experiments were done with SPSIgG #2^{preabsorbed} in comparison to native SPS-IgG #2, and a further control IgG containing no specific antineuronal AB on primary neurons and murine hippocampal brain slices. As expected, native SPS-IgG #2 immunostained neuronal structures in primary cell cultures and dentate gyrus of hippocampal brain sections (Figure 25 A). Surprisingly, SPSIgG #2^{preabsorbed} still showed still strong immunoreaction to neuronal structures in hippocampal slices and dissociated neurons with punctuate pattern similar to the staining pattern of other presynaptic markers (Figure 25 A). This finding strongly suggests the occurrence of additional IgG-AB in SPS-IgG other than anti-GAD65 AB that are directed to so far not determined presynaptic antigens.

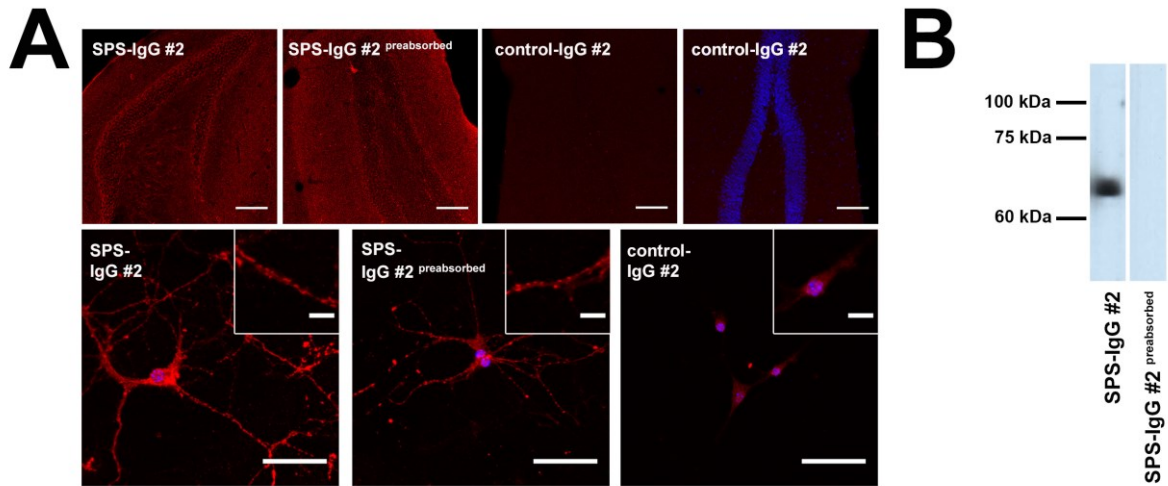


Fig 25 SPS-IgG depleted of GAD65-AB still binds to murine neuronal structures

A) Positive immunolabeling of synapses of dissociated hippocampal neurons and mouse dentate gyrus in hippocampal slices with patient SPS-IgG #2 (red) before depletion and after removal of anti-GAD65 AB (SPSIgG #2^{preabsorbed}). Control IgG #2 showed no specific immunostaining. Blue = DAPI staining for cell nuclei. Insets depict higher magnifications; scale bar (top row, slices): 100 µm, scale bar (bottom row, cells): 50 µm, scale bar (insets): 10 µm. B) Western blot (recombinant GAD65, 15µg per lane) confirming efficient depletion of anti-GAD65 AB from SPS-IgG #2 after affinity chromatography; left lane = patient IgG #2, right lane = patient IgG#2 after preabsorption with recombinant human GAD65.

4.4. Microisland cultures as model system to investigate functional effects of pathogenic antineuronal AB

Availability and amount of patient material (IgG, serum, or CSF) for experimental use in research of AB mediated synapse pathology is often a limiting factor. Also for in vitro physiological experiments with AB preincubation of acute brain slices, relatively high amounts of patient material are necessary. This led to the idea to establish a model system with the advantage of known synaptic connectivity and the possibility of using very little patient material for incubation. These considerations directed to the establishment of a primary cell culture based model system with convenient possibilities to assess functional effects induced by pathogenic AB. The so-called microisland culture system consists of many isolated neurons on a coverslip that are separated from each other by specific preparation of the coverslip coating (for details see material and methods section, 2.3.).

Microisland cultures offer several benefits 1) patient material is only needed in sparse volume similar to usual cell culture preparations 2) in contrast to usual neuronal cultures and brain slices, the circuit complexity is reduced and thus connectivity between neurons is clearly monosynaptic 3) individual cells are located on microislands innervating themselves with so called autapses allowing easy stimulation and recording of depolarization evoked autaptic potentials with the same patch-clamp pipette.

Results B: Functional consequences induced by anti-GAD65 containing SPS-IgG

The structural and functional maturity of the established autapses in culture (Figure 26 A) was confirmed by immunostaining for synaptic vesicle marker synphy and the axonal marker PGP9.5. (Figure 26 C, D) as well as recording of eIPSCs by whole cell voltage clamp recordings in presence of CNQX and AP-5 blocking postsynaptic glutamatergic receptors (Fig 26 B). This established model system can now be used in future experiments for evaluation of AB-induced synaptic dysfunction when patient material is limited. The next application will be functional investigations of preabsorbed SPS-IgG (SPSIgG #2^{preabsorbed}) and specific patient anti-GAD65 AB reconstituted after affinity chromatography on GABAergic autaptic transmission. Due to the very small amounts of reconstituted IgG after affinity purification, microisland cultures represent an ideal model system.

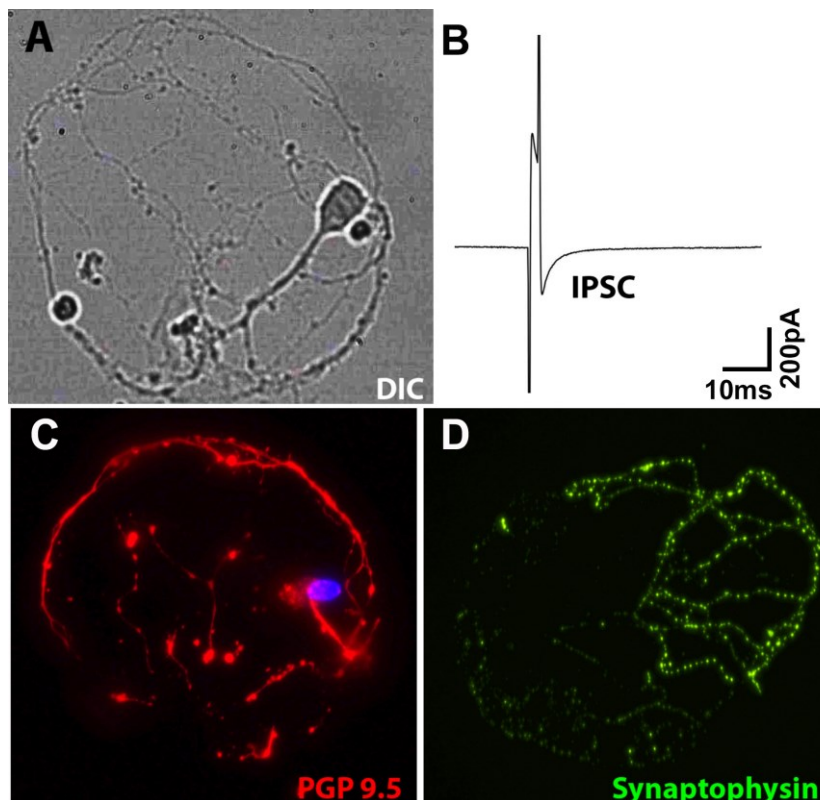


Fig 26 Microisland culture

A) Differential interference contrast (DIC) image of a vital autaptic neuron in culture. B) depolarization (1ms) evoked IPSC recorded by whole cell voltage clamp. First deflection is the stimulus artifact due to depolarization. The IPSC (downward deflection) can be clearly separated. C) immunostaining of a microisland neuron with the axonal marker PGP 9.5. D) immunostaining with anti-synaptophysin AB. reveals occurrence of presynaptic vesicles.

5. Discussion

5.1. Pathophysiological mechanisms of anti-amphiphysin AB

Synaptic neurotransmission depends on reliable compensatory reformation of synaptic vesicles following fusion with synaptic membrane by CME or budding of new vesicles from bulk endosomes. Studies on CME function have relied on genetic KO of CME proteins (Milosevic et al., 2011, Raimondi et al., 2011, Soda et al., 2012) or acute block by inhibitory peptides (Shupliakov et al., 1997). Genetic absence of CME proteins leads to endocytosis defects characterized by appearance of different endocytosis intermediates depending on the point of interference with endocytosis (Di Paolo et al., 2002, Ferguson et al., 2007, Milosevic et al., 2011). The present thesis revealed that pathogenic human AB targeting amphiphysin in paraneoplastic SPS can have effects on structure of presynaptic vesicle pools and the molecular composition of synaptic vesicles.

Results reported here with reduction of synaptic vesicle pools and less endocytic intermediates in GABAergic boutons at high synaptic activity corroborate the findings that CME in GABAergic synapses is functionally primarily affected by specAmph AB (Geis et al., 2010). Here, ultrastructural abnormalities have been uncovered that represent dysfunctional CME after passive-transfer of anti-amphiphysin AB. Beside depletion of the presynaptic vesicle pool, loss of CCV removes the machinery for proper protein sorting and efficient preparation of vesicles for transmitter exocytosis (Faini et al., 2013). ELS are structures that are prevalent during ultrafast endocytosis (Watanabe, 2013). The reduction of ELS during stimulated conditions probably impedes fast replenishment of synaptic vesicles in synapses under sustained activity. Finally, the structural defects characterized in this study are in line with anti-amphiphysin AB induced functional defects like slower endocytosis rates and faster synaptic depression under prolonged high frequency neurotransmission as reported previously (Geis et al., 2010).

The results here are different to observations from animals with genetic deficiency of amphiphysin 1 with probably sufficient compensatory mechanisms (Di Paolo et al., 2002). Further, the findings in this study are different to previous reports showing stimulation induced accumulation of clathrin coated pits stalled at the membrane of lamprey presynaptic boutons that have been injected with inhibitory peptides targeting amphiphysin SH3 domain (Shupliakov et al., 1997). The differential effect of AB can be first explained by the fact that AB bind acutely to endogenous available amphiphysin with only minor possibility of compensatory mechanisms as it is frequently observed in KO animals. Second, in contrast to synap-

Discussion

ses in lamprey, mammalian CNS is far more complex with increased number of synaptic contacts. Moreover, the study using inhibitory peptides targeting lamprey synapses used very long stimulation (30 min) at rather low frequency (0.2 Hz) which might not represent a physiological stimulation as we mimicked with our paradigms.

The protein composition on synaptic vesicles is generally believed to be different depending on which endocytic route is prevalent at a particular synapse (Voglmaier and Edwards, 2007). The present results after molecular analysis of pathologic GABAergic vesicle pools indicate that targeting of v-SNARE isoforms as essential components of vesicle exocytosis to the different synaptic vesicle pools is disturbed. V-SNAREs were previously shown to characterize different vesicle pools (Hua et al., 2011). V-SNAREs who are essential for fast synaptic neurotransmission may not be present in sufficient copy numbers or in the right ratio to guarantee sustained exocytosis at high synaptic activity levels. Syb7 as a marker for the resting pool of vesicles was massively reduced in primary neurons, which is in line with the observations of activity-dependent depletion of vesicle and CCV in spinal presynapses after anti-amphiphysin IgG passive-transfer. V-SNAREs may even be trapped at the synaptic plasma membrane after fusion due to a slowed or blocked endocytic machinery as observed in a previous report (Shetty et al., 2013) which may explain the relative increase of syb2 signal in stimulated neurons after specAmph AB preincubation. Differential distribution of syb-2 may also result from its sorting by AP-180 (Koo et al., 2011) which itself has been shown to have more intense clustering in presence of anti-amphiphysin AB (Geis et al., 2010).

The thesis elucidated that endophilin, an interaction partner of amphiphysin (Micheva et al., 1997), is differentially expressed in GABAergic vesicle pools and seems to be abnormally localized during the influence of anti-amphiphysin AB. As endophilin was shown to be especially important for high frequency neurotransmission (Llobet et al., 2011), this difference in localization might in part explain functional defects caused by specAmph AB that are predominantly apparent during high synaptic activity (Geis et al., 2010). Moreover, triple KO of all endophilin isoforms leads to accumulation of CCVs (Milosevic et al., 2011) reminiscent to the ultrastructural findings of synapses after specAmph treatment at resting conditions reported here. Although these results add important knowledge in a reduced model system of primary hippocampal neurons, they likely do not fully reflect the synaptic dynamics of rat spinal presynaptic boutons in SPS *in-vivo* experiments. This study cannot rule out diverging manifestations of AB induced endocytosis defects in different subtypes of synapses. Future work will also have to elucidate if glutamatergic boutons of primary neurons are equally affected by anti-amphiphysin AB mediated endocytosis deficits.

Discussion

Results of the present dissertation highlight molecular and structural pathomechanisms underlying Stiff person syndrome with pathogenic amphiphysin AB affecting presynaptic CME. It would be highly interesting in future research to perform experimental analysis of postsynaptic receptor trafficking to challenge the hypothesis of an exclusive presynaptic action of anti-amphiphysin AB. Inhibition of postsynaptic endocytic machinery may interfere with endocytosis mediated reduction and recycling of surface receptors and hence also influence synaptic transmission (Wigge et al., 1997). This thesis not only provides important insights into pathophysiological details of a specific autoimmune CNS disorder but may also add principle knowledge for research on other neurological disorders that show reduction (De Jesus-Cortes et al., 2012) or inhibition (Trempe et al., 2009) of endocytic proteins.

5.2. The role of anti-GAD65 AB in SPS

SPS-IgG containing high titer of anti-GAD65 AB delivered to the CNS compartment of experimental animals leads to motor deficits, increased anxiety, cognitive deficits and increased potentiation of excitatory transmission (Geis et al., 2011, Hampe et al., 2013, Hansen et al., 2013, Vega-Flores et al., 2014). The hypothesis of direct pathogenic mechanism of anti-GAD65 AB inducing disease signs in these animal models has long been a matter of debate. The present dissertation provides evidence that SPS-IgG of idiopathic SPS patients mediated an increase in GABAergic presynaptic quantal release probability in dentate gyrus basket cells projecting to granule cells. This finding is not in line with the assumption that anti-GAD65 AB binding reduces enzymatic activity of GAD65. The hypothetical reduction of available neurotransmitter for loading into GABAergic vesicles would have been unmasked by smaller eIPSC amplitudes especially during high frequency stimulation. Against this, results here revealed no AB-induced changes of eIPSC at low and high synaptic activity. The hypothesis that AB-induced inhibition of GAD65 would resemble deficits in GAD65 KO mice was also not corroborated. The frequency dependent deficit of GABAergic transmission observed in GAD65 KO mice (Tian et al., 1999) was not seen at high frequency stimulation after SPS-IgG preincubation. It has to be noted that effects resulting from AB binding might be different compared to complete lack of a protein in a KO model including compensatory regulations in the CNS. Moreover we cannot exclude that we missed AB mediated effects at other IgG concentrations or that incubation time is too short to allow access of AB to their intracellular antigen. Nevertheless, we used IgG concentrations and an incubation time frame that have been validated in previous experiments with AB binding to amphiphysin which is also intracellular located in presynapses (Geis et al., 2010).

Discussion

The results are in accordance with the assumption of additional pathogenic AB present in anti-GAD65-AB-positive SPS patient IgG fractions (Chang et al., 2013) that can account for the functional difference of mIPSC frequency after SPS-IgG preincubation. The already identified target structures for AB that coexist with anti-GAD65 AB in SPS patient serum comprise GABA-A receptor associated protein, gephyrin, and glycine receptors (Butler et al., 2000, Raju et al., 2006). These AB cannot be responsible for presynaptic modifications as their target epitopes are all residing at the postsynaptic compartment of GABAergic synapses. The increased probability of single vesicular fusions allows speculation towards putative additional AB targeting presynaptic antigens that are involved in regulating presynaptic vesicular release, e.g. calcium sensors (Christgau et al., 1992, Pang et al., 2011, Walter et al., 2011) or vesicle proteins regulating spontaneous release mechanisms (Ramirez et al., 2012). These AB might be specific to GABAergic synapses since not all primary hippocampal neurons showed positive immunostaining in cell culture preparations (preliminary observations). Patient symptoms can be explained by chronically increased spontaneous release of presynaptic GABA possibly leading to homeostatic mechanisms that downregulate GABA-A receptors. Chronic spontaneous activity might also induce desensitization of postsynaptic GABA-A receptors. These assumptions would be consistent with reports of reduced GABA-A receptor binding potential in SPS patients (Galldiks et al., 2008). The decrease of inhibitory transmission may lead to comparatively increased excitatory transmission contributing to SPS-symptoms.

However, it remains a matter of debate whether short incubation of anti-GAD65 AB with slices allows AB to reach their target antigens in a similar pattern as compared to long exposure over several days in *in-vivo* animal models. Therefore it cannot be fully excluded that anti-GAD65 antibodies still may have a limited pathogenic effect on GABAergic neurotransmission, but this seems unlikely according to the results shown here. The present experiments could provide important evidence for putative new target antigens present in patient serum or CSF that need to be characterized in future studies. Furthermore, experiments including preabsorbed SPS patient IgG and reconstituted anti-GAD65 fractions will clarify the pathogenic role of existing anti-GAD65-AB (Geis et al., 2010). Here, the established microisland neuronal cultures offer a convenient model system to investigate these experimental questions with a limited amount of patient material. Autapses forming monosynaptic contacts can easily be manipulated and characterized (Ikeda and Bekkers, 2006) and time as well as concentration-dependent processes can conveniently be investigated in standardized series of experiments.

Gene expression analysis showed that SPS-IgG containing GAD65 AB induced no compensatory gene expression changes neither of GAD65 itself or compensatory regulation of its

Discussion

isoform GAD67 which is in line with observations in GAD65 KO mice (Asada et al., 1996). This finding was found in neurons of DIV10 cell cultures. Primary cell cultures are interconnected in less complex networks than brain tissue and synapse formation might not be fully established at that timepoint, so data from *in-vivo* experiments with adult animals and longer exposure time might show different results. For incubation experiments a validated concentration of anti-GAD65 containing IgG was used (Geis et al., 2010) but a dose response relationship is still warranting further experiments with different preincubation concentrations of SPS-IgG. It would also be interesting to perform gene expression analysis of a variety of presynaptic antigens involved in presynaptic release machinery to get further insights into SPS-IgG mediated synaptic changes and to obtain first hints for identification of the putative additional antigen targeted by SPS-IgG. The next steps would imply to perform 2D-gel electrophoresis experiments followed by protein identification by mass spectrometry.

In conclusion, the experiments with anti-GAD65 positive SPS-IgG in this thesis revealed new and unexpected findings suggesting additional presynaptic autoantigens in SPS and might contribute to further research elucidating the synaptic pathophysiology of idiopathic SPS.

Reference list

- Alexopoulos H, Dalakas MC (2010) A critical update on the immunopathogenesis of Stiff Person Syndrome. *Eur J Clin Invest* 40:1018-1025.
- Allen C, Stevens CF (1994) An evaluation of causes for unreliability of synaptic transmission. *Proc Natl Acad Sci U S A* 91:10380-10383.
- Allen TG (2006) Preparation and maintenance of single-cell micro-island cultures of basal forebrain neurons. *Nat Protoc* 1:2543-2550.
- Arkhipov A, Yin Y, Schulten K (2009) Membrane-bending mechanism of amphiphysin N-BAR domains. *Biophys J* 97:2727-2735.
- Asada H, Kawamura Y, Maruyama K, Kume H, Ding R, Ji FY, Kanbara N, Kuzume H, Sanbo M, Yagi T, Obata K (1996) Mice lacking the 65 kDa isoform of glutamic acid decarboxylase (GAD65) maintain normal levels of GAD67 and GABA in their brains but are susceptible to seizures. *Biochem Biophys Res Commun* 229:891-895.
- Asada H, Kawamura Y, Maruyama K, Kume H, Ding RG, Kanbara N, Kuzume H, Sanbo M, Yagi T, Obata K (1997) Cleft palate and decreased brain gamma-aminobutyric acid in mice lacking the 67-kDa isoform of glutamic acid decarboxylase. *Proc Natl Acad Sci U S A* 94:6496-6499.
- Baker MR, Das M, Isaacs J, Fawcett PR, Bates D (2005) Treatment of stiff person syndrome with rituximab. *J Neurol Neurosurg Psychiatry* 76:999-1001.
- Battaglioli G, Liu H, Martin DL (2003) Kinetic differences between the isoforms of glutamate decarboxylase: implications for the regulation of GABA synthesis. *J Neurochem* 86:879-887.
- Bergado-Acosta JR, Muller I, Richter-Levin G, Stork O (2014) The GABA-synthetic enzyme GAD65 controls circadian activation of conditioned fear pathways. *Behav Brain Res* 260:92-100.
- Bradl M, Misu T, Takahashi T, Watanabe M, Mader S, Reindl M, Adzemovic M, Bauer J, Berger T, Fujihara K, Itoyama Y, Lassmann H (2009) Neuromyelitis optica: pathogenicity of patient immunoglobulin in vivo. *Ann Neurol* 66:630-643.
- Brashear HR, Phillips LH, 2nd (1991) Autoantibodies to GABAergic neurons and response to plasmapheresis in stiff-man syndrome. *Neurology* 41:1588-1592.
- Buchwald B, Toyka KV, Zielasek J, Weishaupt A, Schweiger S, Dudel J (1998a) Neuromuscular blockade by IgG antibodies from patients with Guillain-Barre syndrome: a macro-patch-clamp study. *Ann Neurol* 44:913-922.
- Buchwald B, Weishaupt A, Toyka KV, Dudel J (1998b) Pre- and postsynaptic blockade of neuromuscular transmission by Miller-Fisher syndrome IgG at mouse motor nerve terminals. *Eur J Neurosci* 10:281-290.
- Burns ME, Augustine GJ (1995) Synaptic structure and function: dynamic organization yields architectural precision. *Cell* 83:187-194.
- Butler MH, Hayashi A, Ohkoshi N, Villmann C, Becker CM, Feng G, De Camilli P, Solimena M (2000) Autoimmunity to gephyrin in Stiff-Man syndrome. *Neuron* 26:307-312.
- Butler MH, Solimena M, Dirks R, Jr., Hayday A, De Camilli P (1993) Identification of a dominant epitope of glutamic acid decarboxylase (GAD-65) recognized by autoantibodies in stiff-man syndrome. *J Exp Med* 178:2097-2106.
- Chang T, Alexopoulos H, Pettingill P, McMenemy M, Deacon R, Erdelyi F, Szabo G, Buckley CJ, Vincent A (2013) Immunization against GAD induces antibody binding to GAD-independent antigens and brainstem GABAergic neuronal loss. *PLoS One* 8:e72921.
- Chen L, Wang H, Vicini S, Olsen RW (2000) The gamma-aminobutyric acid type A (GABAA) receptor-associated protein (GABARAP) promotes GABAA receptor clustering and modulates the channel kinetics. *Proc Natl Acad Sci U S A* 97:11557-11562.
- Chen Y, Deng L, Maeno-Hikichi Y, Lai M, Chang S, Chen G, Zhang JF (2003) Formation of an endophilin-Ca²⁺ channel complex is critical for clathrin-mediated synaptic vesicle endocytosis. *Cell* 115:37-48.

Reference list

- Christgau S, Aanstoot HJ, Schierbeck H, Begley K, Tullin S, Hejnaes K, Baekkeskov S (1992) Membrane anchoring of the autoantigen GAD65 to microvesicles in pancreatic beta-cells by palmitoylation in the NH₂-terminal domain. *J Cell Biol* 118:309-320.
- Christgau S, Schierbeck H, Aanstoot HJ, Aagaard L, Begley K, Kofod H, Hejnaes K, Baekkeskov S (1991) Pancreatic beta cells express two autoantigenic forms of glutamic acid decarboxylase, a 65-kDa hydrophilic form and a 64-kDa amphiphilic form which can be both membrane-bound and soluble. *J Biol Chem* 266:21257-21264.
- Cremona O, Di Paolo G, Wenk MR, Luthi A, Kim WT, Takei K, Daniell L, Nemoto Y, Shears SB, Flavell RA, McCormick DA, De Camilli P (1999) Essential role of phosphoinositide metabolism in synaptic vesicle recycling. *Cell* 99:179-188.
- Dalakas MC (2008) Advances in the pathogenesis and treatment of patients with stiff person syndrome. *Curr Neurol Neurosci Rep* 8:48-55.
- Dalakas MC (2009) Stiff person syndrome: advances in pathogenesis and therapeutic interventions. *Curr Treat Options Neurol* 11:102-110.
- Dalakas MC, Fujii M, Li M, Lutfi B, Kyhos J, McElroy B (2001) High-dose intravenous immune globulin for stiff-person syndrome. *N Engl J Med* 345:1870-1876.
- Dalakas MC, Fujii M, Li M, McElroy B (2000) The clinical spectrum of anti-GAD antibody-positive patients with stiff-person syndrome. *Neurology* 55:1531-1535.
- Dalmau J, Gleichman AJ, Hughes EG, Rossi JE, Peng X, Lai M, Dessain SK, Rosenfeld MR, Balice-Gordon R, Lynch DR (2008) Anti-NMDA-receptor encephalitis: case series and analysis of the effects of antibodies. *Lancet Neurol* 7:1091-1098.
- David C, McPherson PS, Mundigl O, de Camilli P (1996) A role of amphiphysin in synaptic vesicle endocytosis suggested by its binding to dynamin in nerve terminals. *Proc Natl Acad Sci U S A* 93:331-335.
- David C, Solimena M, De Camilli P (1994) Autoimmunity in stiff-Man syndrome with breast cancer is targeted to the C-terminal region of human amphiphysin, a protein similar to the yeast proteins, Rvs167 and Rvs161. *FEBS Lett* 351:73-79.
- Daw K, Ujihara N, Atkinson M, Powers AC (1996) Glutamic acid decarboxylase autoantibodies in stiff-man syndrome and insulin-dependent diabetes mellitus exhibit similarities and differences in epitope recognition. *J Immunol* 156:818-825.
- De Camilli P, Thomas A, Cofield R, Folli F, Lichte B, Piccolo G, Meinck HM, Austoni M, Fassetta G, Bottazzo G, Bates D, Cartledge N, Solimena M, Kilimann MW, et al. (1993) The synaptic vesicle-associated protein amphiphysin is the 128-kD autoantigen of Stiff-Man syndrome with breast cancer. *J Exp Med* 178:2219-2223.
- De Jesus-Cortes HJ, Nogueras-Ortiz CJ, Gearing M, Arnold SE, Vega IE (2012) Amphiphysin-1 protein level changes associated with tau-mediated neurodegeneration. *Neuroreport* 23:942-946.
- Denker A, Rizzoli SO (2010) Synaptic vesicle pools: an update. *Front Synaptic Neurosci* 2:135.
- Di Paolo G, Sankaranarayanan S, Wenk MR, Daniell L, Perucco E, Caldarone BJ, Flavell R, Picciotto MR, Ryan TA, Cremona O, De Camilli P (2002) Decreased synaptic vesicle recycling efficiency and cognitive deficits in amphiphysin 1 knockout mice. *Neuron* 33:789-804.
- Edwards FA, Konnerth A, Sakmann B (1990) Quantal analysis of inhibitory synaptic transmission in the dentate gyrus of rat hippocampal slices: a patch-clamp study. *J Physiol* 430:213-249.
- Erlander MG, Tobin AJ (1991) The structural and functional heterogeneity of glutamic acid decarboxylase: a review. *Neurochem Res* 16:215-226.
- Essrich C, Lorez M, Benson JA, Fritschy JM, Luscher B (1998) Postsynaptic clustering of major GABA_A receptor subtypes requires the gamma 2 subunit and gephyrin. *Nat Neurosci* 1:563-571.
- Faini M, Beck R, Wieland FT, Briggs JAG (2013) Vesicle coats: structure, function, and general principles of assembly. *Trends Cell Biol* 23:279-288.
- Fekete R, Jankovic J (2012) Childhood stiff-person syndrome improved with rituximab. *Case Rep Neurol* 4:92-96.

Reference list

- Ferguson SM, Brasnjo G, Hayashi M, Wolfel M, Collesi C, Giovedi S, Raimondi A, Gong LW, Ariel P, Paradise S, O'Toole E, Flavell R, Cremona O, Miesenbock G, Ryan TA, De Camilli P (2007) A selective activity-dependent requirement for dynamin 1 in synaptic vesicle endocytosis. *Science* 316:570-574.
- Fesce R, Grohovaz F, Valtorta F, Meldolesi J (1994) Neurotransmitter release: fusion or 'kiss-and-run'? *Trends Cell Biol* 4:1-4.
- Fukunaga H, Engel AG, Lang B, Newsom-Davis J, Vincent A (1983) Passive transfer of Lambert-Eaton myasthenic syndrome with IgG from man to mouse depletes the presynaptic membrane active zones. *Proc Natl Acad Sci U S A* 80:7636-7640.
- Galldiks N, Thiel A, Haense C, Fink GR, Hilker R (2008) 11C-flumazenil positron emission tomography demonstrates reduction of both global and local cerebral benzodiazepine receptor binding in a patient with Stiff Person Syndrome. *J Neurol* 255:1361-1364.
- Geis C, Beck M, Jablonka S, Weishaupt A, Toyka KV, Sendtner M, Sommer C (2009) Stiff person syndrome associated anti-amphiphysin antibodies reduce GABA associated $[Ca^{2+}]_i$ rise in embryonic motoneurons. *Neurobiol Dis* 36:191-199.
- Geis C, Grunewald B, Weishaupt A, Wultsch T, Toyka KV, Reif A, Sommer C (2012) Human IgG directed against amphiphysin induces anxiety behavior in a rat model after intrathecal passive transfer. *J Neural Transm* 119:981-985.
- Geis C, Weishaupt A, Grunewald B, Wultsch T, Reif A, Gerlach M, Dirx R, Solimena M, Perani D, Heckmann M, Toyka KV, Folli F, Sommer C (2011) Human stiff-person syndrome IgG induces anxious behavior in rats. *PLoS One* 6:e16775.
- Geis C, Weishaupt A, Hallermann S, Grunewald B, Wessig C, Wultsch T, Reif A, Byts N, Beck M, Jablonka S, Boettger MK, Uceyler N, Fouquet W, Gerlach M, Meinck HM, Siren AL, Sigrist SJ, Toyka KV, Heckmann M, Sommer C (2010) Stiff person syndrome-associated autoantibodies to amphiphysin mediate reduced GABAergic inhibition. *Brain* 133:3166-3180.
- Grabs D, Slepnev VI, Songyang Z, David C, Lynch M, Cantley LC, De Camilli P (1997) The SH3 domain of amphiphysin binds the proline-rich domain of dynamin at a single site that defines a new SH3 binding consensus sequence. *J Biol Chem* 272:13419-13425.
- Granseth B, Odermatt B, Royle SJ, Lagnado L (2006) Clathrin-mediated endocytosis is the dominant mechanism of vesicle retrieval at hippocampal synapses. *Neuron* 51:773-786.
- Hampe CS, Petrosini L, De Bartolo P, Caporali P, Cutuli D, Laricchiuta D, Foti F, Radtke JR, Vidova V, Honnorat J, Manto M (2013) Monoclonal antibodies to 65kDa glutamate decarboxylase induce epitope specific effects on motor and cognitive functions in rats. *Orphanet J Rare Dis* 8:82.
- Hansen N, Grunewald B, Weishaupt A, Colaco MN, Toyka KV, Sommer C, Geis C (2013) Human Stiff person syndrome IgG-containing high-titer anti-GAD65 autoantibodies induce motor dysfunction in rats. *Exp Neurol* 239:202-209.
- Haucke V, Neher E, Sigrist SJ (2011) Protein scaffolds in the coupling of synaptic exocytosis and endocytosis. *Nat Rev Neurosci* 12:127-138.
- He L, Wu L-G (2007) The debate on the kiss-and-run fusion at synapses. *Trends Neurosci* 30:447-455.
- Henningsen P, Meinck HM (2003) Specific phobia is a frequent non-motor feature in stiff man syndrome. *J Neurol Neurosurg Psychiatry* 74:462-465.
- Heuser JE, Reese TS (1973) Evidence for recycling of synaptic vesicle membrane during transmitter release at the frog neuromuscular junction. *J Cell Biol* 57:315-344.
- Hua Z, Leal-Ortiz S, Foss SM, Waites CL, Garner CC, Voglmaier SM, Edwards RH (2011) v-SNARE composition distinguishes synaptic vesicle pools. *Neuron* 71:474-487.
- Ikeda K, Bekkers JM (2006) Autapses. *Curr Biol* 16:R308.
- Irani SR, Alexander S, Waters P, Kleopa KA, Pettingill P, Zuliani L, Peles E, Buckley C, Lang B, Vincent A (2010) Antibodies to Kv1 potassium channel-complex proteins leucine-rich, glioma

Reference list

- inactivated 1 protein and contactin-associated protein-2 in limbic encephalitis, Morvan's syndrome and acquired neuromyotonia. *Brain* 133:2734-2748.
- Jarius S, Stich O, Speck J, Rasiah C, Wildemann B, Meinck HM, Rauer S (2010) Qualitative and quantitative evidence of anti-glutamic acid decarboxylase-specific intrathecal antibody synthesis in patients with stiff person syndrome. *J Neuroimmunol* 229:219-224.
- Jin H, Wu H, Osterhaus G, Wei J, Davis K, Sha D, Floor E, Hsu CC, Kopke RD, Wu JY (2003) Demonstration of functional coupling between gamma -aminobutyric acid (GABA) synthesis and vesicular GABA transport into synaptic vesicles. *Proc Natl Acad Sci U S A* 100:4293-4298.
- Kash SF, Johnson RS, Tecott LH, Noebels JL, Mayfield RD, Hanahan D, Baekkeskov S (1997) Epilepsy in mice deficient in the 65-kDa isoform of glutamic acid decarboxylase. *Proc Natl Acad Sci U S A* 94:14060-14065.
- Kilkenny C, Browne WJ, Cuthill IC, Emerson M, Altman DG (2012) Improving bioscience research reporting: the ARRIVE guidelines for reporting animal research. *Osteoarthritis Cartilage* 20:256-260.
- Kim J, Namchuk M, Bugawan T, Fu Q, Jaffe M, Shi Y, Aanstoot HJ, Turck CW, Erlich H, Lennon V, Baekkeskov S (1994) Higher autoantibody levels and recognition of a linear NH₂-terminal epitope in the autoantigen GAD65, distinguish stiff-man syndrome from insulin-dependent diabetes mellitus. *J Exp Med* 180:595-606.
- Kittelmann M, Liewald JF, Hegermann J, Schultheis C, Brauner M, Steuer Costa W, Wabnig S, Eimer S, Gottschalk A (2013) In vivo synaptic recovery following optogenetic hyperstimulation. *Proc Natl Acad Sci U S A* 110:E3007-3016.
- Koo SJ, Markovic S, Puchkov D, Mahrenholz CC, Beceren-Braun F, Maritzen T, Dervede J, Volkmer R, Oschkinat H, Haucke V (2011) SNARE motif-mediated sorting of synaptobrevin by the endocytic adaptors clathrin assembly lymphoid myeloid leukemia (CALM) and AP180 at synapses. *Proc Natl Acad Sci U S A* 108:13540-13545.
- Lai M, Hughes EG, Peng X, Zhou L, Gleichman AJ, Shu H, Mata S, Kremens D, Vitaliani R, Geschwind MD, Bataller L, Kalb RG, Davis R, Graus F, Lynch DR, Balice-Gordon R, Dalmau J (2009) AMPA receptor antibodies in limbic encephalitis alter synaptic receptor location. *Ann Neurol* 65:424-434.
- Lai M, Huijbers MG, Lancaster E, Graus F, Bataller L, Balice-Gordon R, Cowell JK, Dalmau J (2010) Investigation of LGI1 as the antigen in limbic encephalitis previously attributed to potassium channels: a case series. *Lancet Neurol* 9:776-785.
- Lancaster E, Lai M, Peng X, Hughes E, Constantinescu R, Raizer J, Friedman D, Skeen MB, Grisold W, Kimura A, Ohta K, Iizuka T, Guzman M, Graus F, Moss SJ, Balice-Gordon R, Dalmau J (2010) Antibodies to the GABA(B) receptor in limbic encephalitis with seizures: case series and characterisation of the antigen. *Lancet Neurol* 9:67-76.
- Livak KJ, Schmittgen TD (2001) Analysis of relative gene expression data using real-time quantitative PCR and the 2^{-Delta Delta C(T)} Method. *Methods* 25:402-408.
- Llobet A, Gallop JL, Burden JJ, Camdere G, Chandra P, Vallis Y, Hopkins CR, Lagnado L, McMahon HT (2011) Endophilin drives the fast mode of vesicle retrieval in a ribbon synapse. *J Neurosci* 31:8512-8519.
- Lobo ME, Araujo ML, Tomaz CA, Allam N (2010) Stiff-person syndrome treated with rituximab. *BMJ Case Rep* 2010.
- Manto MU, Laute MA, Aguera M, Rogemond V, Pandolfo M, Honnorat J (2007) Effects of anti-glutamic acid decarboxylase antibodies associated with neurological diseases. *Ann Neurol* 61:544-551.
- Martin DL, Martin SB, Wu SJ, Espina N (1991) Regulatory properties of brain glutamate decarboxylase (GAD): the apoenzyme of GAD is present principally as the smaller of two molecular forms of GAD in brain. *J Neurosci* 11:2725-2731.

Reference list

- Mata S, Muscas GC, Cincotta M, Bartolozzi ML, Ambrosini S, Sorbi S (2010) GAD antibodies associated neurological disorders: incidence and phenotype distribution among neurological inflammatory diseases. *J Neuroimmunol* 227:175-177.
- Micheva KD, Ramjaun AR, Kay BK, McPherson PS (1997) SH3 domain-dependent interactions of endophilin with amphiphysin. *FEBS Lett* 414:308-312.
- Milosevic I, Giovedi S, Lou X, Raimondi A, Collesi C, Shen H, Paradise S, O'Toole E, Ferguson S, Cremona O, De Camilli P (2011) Recruitment of endophilin to clathrin-coated pit necks is required for efficient vesicle uncoating after fission. *Neuron* 72:587-601.
- Moersch FP, Woltman HW (1956) Progressive fluctuating muscular rigidity and spasm ("stiff-man" syndrome); report of a case and some observations in 13 other cases. *Proc Staff Meet Mayo Clin* 31:421-427.
- Ohkawa T, Satake S, Yokoi N, Miyazaki Y, Ohshita T, Sobue G, Takashima H, Watanabe O, Fukata Y, Fukata M (2014) Identification and characterization of GABA(A) receptor autoantibodies in autoimmune encephalitis. *J Neurosci* 34:8151-8163.
- Pang ZP, Bacaj T, Yang X, Zhou P, Xu W, Sudhof TC (2011) Doc2 supports spontaneous synaptic transmission by a Ca(2+)-independent mechanism. *Neuron* 70:244-251.
- Perera RM, Zoncu R, Lucast L, De Camilli P, Toomre D (2006) Two synaptojanin 1 isoforms are recruited to clathrin-coated pits at different stages. *Proc Natl Acad Sci U S A* 103:19332-19337.
- Peter BJ, Kent HM, Mills IG, Vallis Y, Butler PJ, Evans PR, McMahon HT (2004) BAR domains as sensors of membrane curvature: the amphiphysin BAR structure. *Science* 303:495-499.
- Petit-Pedrol M, Armangue T, Peng X, Bataller L, Cellucci T, Davis R, McCracken L, Martinez-Hernandez E, Mason WP, Kruer MC, Ritacco DG, Grisold W, Meaney BF, Alcalá C, Sillevs-Smitt P, Titulaer MJ, Balice-Gordon R, Graus F, Dalmau J (2014) Encephalitis with refractory seizures, status epilepticus, and antibodies to the GABAA receptor: a case series, characterisation of the antigen, and analysis of the effects of antibodies. *Lancet Neurol* 13:276-286.
- Pittock SJ, Lucchinetti CF, Parisi JE, Benarroch EE, Mokri B, Stephan CL, Kim KK, Kilimann MW, Lennon VA (2005) Amphiphysin autoimmunity: paraneoplastic accompaniments. *Ann Neurol* 58:96-107.
- Praefcke GJ, McMahon HT (2004) The dynamin superfamily: universal membrane tubulation and fission molecules? *Nat Rev Mol Cell Biol* 5:133-147.
- Raimondi A, Ferguson SM, Lou X, Armbruster M, Paradise S, Giovedi S, Messa M, Kono N, Takasaki J, Cappello V, O'Toole E, Ryan TA, De Camilli P (2011) Overlapping role of dynamin isoforms in synaptic vesicle endocytosis. *Neuron* 70:1100-1114.
- Raju R, Rakocevic G, Chen Z, Hoehn G, Semino-Mora C, Shi W, Olsen R, Dalakas MC (2006) Autoimmunity to GABAA-receptor-associated protein in stiff-person syndrome. *Brain* 129:3270-3276.
- Rakocevic G, Raju R, Dalakas MC (2004) Anti-glutamic acid decarboxylase antibodies in the serum and cerebrospinal fluid of patients with stiff-person syndrome: correlation with clinical severity. *Arch Neurol* 61:902-904.
- Ramirez DM, Khvotchev M, Trauterman B, Kavalali ET (2012) Vti1a identifies a vesicle pool that preferentially recycles at rest and maintains spontaneous neurotransmission. *Neuron* 73:121-134.
- Reynolds ES (1963) The use of lead citrate at high pH as an electron-opaque stain in electron microscopy. *J Cell Biol* 17:208-212.
- Richards DA, Bai J, Chapman ER (2005) Two modes of exocytosis at hippocampal synapses revealed by rate of FM1-43 efflux from individual vesicles. *J Cell Biol* 168:929-939.
- Rizzi M, Knoth R, Hampe CS, Lorenz P, Gougeon ML, Lemerrier B, Venhoff N, Ferrera F, Salzer U, Thiesen HJ, Peter HH, Walker UA, Eibel H (2010) Long-lived plasma cells and memory B cells

Reference list

- produce pathogenic anti-GAD65 autoantibodies in Stiff Person Syndrome. *PLoS One* 5:e10838.
- Rizzoli SO, Betz WJ (2005) Synaptic vesicle pools. *Nat Rev Neurosci* 6:57-69.
- Roux A, Uyhazi K, Frost A, De Camilli P (2006) GTP-dependent twisting of dynamin implicates constriction and tension in membrane fission. *Nature* 441:528-531.
- Schindelin J, Arganda-Carreras I, Frise E, Kaynig V, Longair M, Pietzsch T, Preibisch S, Rueden C, Saalfeld S, Schmid B, Tinevez JY, White DJ, Hartenstein V, Eliceiri K, Tomancak P, Cardona A (2012) Fiji: an open-source platform for biological-image analysis. *Nat Methods* 9:676-682.
- Schmid SL (1997) Clathrin-coated vesicle formation and protein sorting: an integrated process. *Annu Rev Biochem* 66:511-548.
- Seidenbecher T, Laxmi TR, Stork O, Pape HC (2003) Amygdalar and hippocampal theta rhythm synchronization during fear memory retrieval. *Science* 301:846-850.
- Shetty A, Sytnyk V, Leshchynska I, Puchkov D, Haucke V, Schachner M (2013) The neural cell adhesion molecule promotes maturation of the presynaptic endocytotic machinery by switching synaptic vesicle recycling from adaptor protein 3 (AP-3)- to AP-2-dependent mechanisms. *J Neurosci* 33:16828-16845.
- Shupliakov O, Low P, Grabs D, Gad H, Chen H, David C, Takei K, De Camilli P, Brodin L (1997) Synaptic vesicle endocytosis impaired by disruption of dynamin-SH3 domain interactions. *Science* 276:259-263.
- Silverstein AM (2001) Autoimmunity versus horror autotoxicus: the struggle for recognition. *Nat Immunol* 2:279-281.
- Soda K, Balkin DM, Ferguson SM, Paradise S, Milosevic I, Giovedi S, Volpicelli-Daley L, Tian X, Wu Y, Ma H, Son SH, Zheng R, Moeckel G, Cremona O, Holzman LB, De Camilli P, Ishibe S (2012) Role of dynamin, synaptojanin, and endophilin in podocyte foot processes. *J Clin Invest* 122:4401-4411.
- Solimena M (1998) Vesicular autoantigens of type 1 diabetes. *Diabetes Metab Rev* 14:227-240.
- Solimena M, Folli F, Aparisi R, Pozza G, De Camilli P (1990) Autoantibodies to GABA-ergic neurons and pancreatic beta cells in stiff-man syndrome. *N Engl J Med* 322:1555-1560.
- Solimena M, Folli F, Denis-Donini S, Comi GC, Pozza G, De Camilli P, Vicari AM (1988) Autoantibodies to glutamic acid decarboxylase in a patient with stiff-man syndrome, epilepsy, and type I diabetes mellitus. *N Engl J Med* 318:1012-1020.
- Sommer C, Weishaupt A, Brinkhoff J, Biko L, Wessig C, Gold R, Toyka KV (2005) Paraneoplastic stiff-person syndrome: passive transfer to rats by means of IgG antibodies to amphiphysin. *Lancet* 365:1406-1411.
- Somogyi J (2002) Differences in ratios of GABA, glycine and glutamate immunoreactivities in nerve terminals on rat hindlimb motoneurons: a possible source of post-synaptic variability. *Brain Res Bull* 59:151-161.
- Sudhof TC, Malenka RC (2008) Understanding synapses: past, present, and future. *Neuron* 60:469-476.
- Sudhof TC, Rizo J (2011) Synaptic vesicle exocytosis. *Cold Spring Harb Perspect Biol* 3.
- Takamori S, Holt M, Stenius K, Lemke EA, Grønborg M, Riedel D, Urlaub H, Schenck S, Brügger B, Ringler P, Müller SA, Rammner B, Gräter F, Hub JS, De Groot BL, Mieskes G, Moriyama Y, Klingauf J, Grubmüller H, Heuser J, Wieland F, Jahn R (2006) Molecular anatomy of a trafficking organelle. *Cell* 127:831-846.
- Takei K, McPherson PS, Schmid SL, De Camilli P (1995) Tubular membrane invaginations coated by dynamin rings are induced by GTP-gamma S in nerve terminals. *Nature* 374:186-190.
- Takei K, Slepnev VI, Haucke V, De Camilli P (1999) Functional partnership between amphiphysin and dynamin in clathrin-mediated endocytosis. *Nat Cell Biol* 1:33-39.

Reference list

- Tian N, Petersen C, Kash S, Baekkeskov S, Copenhagen D, Nicoll R (1999) The role of the synthetic enzyme GAD65 in the control of neuronal gamma-aminobutyric acid release. *Proc Natl Acad Sci U S A* 96:12911-12916.
- Toro C, Jacobowitz DM, Hallett M (1994) Stiff-man syndrome. *Semin Neurol* 14:154-158.
- Toyka KV, Brachman DB, Pestronk A, Kao I (1975) Myasthenia gravis: passive transfer from man to mouse. *Science* 190:397-399.
- Trempe JF, Chen CX, Grenier K, Camacho EM, Kozlov G, McPherson PS, Gehring K, Fon EA (2009) SH3 domains from a subset of BAR proteins define a Ubl-binding domain and implicate parkin in synaptic ubiquitination. *Mol Cell* 36:1034-1047.
- Vega-Flores G, Rubio SE, Jurado-Parras MT, Gomez-Climent MA, Hampe CS, Manto M, Soriano E, Pascual M, Gruart A, Delgado-Garcia JM (2014) The GABAergic septohippocampal pathway is directly involved in internal processes related to operant reward learning. *Cereb Cortex* 24:2093-2107.
- Verstreken P, Koh TW, Schulze KL, Zhai RG, Hiesinger PR, Zhou Y, Mehta SQ, Cao Y, Roos J, Bellen HJ (2003) Synaptotagmin is recruited by endophilin to promote synaptic vesicle uncoating. *Neuron* 40:733-748.
- Vianello M, Tavolato B, Armani M, Giometto B (2003) Cerebellar ataxia associated with anti-glutamic acid decarboxylase autoantibodies. *Cerebellum* 2:77-79.
- Voglmaier SM, Edwards RH (2007) Do different endocytic pathways make different synaptic vesicles? *Curr Opin Neurobiol* 17:374-380.
- Walter AM, Groffen AJ, Sorensen JB, Verhage M (2011) Multiple Ca²⁺ sensors in secretion: teammates, competitors or autocrats? *Trends Neurosci* 34:487-497.
- Watanabe S, Rost BR, Camacho-Perez M, Davis MW, Sohl-Kielczynski B, Rosenmund C, Jorgensen EM (2013) Ultrafast endocytosis at mouse hippocampal synapses. *Nature* 504:242-247.
- Werner C, Haselmann H, Weishaupt A, Toyka KV, Sommer C, Geis C (2014) Stiff person-syndrome IgG affects presynaptic GABAergic release mechanisms. *J Neural Transm*.
- Wessig C, Klein R, Schneider MF, Toyka KV, Naumann M, Sommer C (2003) Neuropathology and binding studies in anti-amphiphysin-associated stiff-person syndrome. *Neurology* 61:195-198.
- Whitney KD, McNamara JO (1999) Autoimmunity and neurological disease: antibody modulation of synaptic transmission. *Annu Rev Neurosci* 22:175-195.
- Wigge P, McMahon HT (1998) The amphiphysin family of proteins and their role in endocytosis at the synapse. *Trends Neurosci* 21:339-344.
- Wigge P, Vallis Y, McMahon HT (1997) Inhibition of receptor-mediated endocytosis by the amphiphysin SH3 domain. *Curr Biol* 7:554-560.
- Wolter S, Loschberger A, Holm T, Aufmkolk S, Dabauvalle MC, van de Linde S, Sauer M (2012) rapidSTORM: accurate, fast open-source software for localization microscopy. *Nat Methods* 9:1040-1041.
- Wu Y, Matsui H, Tomizawa K (2009) Amphiphysin I and regulation of synaptic vesicle endocytosis. *Acta Med Okayama* 63:305-323.
- Yaksh TL, Rudy TA (1976) Chronic catheterization of the spinal subarachnoid space. *Physiol Behav* 17:1031-1036.

Appendix A: Index of figures

Fig 1 Summary of SPS antigens linked to GABAergic neurotransmission.....	3
Fig 2 Overview of the presynaptic compartment of chemical synapses depicting exocytosis and endocytosis mechanisms	5
Fig 3 Amphiphysin structure and interaction partners.....	6
Fig 4 Structural deficits at disturbed endocytosis.....	7
Fig 5 Experimental setup and categorization of synapse types	20
Fig 6 Increased synaptic vesicle density in stimulated spinal boutons (control condition). ..	21
Fig 7 Increased CCV intermediates at high synaptic activity in spinal boutons (control condition).....	22
Fig 8 Increased number of ELS upon stimulation in spinal boutons (control condition).	23
Fig 9 Reduced vesicle density in stimulated boutons after intrathecal passive-transfer with specAmph AB	24
Fig 10 Depletion of CCV during high synaptic activity after intrathecal passive-transfer with specAmph AB	25
Fig 11 Reduction of ELS in spinal cord boutons after intrathecal passive-transfer with specAmph AB	26
Fig 12 Scheme for analysis of dSTORM signals.....	28
Fig 13 specAmph AB induce increase of syb2 expression inside GABAergic presynapses.....	29
Fig 14 specAmph AB mediate decrease of syb7 upon stimulation	30
Fig 15 Stimulation induced different endophilin expression pattern in GABAergic boutons dependent on IgG preincubation	32
Fig 16 Scheme of cluster analysis of dSTORM signals	32
Fig 17 Stimulation evoked dispersion of endophilin signal maxima in presence of specAmph AB	33
Fig 18 Synaptojanin expression in GABAergic boutons is unaffected by AB targeting amphiphysin	34
Fig 19 Stable synaptojanin clustering in presence of AB to amphiphysin	35

Fig 20 Similar GABAergic eIPSC amplitude and kinetic characteristics in presence of anti-GAD65 AB containing IgG	36
Fig 21 SPS-IgG with anti-GAD65 AB does not affect short term plasticity or high frequency transmission of a basket cell – granule cell GABAergic synapse	38
Fig 22 GAD65-IgG increases release probability of spontaneous GABAergic transmission ...	39
Fig 23 Increased mIPSC frequency cannot be attributed to larger GABAergic vesicle pools .	40
Figure 24 Anti-GAD65 AB containing IgG induces no gene expression changes of gad isoforms	41
Fig 25 SPS-IgG depleted of GAD65-AB still binds to murine neuronal structures	42
Fig 26 Microisland culture	43

Appendix B: Abbreviations

BSA	bovine serum albumine
°C	degree celsius
µg	10 ⁻³ g
µm	10 ⁻⁶ meter
µs	10 ⁻³ second
a.u.	arbitrary units
AB	autoantibodies
ACSF	artificial cerebrospinal fluid
AMPA	alpha-amino-3-hydroxy-5-methyl-4-isoxazole propionic acid
ANOVA	analysis of variance
AP-2	adaptor protein 2
AP-3	adaptor protein 3
AP-5	D-2-amino-5-phosphonovalerate
BAR	Bin/Amphiphysin/Rvs
CCD	charge-coupled device
CCV	clathrin coated vesicles
cdk5	cyclin dependent kinase 5
cDNA	complementary deoxyribonucleic acid
CIDP	chronic inflammatory demyelinating polyneuropathy
cm	10 ⁻² meter
CME	clathrin mediated endocytosis
CNQX	6-Cyano-7-nitroquinoxaline-2,3-dione
CNS	central nervous system
CSF	cerebrospinal fluid
CT	comparative threshold
DG	dentate gyrus
DIV	days in vitro
dSTORM	direct stochastic optical reconstruction microscopy
E18	day 18 embryonal state
EDTA	ethylenediaminetetraacetic acid
eIPSC	evoked inhibitory postsynaptic currents
ELS	endosome like structures
EM	electron microscopy
EMCCD	electron multiplying charge-coupled device
FBS	fetal bovine serum
fig.	figure
FWHM	full width half maximum
g	gram

Appendix B: Abbreviations

GABA	γ - aminobutyric acid
GABARAP	GABA _A receptor associated protein
GAD	glutamate decarboxylase
GAD65	glutamate decarboxylase 65
GAD67	glutamate decarboxylase 67
GAPDH	Glyceraldehyde-3-Phosphate Dehydrogenase
GTPase	Guanosintriphosphatase
h	hour
H ₂ O	water
HBSS	Hank's Balanced Salt Solution
Hz	Hertz
i.th.	intrathecal
IgG	immunoglobulin G
IPSC	inhibitory postsynaptic current
kHz	10 ³ Hz
KO	knockout
M	mega
m	meter
M	molar
MEA	mercaptoethylamine
min	minute
mIPSC	miniature inhibitory postsynaptic current
ML	molecular layer
mm	10 ⁻³ meter
mM	10 ⁻³ molar
ms	10 ⁻³ second
ng	10 ⁻⁹ gram
nm	10 ⁻⁹ meter
NMDA	N-methyl-D-aspartate
pA	10 ⁻¹² ampere
PBS	phosphate buffered saline
PDL	poly-D-lysine
PFA	paraformaldehyde
PGP 9.5	protein gene product 9.5
PIP ₂	Phosphatidylinositol-4,5-bisphosphate
PLP	pyridoxal 5' phosphate
PMT	photomultiplier tube
ppr	paired pulse ratio
PRD	proline rich domain
PS	penicillin streptomycin

Appendix B: Abbreviations

PSF	point spread function
qRT-PCR	quantitative reverse transcription polymerase chain reaction
rec	recording
RNA	ribonucleic acid
ROI	region of interest
RT	room temperature
s	second
SEM	standard error of mean
SH3	spectrin homology 3
SNARE	soluble N-ethylmaleimide-sensitive-factor attachment receptors
specAmph	treated with specific autoantibodies to Amphiphysin
SPS	Stiff person syndrome
STED	stimulated emission depletion
stim	stimulation
syb	synaptobrevin
syb2	synaptobrevin 2
syb7	synaptobrevin 7
Syphy	Synaptophysin
Tirf	total internal reflection fluorescent
TTX	tetrodotoxin
V	volt
VGAT	vesicular GABA transporter
v-SNARE	vesicular soluble N-ethylmaleimide-sensitive-factor attachment receptors
Ω	Ohm

Affidavit & eidesstattliche Erklärung

Affidavit

I hereby confirm that my thesis entitled is the result of my own work. I did not receive any help or support from commercial consultants. All sources and / or materials applied are listed and specified in the thesis.

Furthermore, I confirm that this thesis has not yet been submitted as part of another examination process neither in identical nor in similar form.

.....
Place, Date

.....
Signature

Eidesstattliche Erklärung

Hiermit erkläre ich an Eides statt, die Dissertation eigenständig, d.h. insbesondere selbständig und ohne Hilfe eines kommerziellen Promotionsberaters, angefertigt und keine anderen als die von mir angegebenen Quellen und Hilfsmittel verwendet zu haben.

Ich erkläre außerdem, dass die Dissertation weder in gleicher noch in ähnlicher Form bereits in einem anderen Prüfungsverfahren vorgelegen hat.

.....
Ort, Datum

.....
Unterschrift

Danksagung/Acknowledgements (in German)

Besonderer Dank gilt Frau Professor Dr. Claudia Sommer, die mir das interessante Thema der Doktorarbeit überlassen hat und mich im Laufe der Doktorarbeit unterstützt und beraten hat. Die Gruppenseminare der Neurologie in Würzburg haben mir interessante Einblicke in die klinische Forschung geben können und Frau Prof. Sommer ermöglichte mir die Erlernung neuer Methoden und den Besuch von hilfreichen Konferenzen und Workshops. Zudem möchte ich Herrn Professor Dr. Klaus V. Toyka für sein großes Interesse an meiner Forschungsarbeit und seine fortwährende Unterstützung herzlichst bedanken.

Besonderer Dank geht auch an Frau Professor Dr. Marie-Christine Dabauvalle und Herrn Professor Dr. Erhard Wischmeyer, die mir als weitere Gutachter wertvolle Ratschläge bei der Versuchsplanung und Interpretation der Ergebnisse gegeben haben.

Höchsten Dank möchte ich Herrn Professor Dr. Christian Geis aussprechen, der mich täglich bei meiner Forschungsarbeit begleitet und unterstützt hat. Er konnte meine Faszination für die Forschung an Autoimmunerkrankungen durch spannende Experimente fortwährend steigern und seine Unterstützung in allen Lebensbereichen ist für mich von unschätzbarem Wert.

Bei meinen Laborkollegen Dr. Benedikt Grünwald, Holger Haselmann, Christoph Emmerich und Christian Staudenmaier möchte ich mich für die schöne Zeit im Labor und Büro als auch für konstruktive Kritik bei der Versuchsplanung bedanken.

Dr. Martin Pauli möchte ich für die professionelle Einweisung in die *d*STORM Mikroskopie und für die faszinierenden Unterhaltungen wissenschaftlicher als auch privater Natur danken.

Für die spannenden Kooperationen, bei denen ich z.B. neue Techniken wie Elektronenmikroskopie und höchstauflösende Fluoreszenzmikroskopie lernen durfte, möchte ich mich bei Frau Professor Dr. Esther Asan, Herrn Professor Dr. Manfred Heckmann, Herrn Professor Dr. Markus Sauer, Herrn PD Andreas Weishaupt und Herrn PD Dr. Sören Doose bedanken.

Weiterhin danke ich allen technischen Angestellten für die nette Atmosphäre und expe-

Danksagung/Acknowledgements (in German)

rimentelle Unterstützung: Sonja Mildner, Barbara Dekant, Barbara Broll, Helga Brünner, Lydia Biko, Susanne Helmig, Hiltrud Klüpfel, Claudia Sommer (Jena), Karin Reinfurt-Gehm (Anatomie Würzburg) und Sieglinde Schenk (Anatomie Würzburg).

Mein spezieller Dank richtet sich an meinen Bruder Michael und an meine Eltern, Gertrud und Klaus, die mir das Studium ermöglicht haben und stets an mich geglaubt haben.

Ganz besonders möchte ich meiner Freundin Corinna danken, die mich in der finalen Phase der Doktorarbeit aufgemuntert hat und mir durch Ihr Verständnis sowie durch Ihre Motivation das Durchhalten bis zum Finale erheblich erleichtert hat.

Natürlich möchte ich allen danken, die ich vergessen habe zu danken. Es gab viele weitere Leute, die mich in meinem Labor- und Büroalltag begleitet haben und ich danke meinen Freunden, die mir den nötigen Ausgleich zur Arbeit geschenkt haben.

Publications

Peer reviewed journals; original articles (chronological order)

Doppler K, **Werner C**, Henneges C, Sommer C (2012) Analysis of myelinated fibers in human skin biopsies of patients with neuropathies. *J Neurol.* 259:1879-1887.

Doppler K, **Werner C**, Sommer C (2013) Disruption of nodal architecture in skin biopsies of patients with demyelinating neuropathies. *J Peripher Nerv Syst* 18:168-176.

Werner C, Haselmann H, Weishaupt A, Toyka KV, Sommer C, Geis C (2014) Stiff person-syndrome IgG affects presynaptic GABAergic release mechanisms. *J Neural Transm.*

Poster presentations at international conferences

Werner C, Grünewald B, Toyka KV, Sommer C, Geis C (2011) Impaired cerebellar GABAergic feedforward inhibition in CLN3 knockout mice. 9th meeting of the German Neuroscience Society, Göttingen, Germany

Werner C, Grünewald B, Asan E, Sommer C, Geis C (2012) Stiff Person Syndrome: Ultrastructural analysis of spinal synaptic terminals. 8th FENS Forum of Neuroscience, Barcelona, Spain

Werner C, Grünewald B, Asan E, Sommer C, Geis C (2012) Stiff Person Syndrome: endocytosis at a slowed pace. 42nd annual meeting of the Society for Neuroscience, New Orleans, United States of America

Curriculum Vitae

2009~ PhD-Student, Graduate School of Life Science, Julius-Maximilians-Universität, Würzburg and Hans-Berger Department of Neurology, Experimental Neurology, Jena University Hospital

- thesis title: "Effect of autoantibodies targeting amphiphysin or glutamate decarboxylase 65 on synaptic transmission of GABAergic neurons"
supervisor/committee: Prof. Dr. Claudia Sommer, Prof. Dr. Marie-Christine Dabauvalle, Prof. Dr. Erhard Wischmeyer
- Member of the SFB 581(Deutsche Forschungsgemeinschaft)

2004-2008 Diploma, Biology, Julius-Maximilians-Universität, Würzburg

diploma thesis title: „Functional interactors of Bruchpilot protein“

supervisor/committee: Prof. Dr. Stephan Sigrist, Prof. Dr. Erich Buchner

- subjects: neurobiology, animal ecology, pharmaceutical biology

1991-2001 Abitur, Franken Landschulheim Schloss Gaibach, Gaibach

.....
Place, date

.....
Signature